AD 749360

PARAMETER ESTIMATION ALGORITHMS FOR DIGITAL SYSTEMS

by Claus P. Janota

Technical Memorandum
File No. TM 71-131
August 3, 1971
Contract N00017-70-C-1407

Copy No. 7

D D C
OCT 10 1972
C

The Pennsylvania State University
Institute for Science and Engineering
ORDNANCE RESEARCH LABORATORY
University Park, Pennsylvania

DISTRIBUTION OF THIS DOCUMENT IS UNLIMITED

NAVY DEPARTMENT NAVAL ORDNANCE SYSTEMS COMMAND

Reproduced by
NATIONAL TECHNICAL
INFORMATION SERVICE
U S Department of Commerce
Springfield VA 22151

153

ia

DOCUMENT CONTROL DATA - R & D

(Security classification of title, abstract and indexing annotation when overall report is classified)

1. ORIGINATING ACTIVITY (Corporate author) Ordnance Research Laboratory University Park, Pennsylvania	2a. REPORT SECURITY CLASSIFICATION Unclassified 2b. GROUP

3. REPORT TITLE

Parameter Estimation Algorithms for Digital Systems

4. DESCRIPTIVE NOTES (Type of report and inclusive dates)

M.S. Thesis, Engineering Acoustics - September 1971

5. AUTHOR(S) (First name, middle initial, last name)

Claus P. Janota

6. REPORT DATE August 3, 1971	7a. TOTAL NO. OF PAGES 150	7b. NO. OF REFS 42
8a. CONTRACT OR GRANT NO. N00017-70-C-1407 b. PROJECT NO. c. d.	9a. ORIGINATOR'S REPORT NUMBER(S) TM 71-131 9b. OTHER REPORT NO(S) (Any other numbers that may be assigned this report)	

10. DISTRIBUTION STATEMENT

Distribution of this document is unlimited.

11. SUPPLEMENTARY NOTES	12. SPONSORING MILITARY ACTIVITY Naval Ordnance Systems Command Department of the Navy

13. ABSTRACT

The general topic of the work reported in this thesis is the use of algorithms for parameter estimation in a digital signal processor. Such an algorithmic approach to the estimation problem follows naturally when principal components of the overall system are digital. Algorithms for performing the decision functions associated with a maximum likelihood estimator are outlined and presented in general terms. The factors important to comparing various algorithmic approaches are defined and discussed. The confidence intervals for various algorithmic parameter estimation approaches are developed and the results of computer simulation of the system presented. It is demonstrated that the error in estimation can be quite small in relation to the pulse length even for the monochrome pulse case.

DD FORM 1 NOV 65 1473

ib

14. KEY WORDS	LINK A ROLE	LINK A WT	LINK B ROLE	LINK B WT	LINK C ROLE	LINK C WT
Air Search Radar	8					
Digital Systems	8					
Engineering Acoustics	8					
Linear Frequency Shift Pulse	8					
Monochrome Pulse	8					
Parameter Estimation	8					
Quantization	8					
Signal Processing	8					

ABSTRACT

The general topic of the work reported in this thesis is the use of algorithms for parameter estimation in a digital signal processor. The work evolved from the current trend toward sampled, digitized data systems. Such an algorithmic approach to the estimation problem follows naturally when principal components of the overall system are digital.

The general parameter estimation problem is treated in way of introduction. This estimation scheme is then extended to the specific case of signals in the presence of additive gaussian noise. It is shown how an estimation which seeks to minimize the square error for an interesting class of cases leads to a correlator receiver.

The response of such a receiver to two important classes of signals, monochrome pulse and linear frequency shift pulse, is developed. Quantization of this receiver response makes it possible to treat the data in a digital system. The effects of quantization on the input and data representation within the digital system are discussed.

Algorithms for performing the decision functions associated with a maximum likelihood estimator are outlined and presented in general terms. The factors important to comparing various algorithmic approaches are defined and discussed. These factors, cycle repeat count and frame length, are analogous to certain aspects of communication systems.

The confidence intervals for various algorithmic parameter estimation approaches are developed and the results of computer simulation of the system presented. The confidence interval on estimates of echo delay time are shown to be dependent on the ratio of received signal energy to noise ratio. It is demonstrated that the error in estimation can be quite small in relation to the pulse length even for the monochrome pulse.

An air traffic control search radar is used as a specific example of how estimation algorithms may be used in practice. The measures of algorithm performance can be related to specific system requirements when such a model is used.

ACKNOWLEDGMENT

The author wishes to express his gratitude to his advisor, Dr. Carter L. Ackerman, for his interest and encouragement as well as to Mr. Norman B. Miller who initially suggested the topic of this thesis.

The author also acknowledges the assistance rendered by the Ordnance Research Laboratory of The Pennsylvania State University in supporting this investigation under contract with the Naval Ordnance Systems Command.

In addition the author expresses his appreciation for the assistance rendered by the Statistical Consulting Service of The Pennsylvania State University and for the help of numerous persons at the university who provided encouragement and the various services needed to complete this work.

TABLE OF CONTENTS

		Page
Acknowledgments		ii
List of Tables		v
List of Figures		vi
I.	INTRODUCTION	
	1.1 Statement of the Problem	1
	1.2 Importance of the Problem	1
	1.3 Scope of the Problem	3
II.	ANALYSIS OF ESTIMATION	
	2.1 Introduction	4
	2.2 Bayes Estimate	8
	2.3 Maximum Likelihood Estimation	13
	2.4 Signal Parameter Estimation	15
	2.5 The General Radar Problem	21
III.	AMBIGUITY AND RESOLUTION	
	3.1 Noise Free Resolution	24
	3.2 Noise Effects	26
	3.3 Echo Delay Resolution in Radar	27
	3.4 Resolution in Radar	27
IV.	DIGITAL SYSTEMS	
	4.1 The Generalized Decision Process	31
	4.2 Single Monochromatic Carrier Band Pulse, Rectangular Envelope	33
	4.3 The Effect of Continuous Observation	42
	4.4 Linear Swept FM Pulse of Duration T	45
V.	ESTIMATION ALGORITHMS	
	5.1 Introduction	50
	5.2 The General Purpose Programmed Automaton	50
	5.3 Nature of the Input to the Estimation Algorithm	52
	5.4 Measures of Algorithm Performance	56
	5.5 Simultaneous Estimation of Frequency and Echo Delay	71

TABLE OF CONTENTS

Page

VI. ILLUSTRATIVE EXAMPLE OF RADAR ESTIMATION
6.1 A Track-While-Scan Radar 90
6.2 Processing Implications of the Model 93
6.3 A Simulation System 99

VII. SUMMARY AND CONCLUSIONS
7.1 Statement of the Problem 111
7.2 Approach 111
7.3 Conclusions 112
7.4 Suggestions for Further Work 112

APPENDIX A: Quantized Correlation Functions 114

APPENDIX B: Non-Linearity in the Linear FM Ridgeline Response 119

APPENDIX C: Miscellaneous Mathematics 124
C.1 Quotient of Random Variables 124
C.2 Estimation by Intersecting Linear Regression. 128

APPENDIX D: Miscellaneous Algorithms 130
D.1 Algorithm for Estimation, Simple Monochrome Case 130
D.2 Algorithm for Treating the Linear FM Case, Direct Method 131
D.3 Algorithm for Treating the Linear Case, Transformation Method 132
D.4 Algorithm for Generating Correlated Gaussian Pseudorandom Numbers 134

APPENDIX E: ALGOL 60 Language Reference 135

BIBLIOGRAPHY 139

LIST OF TABLES

Table		Page
6.1	Parameters for Model Radar Application	92
E.1	Summary of ALGOL 60 Symbology	137
E.2	ALGOL 60 Expressions	138

LIST OF FIGURES

Figure		Page
2.1	Parameter Estimation Model	5
2.2	Representative Cost Functions.	7
2.3	The Estimation of Known Signals in the Presence of Additive Noise	16
2.4	Summary of Maximum Likelihood Estimation	20
3.1	Uncertainty Surfaces for Representative Signals. (a) Linear Swept Chirp Pulse With Rectangular Envelope (b) Monochrome Pulse With Rectangular Envelope (c) "Noise" Waveform	29
4.1	Uncertainty Surface for Monochrome Pulse of Duration T Rectangular Envelope	36
4.2	Maximum Likelihood Estimator, Carrier Band Signal. .	37
4.3	Quantization of an Analog Waveform	38
4.4	Input-Output Characteristics of a Quantizer.	38
4.5	Typical Monochrome Signal Correlator Response Showing the Effect of Noise	41
4.6	Maximum Likelihood Receiver Time Response for a Multiple Target Situation	44
4.7	Samples for a Multiple Target Situation, for Thresholded Analog Output	44
4.8	Uncertainty Function of Linear F-M Pulse	47
4.9	Uncertainty Region of Linear F-M Pulse of Duration T	48
5.1	Transfer of Samples Into the Processing Array. . . .	54

LIST OF FIGURES

Figure		Page
5.2	Effect of Noise-Only Event on the Estimation Scheme	59
5.3	Effect of Received Signal Energy on Algorithm Bias	63
5.4	Confidence Interval for Estimation Algorithms	67
5.5	ML Detector Response for Two Monochrome Pulses, Large S/N Case	73
5.6	Overlapping Monochrome Responses	74
5.7	Response of a Correlation Receiver to Overlapping Chirp Signals	77
5.8	Overlapping Echoes for F-M Signal	78
5.9	Distribution of First Sample Deviation for Linear F-M Signals	81
5.10	General Algorithm for Signals With Linear Ridgeline Response	83
5.11	Separation of Data Points by Transformation Algorithm	85
5.12	Tests of Data Points in the t' Space, Worst Case Example	87
6.1	Bayes Estimator, M-ary Communications with Known A Priori Density	96
6.2	Frequency Response of a Maximum Likelihood Receiver to a Monochrome Pulse with Rectangular Envelope	98
6.3	The Effect of Bilateral Hamming Weighting on the Secondary Peaks in a Linear F-M Correlator	100
6.4	Effect of Sampling Rate on Estimate of Time Delay	104

LIST OF FIGURES

Figure		Page
6.5	Effect of Sampling Rate on Estimate of Time Delay, Quotient Algorithm	105
6.6	Bias of the Quotient Algorithm	106
6.7	Effect of a Threshold on Confidence Interval	108
6.8	Effect of Threshold on Confidence Interval, Quotient Algorithm	109
A.1	Analytic Model of a Quadrature Correlator	115
A.2	Quadrature Correlation Function Variance as a Function of Sampling Rate	117
B.1	Slope of Ridgeline Response with Delay Time	122
B.2	Behavior of Correlator Peak Output with Delay Time	123

CHAPTER I

INTRODUCTION

1.1 Statement of the Problem

This thesis outlines digital schemes for parameter estimation in the general problem of processing signals with unknown parameters in the presence of noise. Such digital estimation algorithms are a natural consequence of the current trend toward sampled, digitized data systems. The exposition considers several algorithmic approaches to the estimation problem. Differences between the schemes such as processing time requirements, sensitivity to noise, and biases are discussed.

1.2 Importance of the Problem

The reception problem of signals with unknown parameters in noise occurs for M-ary communication and communications links for which an unknown and varying phase is impressed upon the transmitted signal. Some examples of this latter situation are digital communication systems without phase reference, digital communication over fading channels, channels with varying transmission medium conditions, and channels exhibiting multi-path propagation.

A corresponding problem arises in the radar case when a target is present so that the pulse is reflected. Signal attenuation and associated phase shift will result, even for a point target. If the radar application is to be useful, the value of time delay, phase, and

reflected signal amplitude are in some sense unknown at the receiver. In addition, the returned signal may suffer a frequency shift. The radar system further differs from the communication channel in that detection and estimation must often be combined. This occurs whenever no a priori knowledge of the presence of a target exists.

The application of digital schemes for accomplishing the required parameter estimation follows naturally when other components of the receiver are digital in nature. Sampled and quantized data is frequently processed in lieu of analog inputs for convenience. The use of signal correlators and fast digital Fourier transform (FFT) systems in recent years gives added emphasis to digital parameter estimation systems as does the widespread use of digital data recording.

For reasons of flexibility, it is often desirable to use a general purpose computer for accomplishing the digital processing. Such a computer and its associated algorithms can be used to perform parameter estimation as well as to provide control functions for data acquisition or recording. Modifications in signal types can be treated in such a system by algorithm revisions. In addition, the possibility of self modifying systems exists in a general purpose computer due to the inherent flexibility of such machines [11].

The use of digital computers in the correlation and detection of signals has been extensively reported in the literature [2, 25, 29, 37]. Also array processing of signals in various interfering background situations has been treated [42]. Schlachta et al and Leth-Espensen have addressed the problem of time domain tracking of radar targets using a general purpose digital computer [9, 31].

1.3 Scope of the Problem

The basic intent of this thesis is to present a representative set of algorithms for signal parameter estimation. The general detection problem is discussed and a model radar system is presented as an example. The nature of correlation functions is treated to demonstrate the types of errors introduced by noise.

Algorithms for parameter estimation for pure tone and frequency modulated (chirp) pulsed signals are treated. In addition, these signals, modulated in a pulse with rectangular or Gaussian envelope, result in correlation functions which are amenable to detailed analysis.

Some discussion of the implications of alternate algorithms on data rates and errors is included, as are some applications areas of interest.

CHAPTER II

ANALYSIS OF ESTIMATION

2.1 Introduction

In this chapter the general problem of estimation of signal parameters is discussed. The parameter estimation problem occurs in the three broad areas: digital communications, radar, sonar or seismology, and pattern recognition and classification. The discussion here will concentrate on the communication and radar areas.

A model of the general estimation problem is shown in Figure 2.1 and consists of the following four components [35].

a. Parameter Space. The parameter space defines the totality of values which may be assumed by the source. This space for example, may consist of all possible states in a binary communication system or all allowed target dopplers in a radar application.

b. Probabilistic Mapping from Parameter Space to Observation Space. This is the probabilistic law that maps a selected value from the parameter space onto the observation space.

c. Observation Space. The observation space is the set of all outcomes of the mapping of a parameter onto an observation. This will generally be a

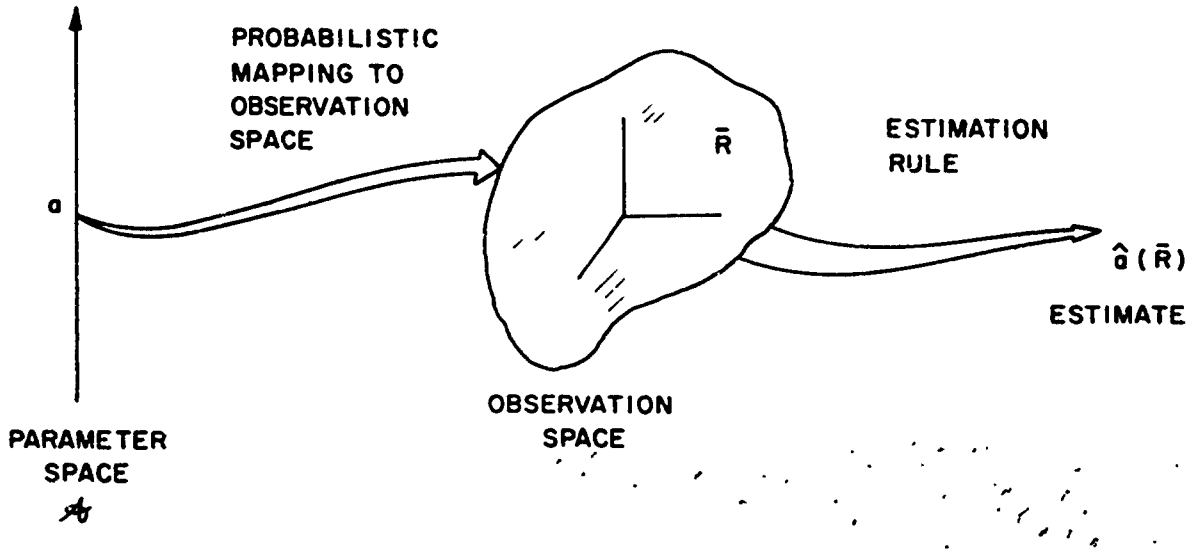

Figure 2.1 Parameter Estimation Model

finite dimensioned space. An observation will be denoted by a vector $\overline{R}$.

d. Estimation Rule. After observing an outcome $\overline{R}$, we shall want to estimate the value of the parameter a. This estimate may be denoted as $\hat{a}\ (\overline{R})$.

In the communications problem, the a priori probability of selection of a specific value of the parameter from the parameter space is generally known. That is, the probability distribution of the unique messages is known, perhaps uncertainly. If it is possible to determine the conditional observation density $p(\overline{R}|a)$ a method of detection optimization is available [30, 35]. This conditional observation density $p(\overline{R}|a)$ will be describable if the effect of the channel on the parameter a is known. In most cases, the assumption of additive noise is valid, that is,

$$R(t) = x(t) + n(t), \tag{2.1}$$

where n(t) is the additive noise. Then, x(t) is the pure signal input to the channel, and R(t) the measured channel output. It is now necessary to consider a cost function $C(\hat{a},a)$. This function is dependent on the value of both the parameter a and its estimated value $\hat{a}$. The cost function defines the "seriousness" of an error in the estimation of the parameter a. The error is $(\hat{a}-a)$. The choice of the cost function is dependent on the situation of interest. One practical way to assign the cost function is in terms of the magnitude of the error (Figure 2.2a). Another form which is often used because of its mathematical tractability is to consider the

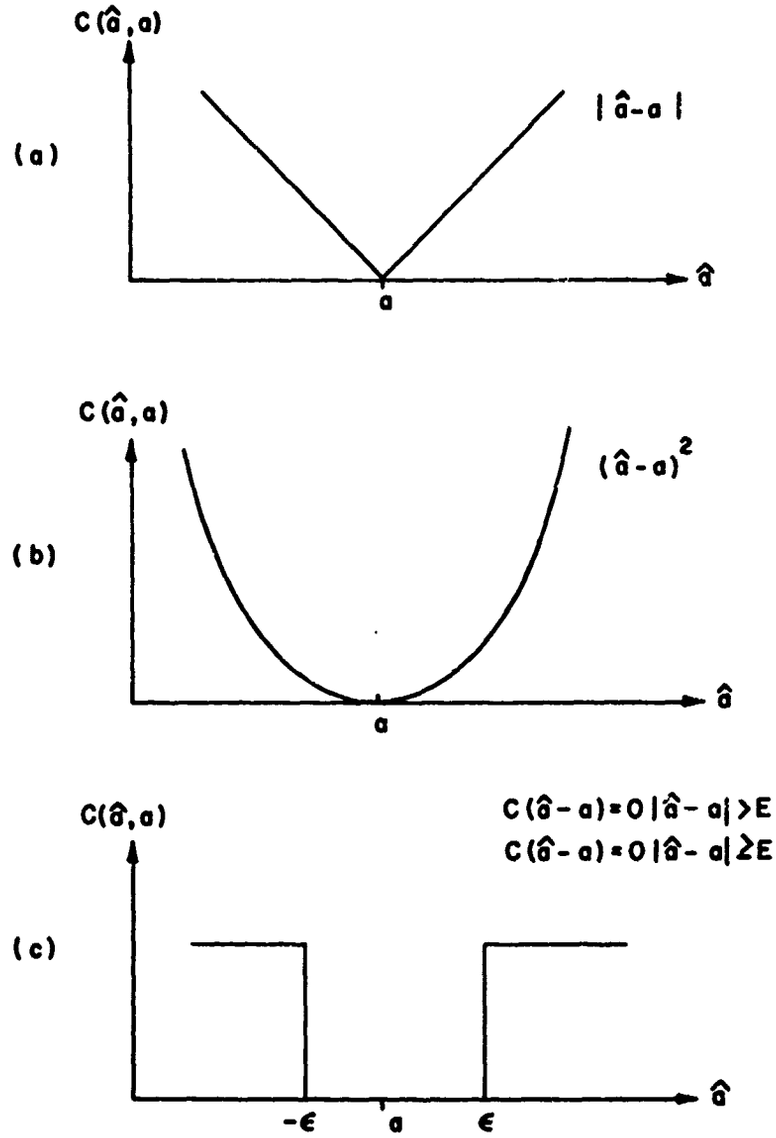

Figure 2.2 Representative Cost Functions

squared error (Figure 2.2b). In some situations, small errors are inconsequential, but errors above a certain value are equally serious. Such a cost function is shown in Figure 2.2c.

To avoid mathematical difficulties most authors use the squared error cost function [13, 15, 32, 35]. The exposition herein will concentrate on this form of the cost function as well and it will be shown that this form of cost function is equivalent to an important general problem in estimation. This function is

$$C(\hat{a},a) = (a-a)^2. \tag{2.2}$$

In typical radar applications, the a priori probability density of the parameter a is generally not known. This situation is often treated by assuming a uniform probability density over some allowed range of the parameter. For example, the target is assumed to be equally likely at all ranges over which a radar receiver is designed to operate. Obviously, this state of affairs is not generally the case but is reasonable in light of complexities imposed by multi-target requirements, the effect of clutter and other operational factors.

2.2 Bayes Estimate

The average cost of the errors in estimation is

$$R_c(a) = \int_{-\infty}^{\infty} C(\hat{a},a)\ p(\overline{R}|a)d\overline{R}. \tag{2.3}$$

This is termed the conditional risk. The average risk is derived by averaging over all values of a,

$$R_a(a) = \int_{-\infty}^{\infty} \int_{-\infty}^{\infty} C(\hat{a},a)\ p(\bar{R},a)\ da d\bar{R}. \tag{2.4}$$

The Bayes estimation procedure is that procedure which minimizes the average risk R_a. Then, for the cost in Equation (2.2), the average risk is

$$R_a(a) = \int_{-\infty}^{\infty} \int_{-\infty}^{\infty} [\hat{a}\ (\bar{R})-a]^2\ p(a,\bar{R})\ da d\bar{R} \tag{2.5}$$

From basic mathematical statistics, [16],

$$p(a,\bar{R}) = p(a|\bar{R})\ p(\bar{R}). \tag{2.6}$$

Equation (2.5) then reduces to

$$R_a(a) = \int\left\{\int [\hat{a}(\bar{R})-a]^2\ p(a|\bar{R})\ da\right\} p(\bar{R}) d\bar{R}\ . \tag{2.7}$$

This function will henceforth be denoted as $R_{ms}(a)$, the mean square cost. Since the function in braces is clearly non-negative, we may minimize $R_{ms}(a)$ by minimizing the inner integral. Find the minimum of the inner integral by differentiating with respect to $a(\bar{R})$ and setting the result equal to zero.

$$\frac{d}{da} \int_{-\infty}^{\infty} [\hat{a}(\bar{R})-a]^2\ p\ (a|\bar{R})\ da \tag{2.8}$$

$$= -2 \int_{-\infty}^{\infty} ap(a|\bar{R})da + 2\hat{a}(\bar{R}) \int_{-\infty}^{\infty} p(a|\bar{R})\ da\ .$$

The second integral is obviously equal to 1 we then have

$$\hat{a}_{ms}(\bar{R}) = \int_{-\infty}^{\infty} ap(a|\bar{R})\, da \quad , \tag{2.9}$$

where $\hat{a}_{ms}(R)$ is the estimate which minimizes $R_{ms}(a)$. This term is the mean of the a posteriori density. Similar results may be found for other cost functions. A general extension of Equation (2.9) occurs for the cost function

$$c(\hat{a},a) = f(a)\ (\hat{a}-a)^2. \tag{2.10}$$

The Bayes estimate is [29],

$$\hat{a}(\bar{R}) = \frac{\int_{-\infty}^{\infty} a\ f(a)\ p\ (a|\bar{R})\ da}{\int_{-\infty}^{\infty} f(a)\ p\ (a|\bar{R})\ da} . \tag{2.11}$$

The Bayes estimate of the absolute value criterion in Figure 2.2a is the minimum of

$$R_{abs} = \int_{-\infty}^{\infty} [\,|a-a(\bar{R})|\,]\ p(a|R)p(\bar{R})\ dR\ da. \tag{2.12}$$

The result of carrying out the calculation is shown in Equation (2.13) [35],

$$\int_{-\infty}^{\hat{a}\,abs(\bar{R})} p(a|\bar{R})da = \int_{a_{abs}(\bar{R})}^{\infty} p(a|\bar{R})\ da\,. \tag{2.13}$$

Hence, the Bayes estimate for an absolute value criterion is the median of the a posteriori density.

Similarly, the uniform cost function shown in Figure 2.2c leads to a Bayes estimate which is the maximum of the a posteriori density [35].

Two properties of the Bayes estimate for a large class of cost functions are presented below without proof. The properties are due to Sherman and are useful in justifying the use of the mean square estimate for general problems for which the exact cost function may lead to unsolvable mathematics [33].

a. Property 1. If the cost function $C(\hat{a},a)$ is a symmetric, convex upward function and its a posteriori density $p(a|\overline{R})$ is symmetrical about its conditional mean, the estimate that minimizes the risk is identical to $\hat{a}_{ms}$. Here $\hat{a}_{ms}$ is the conditional mean.

b. Property 2. In the case where the cost function is a symmetric, nondecreasing function, an a posteriori density $p(a|\overline{R})$ which is symmetrical about the conditional mean, is unimodal, and satisfies the condition

$$\lim_{x\to\infty} c(\hat{a},a)\ p(a|\overline{R}) = 0 \tag{2.14}$$

leads to a best estimate which is again $\hat{a}_{ms}$.

The proof of these two properties is available in the literature [36].

Whenever it is desired to estimate more than one parameter, a straightforward extension of the above presentation is possible. Such a situation occurs in the typical radar situation in which both the range to the target and its velocity must be estimated. We then define the error vector

$$\bar{a}_\varepsilon(\bar{R}) = \begin{bmatrix} \hat{a}_1(\bar{R}) - a_1 \\ \hat{a}_2(\bar{R}) - a_2 \\ \vdots \\ \hat{a}_k(R) - a_k \end{bmatrix} = a(\bar{R}) - \bar{a} \ . \tag{2.15}$$

For the mean square error criterion, the cost function is:

$$C(\bar{a}_\varepsilon(\bar{R})) = \sum_{i=1}^{k} a_{\varepsilon_i}^2 (\bar{R}) \tag{2.16}$$

and the associated risk is then

$$R_{ms} = \int_{-\infty}^{\infty} \int_{-\infty}^{\infty} C(\bar{a}_\varepsilon(\bar{R}))\ p(\bar{R},\bar{A})\ d\bar{R}\ d\bar{A}$$

or

$$R_{ms} = \int_{-\infty}^{\infty} p(\bar{R}) d\bar{R} \int_{-\infty}^{\infty} \left[\sum_{i=1}^{k} (\hat{a}_i(\bar{R}) - A_i)^2 \right] p(\bar{A}|\bar{R})\ d\bar{A} \ . \tag{2.18}$$

It can be seen that to minimize R_{ms}, we may minimize each error term separately. Hence, for the multi-parameter estimation problem, the Bayes criterion may be applied to the parameters on a one-by-one basis.

2.3 Maximum Likelihood Estimation

In situations where the a priori distribution of a is not known, the estimation problem is best treated as the estimation of a non-random parameter. Using the Bayes criterion for this case fails to lead to useful results [35]. Some other measures of the quality of the estimate are therefore considered. The first of these is the expectation of the estimate:

$$E\,[\hat{a}(\overline{R})] = \int_{-\infty}^{\infty} \hat{a}(R)\; p(\overline{R}|a)\; d\overline{R}\;. \tag{2.19}$$

The possible values of the expectation can be grouped into three classes [35].

1. If $E\,[\hat{a}(\overline{R})] = a$, for all values of a the estimate is said to be unbiased.
2. If $E\,[\hat{a}(\overline{R})] = a+\beta$, β independent of a, the estimate is said to contain a fixed bias. It is always possible to obtain an unbiased estimate from such a biased estimate.
3. If $E\,[\hat{a}(\overline{R})] = a + f(a)$, the estimate has an unknown bias. Because the bias depends on the unknown parameter we cannot readily remove its effect from the observation.

The expectation of an estimate is not very satisfactory since it can lead to large errors if the a posteriori density has a large second moment.

A second measure of quality is the variance of estimation error. It seems reasonable to require a good estimate to have a small variance. One commonly used estimate which satisfies this condition is the maximum-likelihood estimate. In this procedure, it is desired to maximize the so-called likelihood function $p(\overline{R}|a)$. This estimate is a good estimate but not necessarily the best estimate possible by all criteria.

One useful form in which this estimate occurs is in terms of the log likelihood function $\ln [p(\overline{R}|a)]$. Since the logarithm is monotonically increasing, maximizing $\ln [p(\overline{R}|a)]$ insures maximization of $p(\overline{R}|a)$. When conditions of differentiability are met, the maximum of $\ln [p(\overline{R}|a)]$ can be found by solving the equation

$$\frac{\partial \{\ln [p(\overline{R}|a)]\}}{\partial a} = 0 . \tag{2.20}$$

This maximum likelihood estimate corresponds mathematically to the limiting case of a maximum a posteriori estimate in which the prior knowledge approaches zero [35].

The Cramer-Rao bound of the variance of any estimate will now be stated without proof [7, 12].

If $\hat{a}(\overline{R})$ is any unbiased estimate of a, then

$$\mathrm{Var}\ [\hat{a}(\overline{R}) - a] \geq \left(E\left\{ \left[\frac{\partial \ln p(\overline{R}\ a)}{\partial a} \right]^2 \right\} \right) \tag{2.21}$$

Or, equivalently:

$$\mathrm{Var}\ [\hat{a}(\overline{R}) - a] \geq \left\{ -E\left[\frac{\partial^2 \ln p(\overline{R}|a)}{\partial a^2} \right] \right\}^1 , \tag{2.22}$$

if the following conditions are assumed to be satisfied:

$$\frac{\partial p\ (\bar{R}|a)}{\partial a} \quad \text{and} \quad \frac{\partial^2 p\ (\bar{R}|a)}{\partial a^2}$$

exist and satisfy basic conditions of integrability.

This bound in essence states that any estimate is limited in its precision by the a posteriori variance. Cramer has shown that the equality holds when $\hat{a}(\bar{R})$ is a sufficient statistic for the estimate of the parameter a [7].

2.4 Signal Parameter Estimation

The above discussion may be extended readily to the estimation of signal parameters. For example, in M-ary digital communications one of a finite number of symbols or message blocks is chosen for transmission. Associated with each of the M messages $m_1, m_2 \ldots m_M$ is a transmitted waveform $s_1(t), s_2(t) \ldots s_M(t)$ (Figure 2.3). These waveforms are corrupted by an additive noise. Initially, we consider all channel noise as white Gaussian noise $n_w(t)$ with power-density spectrum

$$S_n(w) = \frac{N_o}{2} \quad .$$

The received waveform will then take the form

$$r(t) = s_k(t) + n_w(t)$$

when message k has been transmitted. Without loss of generality, this result may be stated as

$$q(t) = s_k(t) + n(t)$$

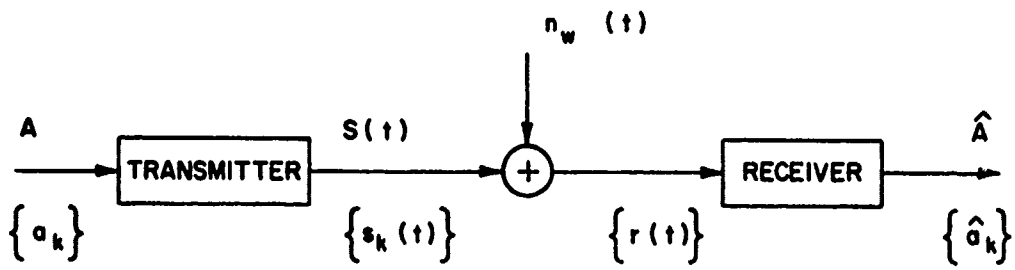

Figure 2.3 The Estimation of Known Signals in the Presence of Additive Noise

where n(t) is the noise component in the signal space. Letting the time functions, n(t) and q(t) be denoted by vectors we then get:

$$\bar{q} = \bar{s} + \bar{r} .$$

The random vector $\bar{r}$ $(r_1, r_2 \ldots . r_m)$ is represented by M independent Gaussian variables, each with zero mean. The variance is $r^2 = \frac{N_o}{2}$. The joint probability density function of vector $\bar{r}$ in such a case has spherical symmetry.

$$f_n(\bar{n}) = \frac{1}{(2\pi\sigma^2)^{M/2}} e^{-|\bar{n}|^2/2\sigma_N^2}$$

$$= \frac{1}{(\pi N_o)^{M/2}} e^{-|\bar{n}|^2/N_o} . \qquad (2.23)$$

The likelihood function $p(\bar{R}|a)$ then becomes

$$p_{\bar{q}}(\bar{q}|m_i) = \frac{1}{(\pi N_o)^{M/2}} e^{|\bar{n}|^2/N_o} \qquad (2.24)$$

However, when a specific message m_i is sent,

$$\bar{q} = \bar{s}_i + \bar{n}$$

and

$$\bar{n} = \bar{q} - \bar{s}_i .$$

Equation (2.24) can then be written as:

$$p_{\bar{q}}(\bar{q}|m_i) = \frac{1}{(\pi N_o)^{M/2}} e^{-|\bar{q} - \bar{s}_i|^2/N_o} .$$

The log likelihood function is given by:

$$\ln\left[p_{\bar{q}}\,(\bar{q}|m_i\right] = \ln\left[\frac{1}{(\pi N_o)^{M/2e}} - \frac{1}{N_o}\,|\bar{q} - \bar{s}_i|^2\right]. \qquad (2.25)$$

It is this function which is to be maximized if the a posteriori probability is to be maximal. The first term on the right in Equation (2.25) is a constant and therefore need not be considered in the maximization. The term $|\bar{q} - \bar{s}_i|^2$ is the square of the vector $\bar{q} - \bar{s}_i$. Hence,

$$|\bar{q} - \bar{s}_i|^2 = \sum_{k=1}^{M} (q_k - s_{i_k})^2 \qquad (2.26)$$

$$= \sum_{k=1}^{M} q_k^{\,2} + \sum_{k=1}^{M} S_{i_k}^{\,2} - 2 \sum_{k=1}^{M} q_k\, S_{i_k}$$

$$= |\bar{q}|^2 + |\bar{S}_i|^2 - 2\,\bar{q}\cdot\bar{S}_i\ ,$$

where $|\bar{S}_i|^2$ is the energy of the signal E_i and

$$\bar{q}\cdot\bar{S}_i = \int_{-\infty}^{\infty} q(t)\, S_i(t)\, dt\ .$$

The signal energy E_i and the terms q^2, N_o are constants in the decision function. It is desired, therefore, to maximize

$$I(g,s) \triangleq -\frac{1}{N_o}\left[|\bar{q}|^2 + E_i - 2\int_{-\infty}^{\infty} q(t)\, S_i(t)\, dt\right].$$

The desired result is then

$$\text{Max } [I(g,s)] \rightarrow \text{Max} \left[\int_{-\infty}^{\infty} q(t)\ S_i(t)\ dt \right], \tag{2.27}$$

where the symbol $\rightarrow$ is used to denote implication.

This result is of the form of a convolution integral,

$$\Phi(\tau) = \int_{-\infty}^{\infty} q(t)\ S_i\ (t + \tau)\ dt.$$

The function $\Phi(\tau)$ has its maximum value at $\tau=0$.

The estimation procedure consists of impressing the received signal on a bank of correlators, one for each of the m signals transmitted, the output of which is sampled so that $\tau = 0$. The decision is made in favor of the signal for which the output is largest. Figure 2.4 summarizes such a parameter estimation scheme for the M-ary digital communication receiver. The parameter to be estimated in this case is which of M possible messages transmitted was received.

It can be seen from Equation (2.26) that this estimation procedure minimizes the square error, hence, corresponds to a Bayes estimate for a square cost function. No assumption as to a priori probabilities for messages m_1, $m_2 \ldots$ m_k has been made.

The presence of a phase reference for such a scheme is a requirement since the output of the various correlators must be sampled at time t such that $\tau = 0$.

$p(\bar{R} \mid a)$; LIKELIHOOD FUNCTION

$\Downarrow$ MAXIMIZE

MINIMUM VARIANCE ESTIMATE

$\Downarrow$

FOR ADDITIVE GAUSSIAN NOISE
IS EQUIVALENT TO:

$\Downarrow$

BAYES ESTIMATE WITH NO PRIOR KNOWLEDGE
$C(\hat{a}, a) = (\hat{a} - a)^2$

$\Downarrow$

$$\phi(\tau)_{qs_i} = \int_{-\infty}^{\infty} g(t)\, s_i(t+\tau)\, dt$$

$\Downarrow$

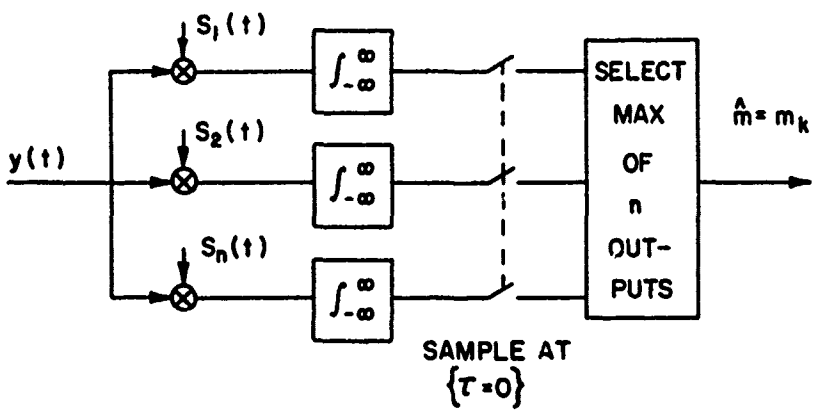

Figure 2.4 Summary of Maximum Likelihood Estimation

In practice, each message exists only for a finite duration of time T. The message may be preceded or followed by another. A specific message, however, is defined only for some finite time interval; hence, the limits of integration on the convolution integral may be changed so that

$$\Phi(\tau) = \int_{-T}^{-T} q(t)\, s_i(t - \tau)\, dt. \tag{2.28}$$

2.5 The General Radar Problem

In the radar estimation problem, a number of parameters may be estimated. Confining the discussion to estimation of echo delay time (t_o) and target velocity dependent echo frequency shift (ν), a similarity to the above estimation problem can be seen.

Define the signal as

$$S(t) = a(t) \cos [w_o t - \Phi(t)] \tag{2.29}$$

where $w_o = 2\pi fo$ and fo represents the carrier frequency,

$a(t)$ = the amplitude function with time t, and

$\Phi(t)$ = the phase function with time.

Going over to complex notation, we may write

$$S(t) = \mathrm{Re}\ \{\psi(t)\}\ , \tag{2.30}$$

the real part of a complex function defined as follows:

$$\psi(t) = a(t)\, e^{i[w_o t - \Phi(t)]}\ .$$

The signal $\psi(t)$ is transmitted and the received signal may be written as

$$\psi(t - t_o) ,$$

where $t = 0$ is the time origin of the transmission and t_o the round trip delay time. The observed receiver input can then be written as

$$\psi(t - t_o - \tau) ,$$

where τ is the time difference between the round trip delay time t_o and the observation time.

To estimate t_o, we must contrive a means of detecting the instant when $\tau = 0$.

If the target from which the echo is received is in motion, the reflected signal will be shifted in frequency by the doppler shift frequency f_d given by

$$f_d = \frac{2v\ fo}{c} , \quad v = f_d - f_o , \tag{2.31}$$

where f_o = the transmitted frequency,

v = radial component of target velocity, and

c = velocity of propagation in the medium.

The received signal will therefore be one of an infinite set of signals corresponding to all allowed radial target velocities.

To estimate ν, the target velocity dependent echo frequency shift, or f_d, the doppler dependent frequency, using a maximum likelihood procedure requires that the echo signal be impressed on an

infinite number of correlators, each corresponding to a different target radial velocity. In practice this impossible situation is approximated by correlators corresponding to specific velocities or by uniformly spaced frequency shifted references.

CHAPTER III

AMBIGUITY AND RESOLUTION

3.1 Noise Free Resolution

In Chapter II, it was demonstrated how an application of estimation criterion leads to a receiver which incorporates a convolution principle, a correlator. This result could equivalently have been expressed in terms of a matched filter receiver [21]. In the absence of channel and receiver noise, the response of the receiver to a signal can be completely described in terms of the correlation function.

Referring to the previous discussion of M-ary communications, it can be seen that two distinct situations occur. The first of these is the case for which

$$q_k = s_k + n_w(t) = s_k$$

and

$$\phi(\tau)_{q_k s_i} = \int_{-\infty}^{\infty} s_k(t)\, s_i(t-\tau)\, dt,$$

for $i = k$.

This result is in the form of an autocorrelation function

$$\phi(\tau)_{ii} = \int_{-\infty}^{\infty} s_i(t)\, s_i(t-\tau)\, dt. \tag{3.1}$$

Some properties of the autocorrelation function are stated below from the literature [21, 22, 28]. These properties are of value in the formulation of estimation schemes.

a. The autocorrelation function is an even function. That is,

$$\phi(\tau)_{ii} = \phi(-\tau)_{ii} \tag{3.2}$$

b. Its value at the origin is the maximum value in magnitude.

$$\phi(0)_{ii} > |\phi(\tau)_{ii}|, \quad \text{for } \tau \neq 0 . \tag{3.3}$$

c. Its first derivative is expressed as

$$\phi'(\tau)_{ii} = \int_{-\infty}^{\infty} s_i(t)\, s_i'(t-\tau)\, dt. \tag{3.4}$$

In the unmatched case,

$$\phi(\tau)_{q_k s_i} = \int_{-\infty}^{\infty} s_k(t)\, s_i(t-\tau)\, dt, \tag{3.5}$$

where $i \neq k$.

This a correlation between two signal waveforms which are assumed not identical. When the M messages are selected to be orthogonal, all unmatched correlations will result in zero mean receiver output and the output of the matched correlator will be clearly distinguished. The result presented in Equation (2.27) insures, however, that all cross correlation outputs will be less than that for the matched correlator for any choice of signals. This result agrees with the description of a correlation in terms of "closeness of fit."

The consequence of these observations for a noise free receiver is that there is no ambiguity in the estimation. If, for example, the phase is not known, the maximum output of the receiver will occur at time such that $\tau = 0$ on the correlator which is matched to the transmitted waveform. In estimating the time of arrival in the absence of noise the resolution is determined solely by limitations due to measurement errors. This result is a direct consequence of the second property of the autocorrelation function; the zero time delay response corresponds to the maximum value of output.

3.2 Noise Effects

The estimation problem as stated includes an additive noise which for the linear estimator proposed remains as an additive effect on the output of the correlators. The correlator outputs will all exhibit time dependent random fluctuations about the response anticipated and the decision process will yield an uncertain result. Properties of the estimation scheme presented so far only insure that the most likely decision will be in favor of zero time delay and the correlator matched to the transmitted message.

It follows directly that members of the message space (m_1, $m_2 \ldots m_k$) which are similar to one another in the sense of correlation integral will be difficult to distinguish in the presence of noise.

Similarly, if the time delay is to be estimated, waveforms for which secondary maxima of the autocorrelation function approach the peak value of this function will result in poor resolution of t.

An extensive effort has been devoted to finding signal sets which satisfy various criteria of resolvability [19, 23, 30, 39]. Many factors must be considered in the selection of such signal sets, not the least of which is the feasibility of implementation.

3.3 Echo Delay Resolution in Radar

It is possible to define a number of measures of range resolution and the one which is chosen here is the delay resolution constant [3]. This constant is:

$$\Delta\tau = \frac{1}{2\,W_e}\,, \tag{3.6}$$

where W_e is the effective bandwidth.

This measure does not depend either on the transmitted pulse length or specific signal characteristics. A long duration pulse can have large bandwidth if the signal has rapid and/or irregular changes in its structure.

3.4 Velocity Resolution in Radar

Define the frequency function

$$\psi(f) = F[\psi(t)]\,,$$

where $F[\psi(t)]$ is the Fourier transform of the complex time function for which

$$S(t) = \mathrm{Re}\{\psi(t)\}\,.$$

For a doppler frequency f_d described in Chapter II as

$$f_d = \frac{2vf_o}{c}\,,$$

the received spectrum may be represented as

$$\psi(f_o - f_d) = \psi(\nu) \ .$$

This formulation leads to a velocity resolution constant of

$$\Delta v = \frac{c}{2 f_o T_e} ,$$

where T_e is the effective duration of the transmitted signal [3]. Again the resolution measure is not dependent on the detailed structure of the signal but rather on the generalized form of T_e.

A surface described by the absolute value noise free correlator output for all values of echo delay and doppler frequencies is often referred to as the uncertainty surface for such an estimation scheme.

Throughout this thesis, the absolute value of the noise free correlator output $|Y(\tau,\nu)|$ will be referred to as the uncertainty surface in keeping with the notation of Woodward [39]. This is to distinguish from the square of this response

$$|Y(\tau,\nu)|^2$$

which is known as the ambiguity function.

Some representative uncertainty surfaces for common signals are shown in Figure 3.1.

It will be shown in subsequent chapters that the attainable resolution, in contrast to the above resolution constants, is a function of the strength of the received signal in relation to noise and depends on the type of processing of the data. The resolution constants $\Delta\tau$, Δv are useful, however, in determining how near one

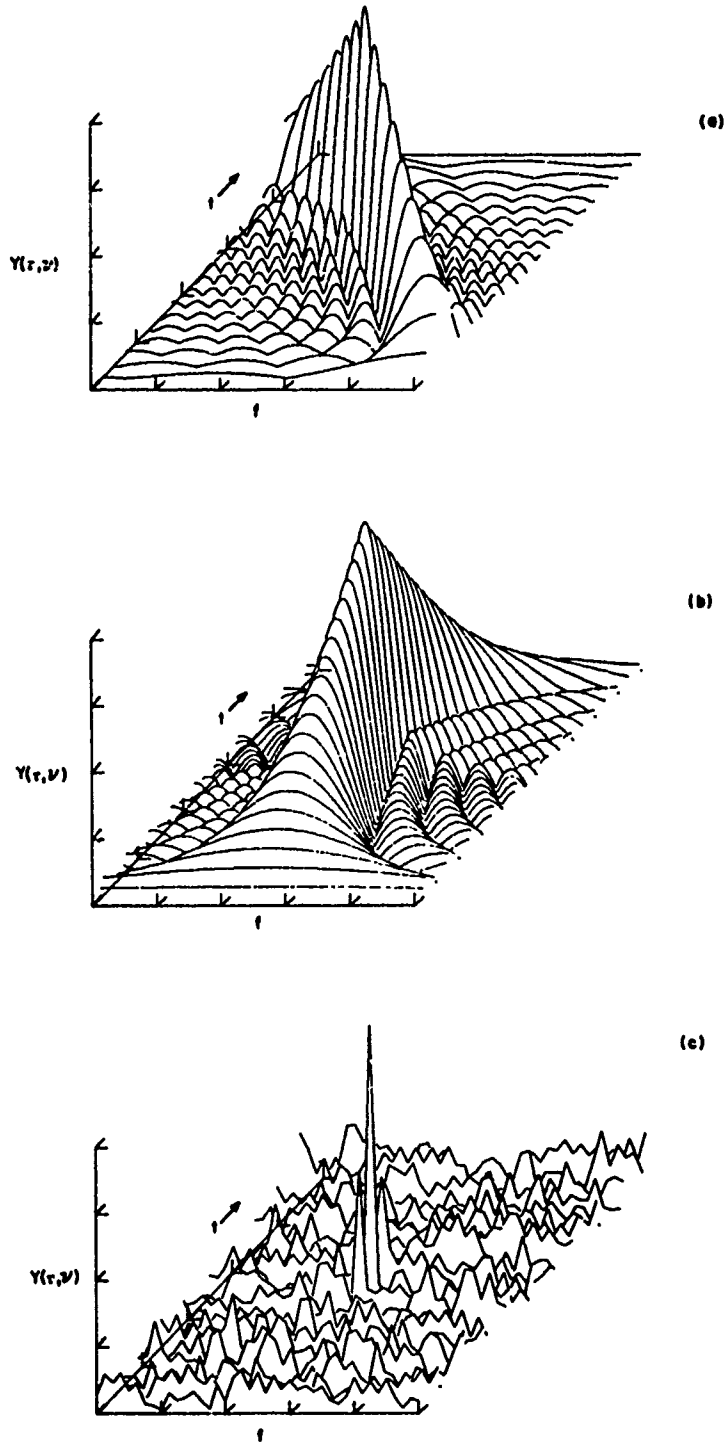

Figure 3.1 Uncertainty Surfaces for Representative Signals. (a) Linear Swept Chirp Pulse With Rectangular Envelope (b) Monochrome Pulse With Rectangular Envelope (c) "Noise" Waveform.

another two signals can be in time delay and velocity dependent frequency and still be distinguishable to a maximum likelihood receiver.

CHAPTER IV

DIGITAL SYSTEMS

4.1 The Generalized Decision Process

The required structure of a maximum likelihood receiver has been developed from fundamental estimation criteria. Recalling the receiver, we note that the major system components are as indicated below:

a. Correlators for each possible transmitted waveform or an approximation to this when an infinite number of echo frequencies can occur.

b. A decision making system which chooses the largest from among the correlator outputs. In the absence of a phase reference, the decision must be made in terms of the largest correlator output within an allowed time or phase interval.

If digital systems are to be used for any part of the receiver, one may ask which of these two components is amenable to such an implementation. A considerable amount of work has been devoted to using digital schemes for accomplishing the correlation. Some concepts reported in the literature are:

a. Sign correlators in which both the received signal and reference signals are represented in terms of two state samples [2].

b. Digital multipliers in which both the received signal and reference signals are quantized and represented by multi-state digital words [38]. A discussion of this type of system appears in Appendix A.

c. Fast Fourier transform algorithms applied to sampled and quantized received signals [6].

d. Matched filter techniques using digital filters in conjunction with sampled and quantized inputs [37].

Alternately the output of analog correlators may be sampled and quantized. In either case, the output of the correlator bank will exist in some digital form which can then be input to a digital decision process. In some cases, the digital result is converted again to analog form for further processing, but this exposition will concentrate on those systems in which the decision making function is digital in nature. Specifically, decision algorithms implemented on a general purpose computer are treated.

The input to the decision algorithm is of necessity a sampled, quantized representation of the output of each correlator. For systems with known time origin the samples correspond to that time for which $\tau = 0$. Otherwise, it will be necessary to provide the algorithm with sufficient data points from each correlator output so that the decision as to maximum correlation within an allowed time span can be made. For generality, the system without a time reference will be

treated in what follows and the result can be easily seen to apply for systems with such a time reference.

The decision process can then be summarized as:

> From the totality of sample points which define the correlator output select the one for which the value of correlation is maximum. Report the corresponding value of $\hat{\tau}$ as the echo delay time estimate and $\hat{\nu}$ as the estimate of target doppler dependent frequency shift.

Additional complicating factors occur in the radar case since it is possible to have a multitude of echoes in the total receive interval. The effect of an ill-defined time origin for a specific echo as well as interactions between closely spaced events must be accounted for in a practical system.

The situation is similarly complicated in certain communications applications where multi-path propagation or distributed scatterers are involved.

4.2 Single Monochromatic Carrier Band Pulse, Rectangular Envelope

Consider as an example of a radar application a system which transmits a single monochromatic pulse with rectangular envelope of duration T.

The transmitted signal will then be:

$$S(t) = \cos 2\pi f_o t \qquad 0 < t < T \qquad (4.1)$$
$$= 0 \qquad \text{otherwise,}$$

or

$$\psi(t) = e^{j\omega_o t} ,$$

where $\omega_o = 2\pi f_o$, and f_o the carrier frequency.

The delayed, doppler shifted echo signal is then

$$\psi'(t-\tau) = e^{j2\pi(f_o-\nu)(t-\tau)} ,$$

where ν is the doppler frequency shift and τ the delay t_o-t. Here t_o is the true echo delay time.

As a measure of the "distance" between the waveforms, consider the integrated square of the magnitude of the difference in accordance with Urkowitz [3]:

$$\begin{aligned}
\varepsilon^2 &= \int_{-\infty}^{\infty} \left|\psi(t) - \psi'(t-\tau)\right|^2 dt \\
&= 2 \int_{-\infty}^{\infty} \left| \psi(t)\right|^2 dt - 2\,\mathrm{Re}\int \psi^*(t)\psi'(t-\tau)\, dt \\
&= 2 \int_{-\infty}^{\infty} \left| u(t)\right|^2 dt \\
&\quad -2\,\mathrm{Re}\left\{ e^{j2\pi(f_o-\nu)\tau} \int_{-\infty}^{\infty} u(t)\, u^*(t-\tau)\, e^{j2\pi\nu t}\, dt \right\}. \qquad (4.2)
\end{aligned}$$

To minimize the difference for $\tau \neq 0$ it suffices to minimize the magnitude of the last term. The integral in the last term is defined as the combined correlation function:

$$\begin{aligned}
Y(\tau,\nu) &= \int_{-\infty}^{\infty} u(t)\, u^*(t-\tau)\, e^{j2\pi\nu}\, dt, \quad |\tau| < T \qquad (4.3) \\
&= 0 \qquad \text{otherwise} ,
\end{aligned}$$

For the monochrome pulse,

$$u(t) = 1 , \quad 0 < t < T$$
$$= 0 \quad \text{otherwise}$$

hence

$$Y(\tau,\nu) = \frac{\sin \pi\nu T \left(1 - \frac{|\tau|}{T}\right)}{\pi\nu}, \quad |\tau| < T$$

and

$$|Y(\tau,\nu)| = \left|\frac{\sin \pi\nu T \left(1 - \frac{|\tau|}{T}\right)}{\pi\nu}\right|, \quad |\tau| < T , \quad (4.4)$$

where Equation (4.4) is the uncertainty function. Note that, in going from Equation (4.2) to Equation (4.3), the rapid fluctuations due to the carrier are rejected. A plot of $|Y(\tau,\nu)|$ is shown in Figure 4.1.

A physical realization of a receiver for a carrier band signal is shown in Figure 4.2. The input to the digital decision algorithm consists of sampled values of correlation output. There is a sample for each target doppler dependent frequency reference for each echo delay interval. The inputs to the digitizer arrive in the order:

$$X(\tau_1,\nu_1), X(\tau_1,\nu_2),\ldots X(\tau_1,\nu_m),\ldots X(\tau_2,\nu_1),\ldots X(\tau_n,\nu_m),$$

where

$X(\tau_i,\nu_j) = |Y(\tau_i,\nu_i) + n_i|$, and n_i the noise component at τ_i.

The effect of the digitizer is to represent the value of analog voltage in terms of a finite number of binary digits. The binary digits which represent a specific value of $X(\tau,\nu)$ comprise a digital datum which is subject to manipulation in a programmed automaton. The process of quantization is shown pictorially in Figure 4.3. All values

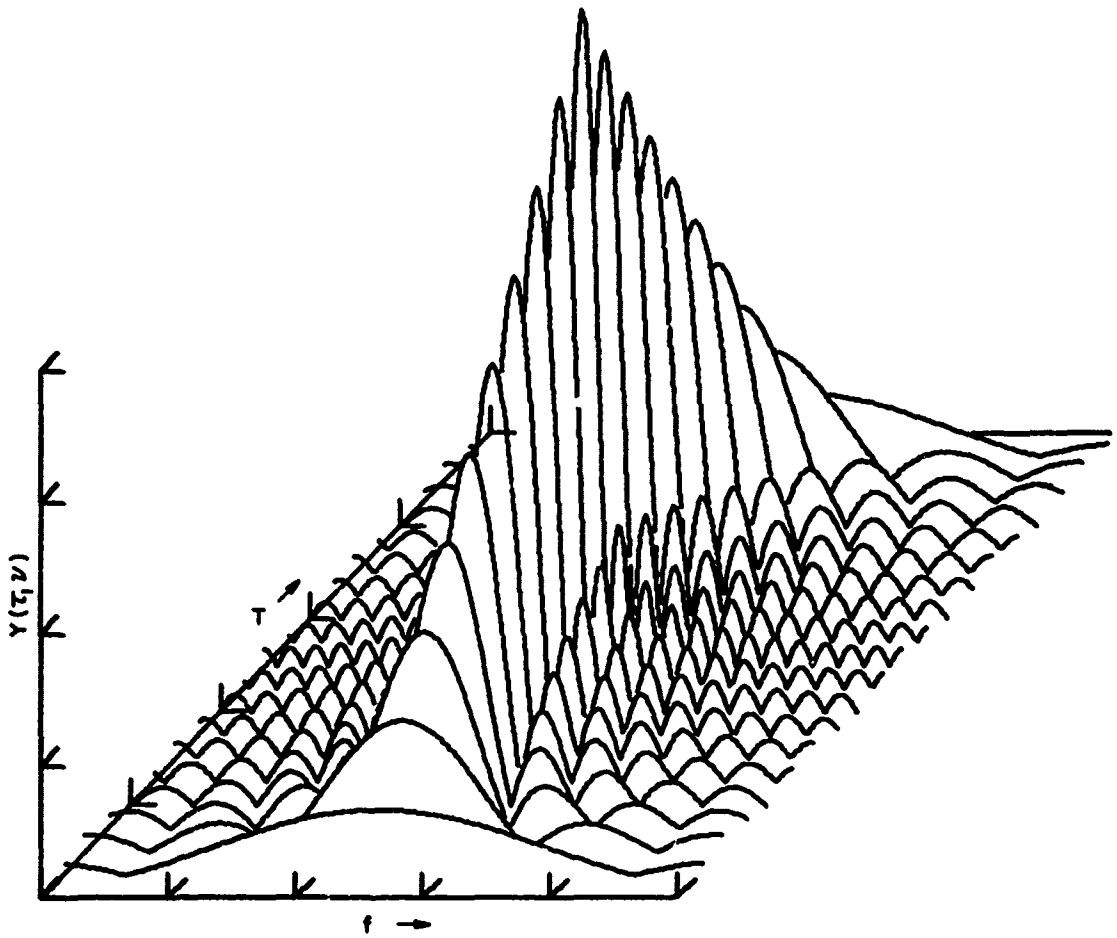

Figure 4.1 Uncertainty Surface for Monochrome Pulse of Duration T Rectangular Envelope

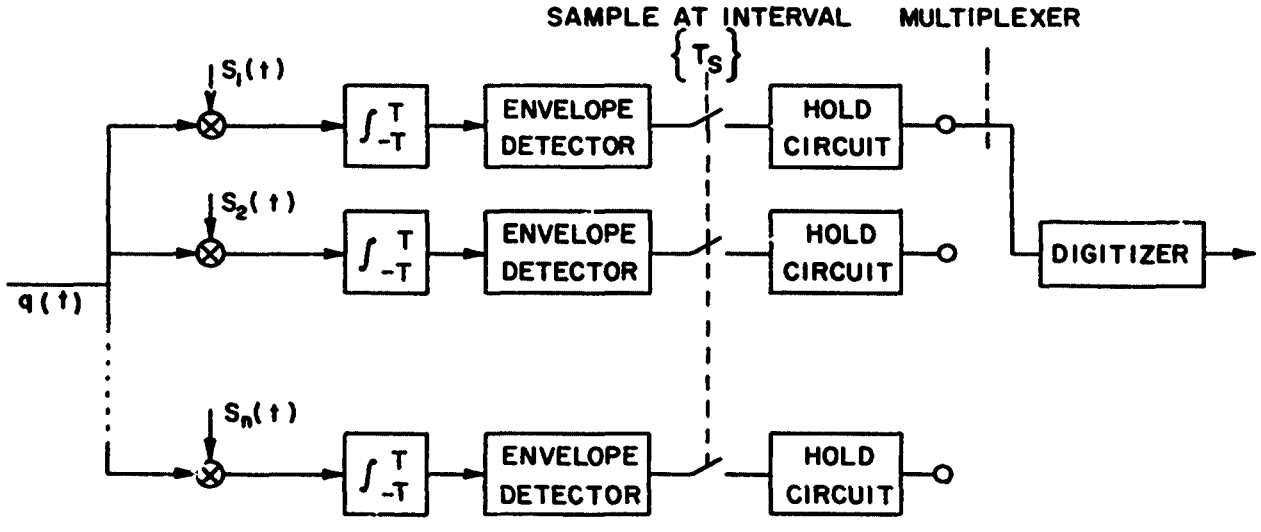

Figure 4.2 Maximum Likelihood Estimator, Carrier Band Signal

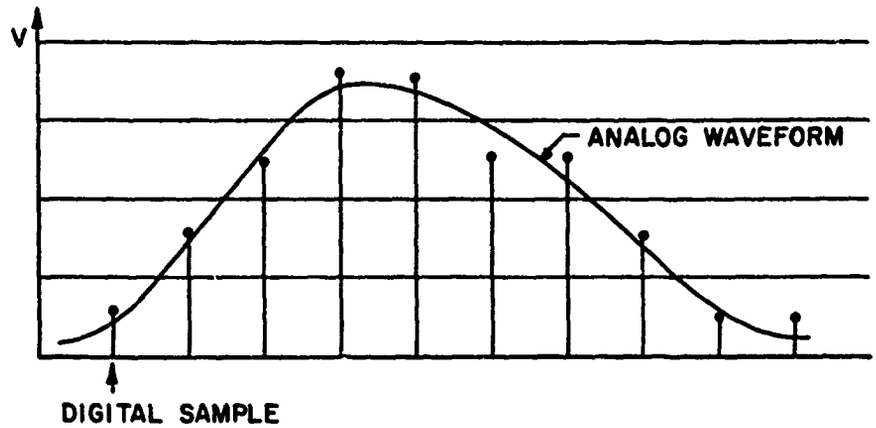

Figure 4.3 Quantization of an Analog Waveform

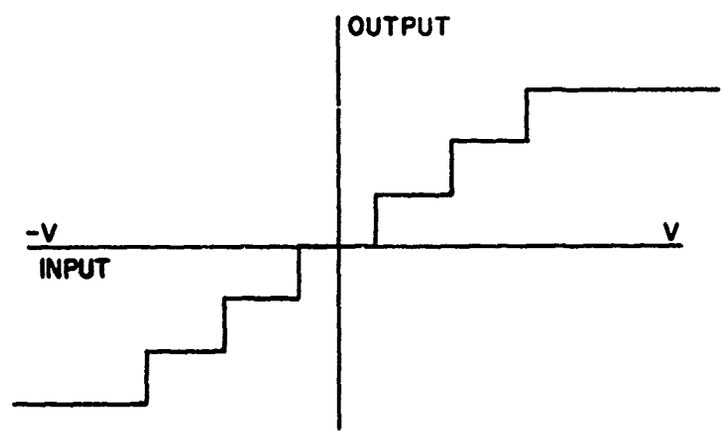

Figure 4.4 Input-Output Characteristics of a Quantizer

of the analog waveform which are within a resolution interval of one another will map into an identical binary representation. Typical input-output characteristics of a quantizer is shown in Figure 4.4.

The selection of number of correlators and the sampling rate of the correlator output time function is determined by operational requirements. As previously detailed, there is no theoretical limit on the resolution possible in the absence of noise other than that imposed by system limitations. As the resolution is increased, however, the number of samples $X(\tau,\nu)$ presented to the digitizer per unit time increases correspondingly. Furthermore, the number of binary digits required to represent the sample increases.

As an example of this latter situation, we note from Figure 4.1 that the uncertainty function of the monotone pulse is a monotonically decreasing function in the vicinity of the peak $X(0,0)$ with both τ and ν.

Substituting $\nu = 0$ in Equation (4.4), we get

$$|Y(\tau, 0)| = |- \frac{|\tau|}{T} . \tag{4.5}$$

For a sample interval such that samples are spaced T_s, the percentage of difference between noise free samples is:

$$||Y(\tau,0)| - |Y(\tau-T_s,0)|| = \frac{T_s}{T} . \tag{4.6}$$

A digital representation of $X(\tau,0)$ must therefore contain a sufficient number of binary digits, so that

$$a(i + 1) - a(i) \leq \frac{T_s}{T}, \tag{4.7}$$

where $a(i + 1)$ and $a(i)$ are digital states.[1]

Similar arguments can be applied to the correlator spacing for doppler dependent frequency. The sampling theorem according to Hartley, Gabor, and Shannon, however, states that any signal essentially limited to an interval of time T and a bandwidth W contains 2WT degrees of freedom [20]. There exist 2WT samples of the signal waveform which contain all of the information of the original signal. This fact places an upper bound on the number of samples required in a receiver of finite bandwidth.

The development in Section 3.1 demonstrated that the maximum a posteriori probability always occurs at $\tau = 0$ on the correlator matched to the doppler dependent frequency. With a maximum likelihood receiver, one can do no better than to select as the estimate of frequency the one corresponding to the maximum $X(\tau_i,\nu_i)$. Figure 4.5 shows the effect of added noise on the correlator output. It can be seen that the noise introduces uncertainty into the measurement of $X(\tau,\nu)$ with the result that, for large values of noise power in relation to signal power, the observation of the maximum $X(\tau_i, \nu_i)$ leads to a poor estimate of the parameters τ and ν .

The discussion thus far has ignored the fact that the signal energy at the receiver is unknown. This omission in no way alters the

[1]The interval need not be uniform. Here, we will assume that values of $X(\tau,\nu)$ are uniformly distributed $(X;\ 0 < x < 1)$. For this case, it can be shown that, for optimum operation in a mean square sense, the quantization steps should be uniform [27].

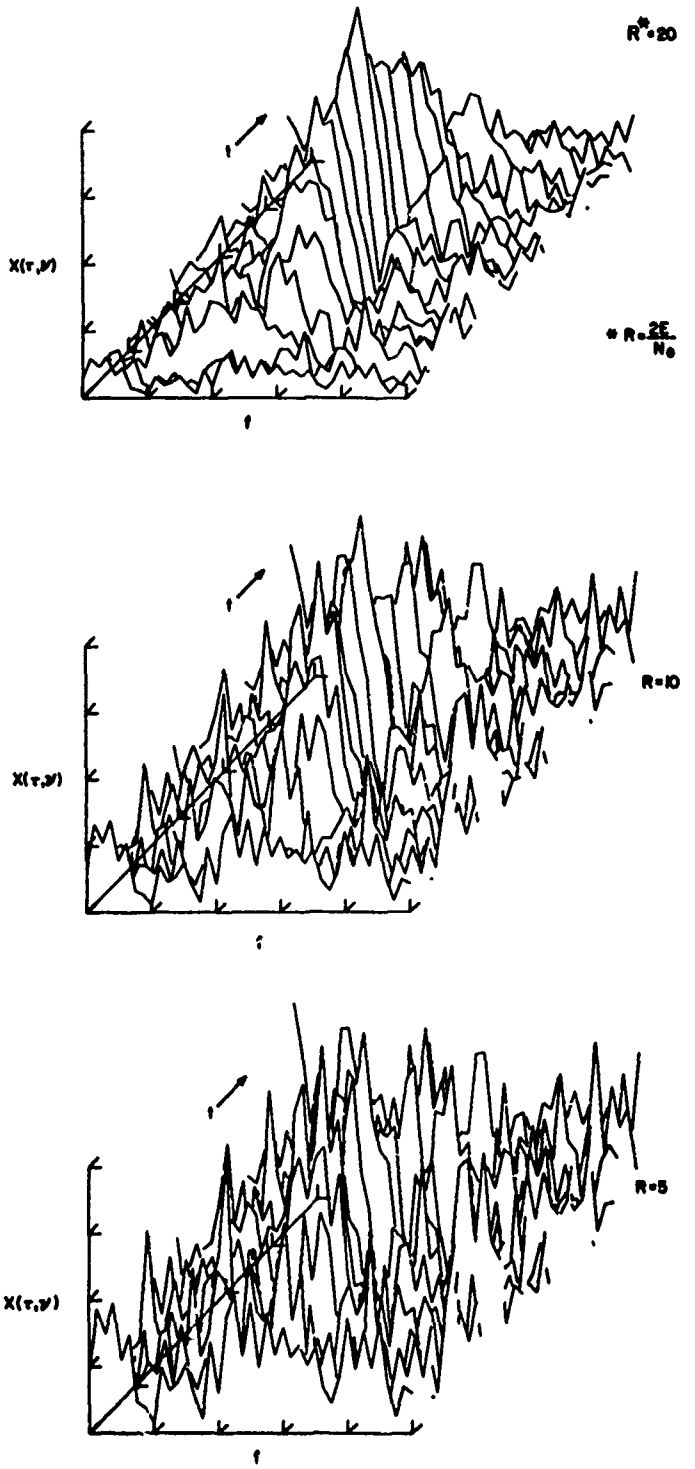

Figure 4.5 Typical Monochrome Signal Correlator Response Showing the Effect of Noise

decision rule as can be seen by noting Equation (2.27). It will be shown later that the value of signal energy is important in determining the accuracy of the estimate, however. The ratio of signal energy to noise energy at the receiver will be a function of range dependent signal attenuation, medium characteristics, target strength to list the major factors.

4.3 The Effect of Continuous Observation

In the foregoing treatment, the transition from the theoretical form of the correlation operation

$$\phi(\tau)_{q_k s_i} = \int_{-\infty}^{\infty} s_k(t)\, s_i(t-\tau)\, dt \tag{4.8}$$

to the practical form

$$\phi(\tau)_{q_k s_i} = \int_{-T}^{T} s_k(t)\, s_i\,(t-\tau)\, dt \quad |\tau| < T$$

$$= 0 \qquad\qquad |\tau| > T$$

for a signal of duration T has been made without conceptual difficulty. The implication, however, is that we have prior knowledge of the interval of echo delay during which the signal is to occur. In many practical systems, however, this knowledge is denied the observer.

In a typical application, τ will take on a range of values determined by system design. The theory insures that for all of these values of τ, the peak a posteriori probability will still occur when $\tau = 0$. Considering the majority of applications, it is found that the ideal situation of a single echo in the total listen period is unusual. Generally other echoes are observed from ground clutter, other aircraft,

etc. Each of these echoes leads to a system response where $|\tau - t_i| < T$, where t_i is the echo delay time associated with target i. Figure 4.6 shows a receiver response to a two target case when the frequency is matched to the correlator.

For the multiple echo case, we will wish to note the peak in some time interval 2T. The problem then is one of knowing the origin of the time interval. Figure 4.7 shows the effect of impressing a threshold on the correlator output. It can be seen that those samples surpassing the threshold roughly define the time interval for which $\tau < T$. The threshold must be selected high enough to avoid very many noise related correlator outputs which appear as false targets. The process of thresholding can be done either by analog means or in the digital processing. By assuming that the noise is stationary, the threshold reduces to a time invariant one.

Thresholding may also be used to reduce the number of samples presented to the digitizer. Since only samples which surpass the threshold are transferred to the digital processing, a means must be included to identify the datum in time and doppler frequency.

In many radar applications, no prior certainty as to the presence of a target exists. The effect of a threshold then is to preclude noise events surpassing the threshold value. The process of estimation is intimately tied to that of detection in such a system. And, no matter how the threshold value is chosen there will be some cases for which a noise event is classified as a target, or a target is overlooked. In analogy to detection theory, the threshold is so chosen

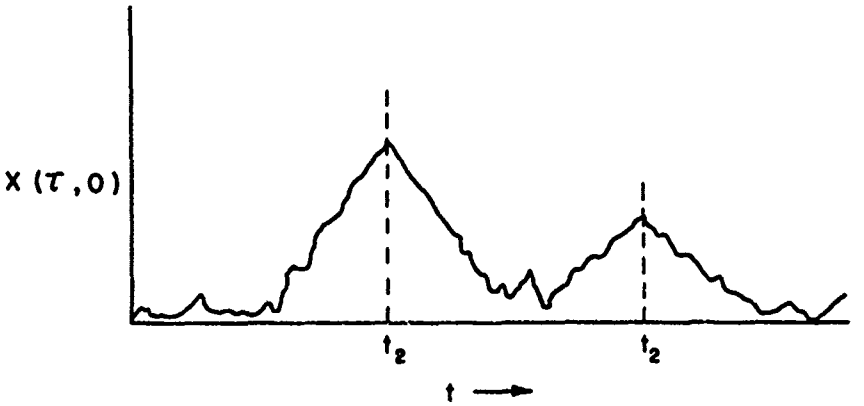

Figure 4.6 Maximum Likelihood Receiver Time Response for a Multiple Target Situation

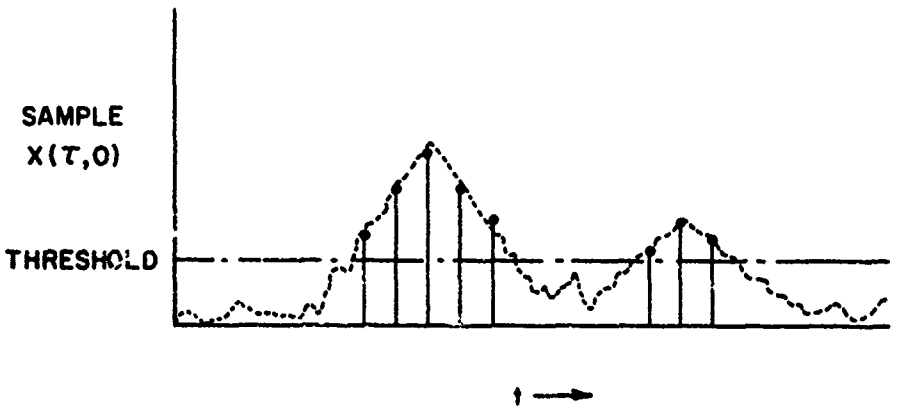

Figure 4.7 Samples for a Multiple Target Situation, for Thresholded Analog Output

as to give maximum performance against a target with a false alarm rate in keeping with system objectives.

The peak value of the uncertainty function in the absence of noise is proportional to the echo energy. This can be seen when $\tau = 0$ is substituted in Equation (4.8) when the echo is matched to a signal replica. The amplitude of the peak can be used as a rough measure of the strength of an echo for this reason. It is a rough measure since it reduces to the limit of no relationship to echo strength when the peak is of noise origin solely. In referring to Figure 4.7, it can be seen that the time duration over which the uncertainty function exceeds the threshold is determined by the peak value of the matched correlator output.

4.4 Linear Swept F-M Pulse of Duration T

In some situations which will be described shortly, it is advantageous to transmit a signal for which the frequency varies linearly over the pulse duration. The complex modulation function for this signal is

$$u(t) = e^{jBt^2}, \quad 0 < t < T \qquad (4.9)$$
$$= 0 \qquad \text{elsewhere},$$

B is measured in radians/sec^2. It can be seen that

$$u(t)\, u^*(t-\tau) = 0 \quad \text{for } |\tau| > T. \qquad (4.10)$$

Then, from Equation (4.2) write

$$Y(\tau,\nu) = \int_{\tau}^{T} e^{-jBt^2} e^{jB(t-\tau)^2} e^{j2\pi\nu t} \, dt$$

$$= \int_{\tau}^{T} e^{j[-Bt^2 + B(t-\tau)^2 + 2\pi\nu t]} \, dt$$

$$= e^{jB\tau^2} \int_{\tau}^{T} e^{-2j[B\tau-\pi\nu]t} \, dt$$

$$= \frac{e^{jB\tau^2}}{2j(B\tau-\pi\nu)} \left[e^{-2j(B\tau-\pi\nu)+} - e^{-2j(B\tau-\pi\nu)\tau}\right].$$

Expressing the exponentials in terms of cos (·) + j sin (·) and obtaining the squared magnitude, the result is

$$|Y(\tau,\nu)| = \left|\frac{\sin(B\tau-\pi\nu)(1 - \frac{|\tau|}{T})\,T}{B\tau-\pi\nu}\right| \left(1-\frac{|\tau|}{T}\right), \quad |\tau| < T. \tag{4.11}$$

This function is plotted in Figure 4.8 for a signal for which $B = T/\text{sec.}^2$ The "ridgeline" defining the peak response as a function of time defines approximately a straight line in the time/frequency domain. The details of this ridgeline response are given in Appendix B.

Considering only that portion of the uncertainty surface which exceeds a value half the peak value,

$$|Y(\tau,\nu)| \geq .5A,$$

where A is the peak value, it is possible to obtain an insight into the resolution of such a signal. In Figure 4.9, the values of $|Y(\tau,\nu)|$ satisfying this criterion are shown projected onto the time/frequency plane.

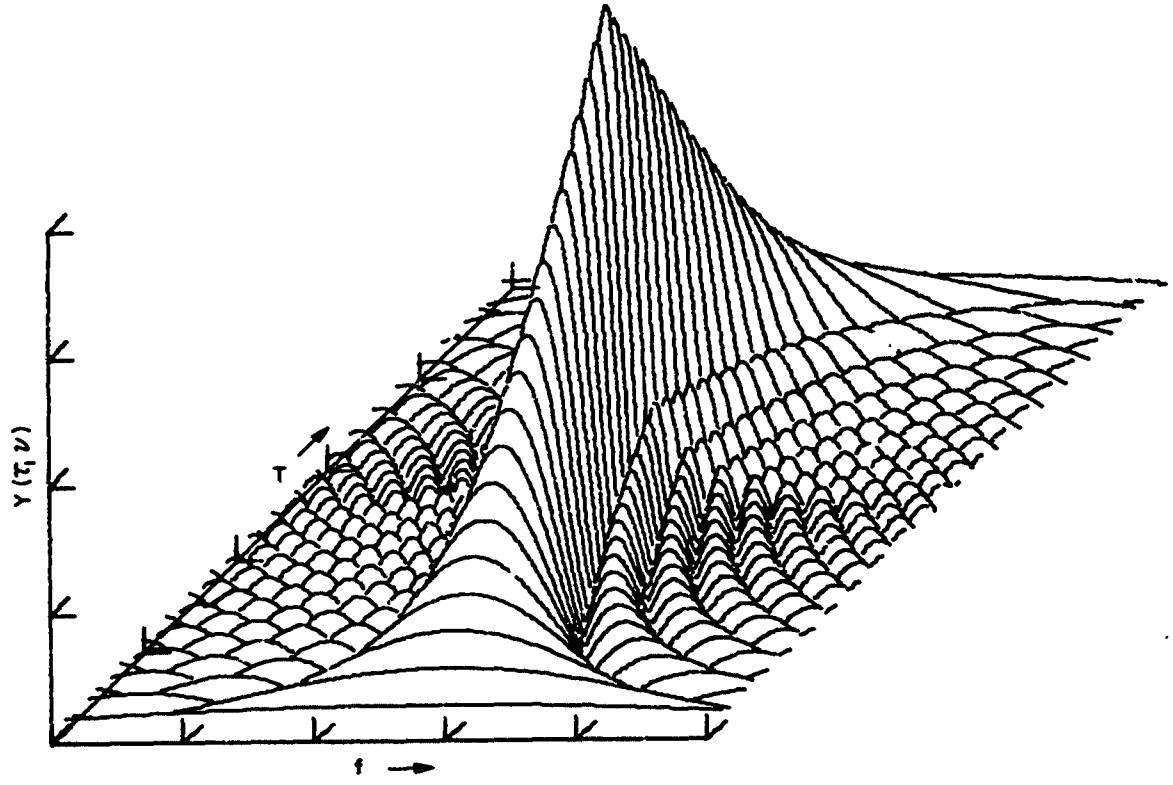

Figure 4.8 Uncertainty Function of Linear F-M Pulse

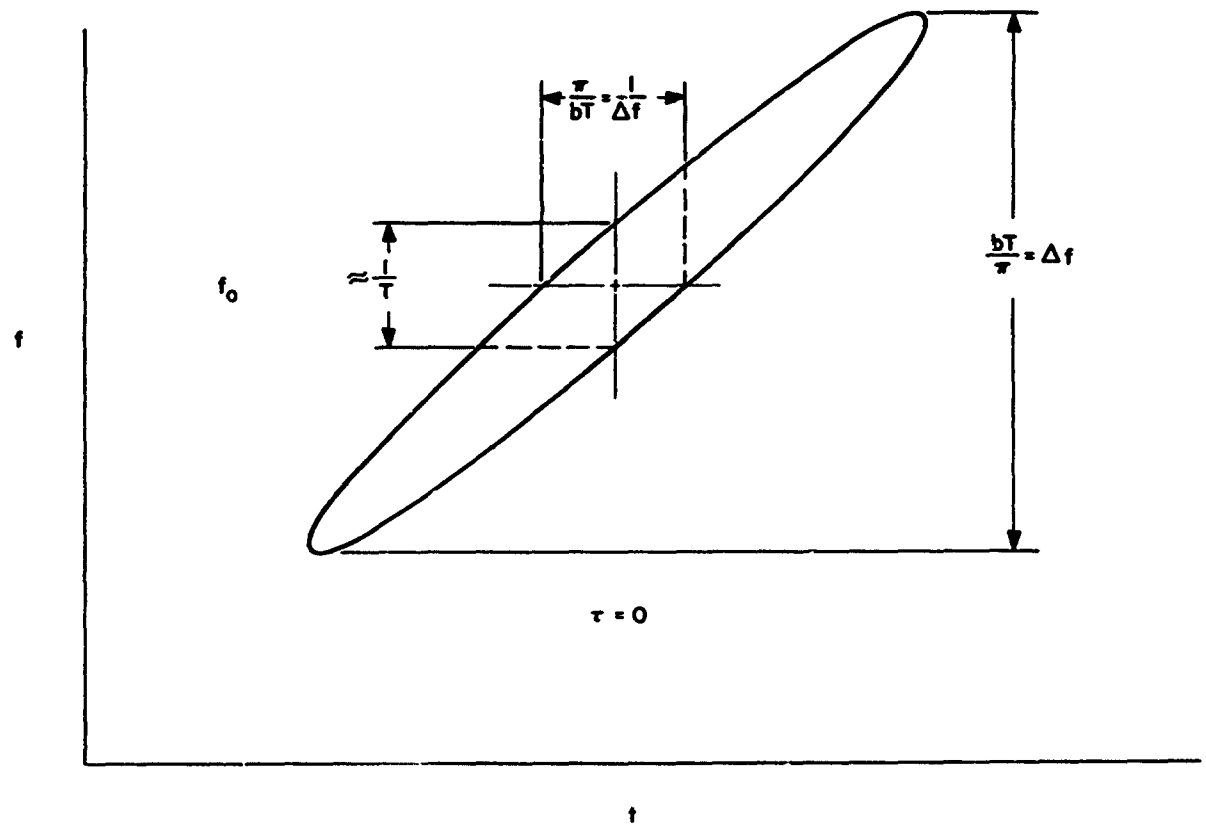

Figure 4.9 Uncertainty Region of Linear F-M Pulse of Duration T

It can be seen from this figure that it is possible to attain good resolution in time in spite of a long pulse by choice of sweep rate. This is an important property of this type of signal since it is often advantageous to transmit a long pulse and thereby a large amount of energy. The problem of resolving targets lying along the ridgeline is a difficult one, however. Also, the combined resolution of time delay and frequency is limited and the maximum time resolution is dependent on independent knowledge of target velocity.

CHAPTER V

ESTIMATION ALGORITHMS

5.1 Introduction

In Chapter III and Chapter IV the theory and response characteristics of a maximum likelihood estimator were developed. The nature of the decision process necessary to implement such an estimator in a digital system was presented. In this chapter, the logic functions previously stated are expanded in the form of algorithms to be executed in a general purpose computer. The concept of the general purpose programmed automaton is presented as background.

Various measures of algorithm performance are investigated in this chapter and subsequently studied in a model application in Chapter VI.

5.2 The General Purpose Programmed Automaton

The function of a programmed automaton is to operate on a set of data according to a list of instructions. Both the data and instructions exist in the form of a finite alphabet or representation. A realization of a programmed automaton is the digital computer. Such a computer operates on data in the form of digital states by means of a set of instructions, i.e., a program.[2]

---

[2]The digital states may or may not be describable in terms of a binary representation. The binary computer is used universally although systems with a different number of primitive states are not ruled out.

The term "general-purpose" as applied to automata describes a capability to perform any mapping whatsoever by revision of the program. In the literal sense of the definition, no realizable automaton is truly general-purpose since a mapping rule may be of such complexity as to overpower the storage capability of the machine. In practice, the definition is extended to those machines capable of performing rather complex mappings which are used in a role where provisions of easy program modifications are required.

Modern general-purpose programmed automata consist of the following basic elements:

a) A memory unit in which both the data words and instruction words are retained in one or another accessible form.

b) An arithmetic unit which accomplishes the various operational functions involved in the manipulation of data.

c) A control unit which serves as the timing and sequencing unit. The control unit generally accomplishes its function in a sequential form performed during a machine cycle.

d) Input-output units through which information exchange to other media occurs.

Instructions which define the mapping are the detailed rules which govern the operations of the digital computer. The mapping, aside from the minute considerations for a specific machine is an

algorithm describable in a generalized way. Algorithms are stated in the form of higher level language statements or perhaps flow diagrams.

Attempts at using machine translation to go from man compatible formulation of an algorithm to the specific machine instructions to accomplish the mapping have resulted in the development of higher level languages. Among languages of this kind are FORTRAN, PL1, COBAL, SAKO and others. A language development stemming from a major international undertaking is the Universal Algarithmic Language ALGOL 60. The advantage of this formulation is that clear and concise statements of algorithm functions can be made. This language has been used extensively in the literature to present algorithms in a machine independent form. Generally, the language is not directly applicable to any machine without extension.

In the following descriptions of the various algorithms, the syntactic intent of ALGOL 60 is adhered to [26]. Since the algorithms are intended only to convey techniques, no attempt at completeness has been made.

5.3 Nature of the Input to the Estimation Algorithm

In keeping with the previously stated method of obtaining samples of the correlator response as shown in Figure 4.2, we now make the following assumptions:

a) For each time sample there are samples for all correlators. All correlators are assumed samples at the same instant.

b) The correlators are always sampled in the same sequence and these samples are presented to a digitizer in a fixed order.

c) Only samples of $|X(\tau_i,\nu_i)| > \eta$, where η is a pre-selected threshold value, are transferred to the computer. See Figure 4.2 and Figure 4.7.

The foregoing assumptions are made quite arbitrarily and may not apply in all situations. This method of treating the data is treated as a representative example only and other methods could be adopted as well.

These samples are transferred to the computer memory unit by some input means and initially we assume that all data is available in memory when the estimation algorithm is activated. They appear in the computer memory as a triple array.

```
integer m, i  max ;
integer array t[1:m], f[1:m], x[1:m],
```

where max is the total number of samples to be processed. The content of t[i], f[i], x[i] correspond to the ith datum sample time, doppler dependent frequency, and X(t,f), respectively.

The order of the samples is maintained in the process of thresholding and this fact can be used to simplify the algorithm. Figure 5.1 shows how the samples are transferred into the data array. On inspection of the sample transfer process it can be seen that all samples corresponding to a single sample time t_i are continguous in the data array.

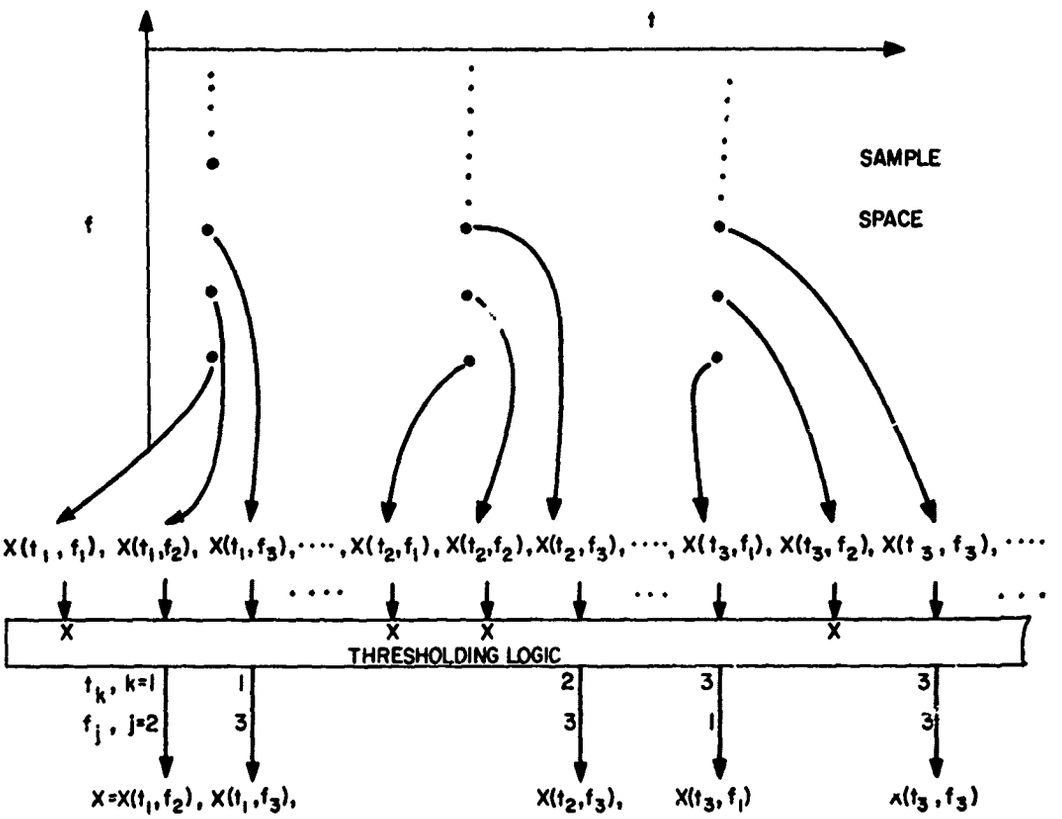

Figure 5.1 Transfer of Samples Into the Processing Array

The algorithm to select the largest value of $X(t_i,f_i)$ from all samples then follows naturally. This procedure is outlined below:

```
procedure MAX (x,t,f,m, Testimate, Festimate)
integer m, Testimate, Festimate; integer array x,t,f;
comment: MAX selects the largest value of m samples
         and returns the corresponding values of time
         delay and frequency as the estimate of these
         parameters.
begin
   integer  xtestvalue, i;
   xtestvalue: = Testimate: = Festimate: = 0;
   for i: = 1 step 1 until m do
   if x[i] > xtestvalue then
      begin Testimate: = t[i]; Festimate: = f[i];
      xtestvalue: = x[i]
      end
end MAX
```

This example of an algorithmic approach to the estimation procedure demonstrates a characteristic of all digital systems, that of uncertainty introduced by the digitization process. Two values of correlator output $X(t_i, f_j)$ and $X(t_k,f_e)$ differing by less than a resolution interval cannot be logically distinguished without imposing an arbitrary criterion. The criterion in the case of this algorithm has been chosen in such a way that the first of a number of peaks of equal value is defined as the maximum.

5.4 Measures of Algorithm Performance

In the design of algorithms, various approaches can be taken. One therefore needs some performance measures for algorithms on the basis of which a choice between various techniques can be made. Some of the criteria may be mutually exclusive to some extent and this leads to trade-off in light of specific requirements.

The algorithm described in Section 5.3 is both direct and simple. Each data sample is tested only once. In addition, it is possible to deal with the data as it is presented. Both of these characteristics are important in a processor and are defined as measured below:

a) Define the Cycle Repeat Count C as the mean number of references to a datum X(t,f) during the algorithm execution for purposes of logic testing.

b) Further we define the Frame Length F as the count of data points (samples) prior to thresholding required for logical completeness of the algorithm.

In the afore described procedure, to find the maximum x(t,f) each datum is processed on a one-at-a-time basis; hence, F=1, C=1. In a real time process such as that of signal parameter estimation, the frame length determines the minimum waiting time after a significant datum is available until a decision can be attempted.

Consider now the case of multiple returns. For each signal, the echo delay time t_k and doppler dependent frequency shift ν are to be estimated. In the case where the returns are well separated in

time, we note the first sample which passes the threshold and select the maximum x(t,f) for all samples within a time span equivalent to twice the pulse length. Repeating this process for all returns completes the algorithm. The formal statement of this scheme follows:

```
procedure MULTMAX (x, t, f, m, tout, fout, xout,n, Tp,Ts)
integer m, n; integer array x, t, f, tout, fout, xout;
value n, Tp, Ts; real Tp, Ts;
comment, MULTMAX selects the largest value of samples within
         a 2Tp interval with time spacing Ts and outputs the
         parameters x, t, f of this sample as xout, tout,
         fout. This process is repeated for all m samples
         input. A maximum of n estimates can be output.
begin
   integer Testimate, Festimate, xtestvalue, k, low, i;
   k: = 0 ; i: = 2 ;
A: xtestvalue: = 0; low: = t[i] -1; i = i - 1;
   for i: = i + 1 while (t[i]-low)< 2* Tp/Ts)∧ (i≤ m) do
B: if x [i]> xtestvalue then
      begin Testimate: = t[i]; Festimate: = f[i];
      xtestvalue: = x[i]
      end
   k: = k + 1;
   if k > n then LISTOVI FLOW;
   tout [k]: = Testimate; fout [k]: = Festimate;
   xout [k]: = xtestvalue;
   if i ≠ m go to A
END MULTMAX
```

In this procedure, Ts is the time interval between successive time samples and Tp the pulse length T. The value of the cycle repeat count is C = 1. The data points can be processed as they are generated on an as available basis. Hence, F = 1, but the final estimate is not available until all samples in the 2T interval are processed.

Consider now the effect of a noise event which exceeds the threshold in the absence of a signal. This situation is depicted in Figure 5.2. An algorithm which considers all samples in a time interval 2T as belonging to the same event does not account properly for such an occurrence. The most serious error is in splitting up the signal related samples in such a way that the estimation rule stated in Section 4.1 is violated. One may ask if it is ever possible to design an algorithm which can properly account for the effects of noise. The noise effects cannot be eliminated totally for any system which is realizable, that is, a system which must rely on a finite processing time and bandwidth [21]. It is possible, however, to apply the logic capability of the computer to circumvent some of the noise problems. The sampling theorem asserts that time samples spaced at 1/2W are independent as far as a noise limited to the bandwidth W is concerned [32][3]. Therefore, noise samples spaced so that

[3]Strictly speaking, a time limited signal of finite bandwidth cannot exist. Losses in practical systems limit the maximum frequency and one considers such a signal as both time and band limited.

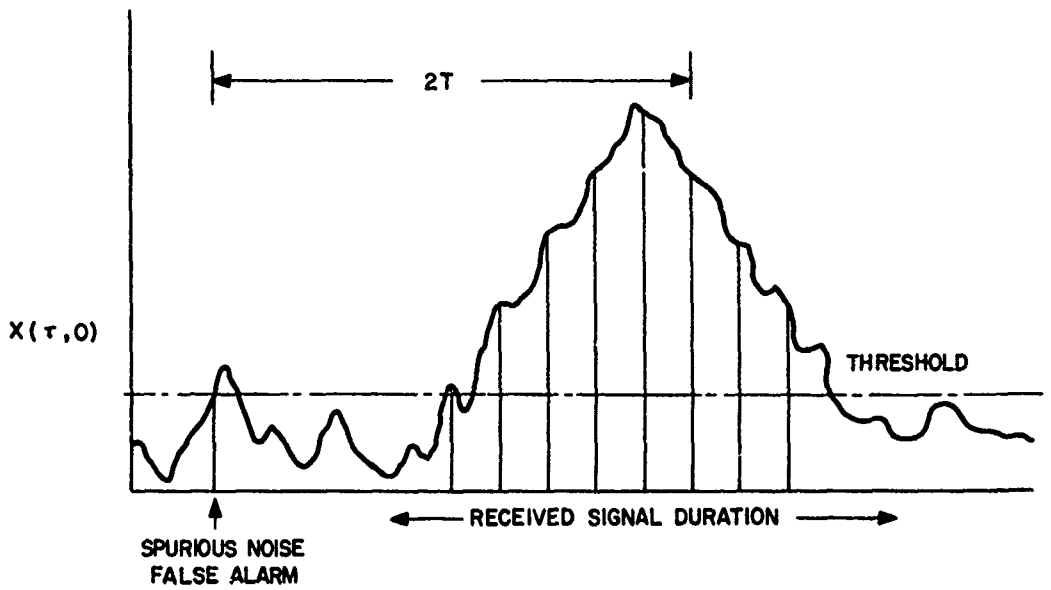

Figure 5.2 Effect of Noise-Only Event on the Estimation Scheme

$$T_s \geq \frac{1}{2W}$$

are independent. When the threshold is set so that the probability $P_\varepsilon = P_r\ (X_n > \eta)$ is small, the probability that α independent samples of β will surpass the threshold is given by the binomial distribution

$$f(\alpha) = \binom{\beta}{\alpha} P_\varepsilon^{\ \alpha}\ (1-P_\varepsilon)^{\beta-\alpha},$$

where

$$\binom{\beta}{\alpha} = \frac{\beta!}{(\beta-\alpha)!\alpha!}\ .$$

For example, the probability that two of three successive independent noise samples exceed the threshold is

$$f(2) = 3\ P_\varepsilon^{\ 2}\ (1-P_\varepsilon)\ .$$

We can take advantage of this characteristic of noise-only threshold surpassing events to build a degree of noise immunity into the algorithm. The procedure to accomplish such a test is presented formally below:

```
boolean procedure NOISE (low, tcurrent)
value low, tcurrent,    ; integer low, tcurrent;
comment NOISE is a logical function which has the
        following logic values for delt where
            delt = current time - time origin for this echo:
FALSE if delt = 0, 1, or 2, or if (2 or 3) of first
        3 time samples were present.
TRUE otherwise.
```

It is assumed that sample spacing is sufficient to insure noise independence.

```
begin
   integer delt; boolean array a [1:2];
   delt: = tcurrent - low; NOISE: = FALSE;
   if delt = 0 then a [1]: = a [2]: = FALSE;
   if delt > 3 then NOISE: = ¬(a [1]∨a[2]);
   if (delt = 1)∨(delt = 2) then a[delt]: = TRUE;
END NOISE
```

This routine enters into the estimation algorithm by way of calls to this logic function at statement labeled B:. The revised structure will then take the form:

```
B:  if NOISE (low, t[i]) then go to A;
    if x[i] > xtestvalue then
        begin Testimate: = t[i];.....
```

The inclusion of this type of a test for noise events corresponds to a somewhat higher threshold. The apparent increase in the threshold value will be large when Ts approaches the pulse length T and decreases as Ts/T becomes small. On the average, for a number of trials,

$$\left\langle \frac{\Delta\eta}{\eta} \right\rangle = Ts/2T \ ,$$

where $\Delta\eta$ is the change in threshold implied by imposing the above requirement.

Another measure of algorithm performance is the degree of immunity to biases. The preceding algorithm gives essentially an unbiased estimate of the parameter of interest. Some bias is introduced, however, by the fact that the received signal energy is unknown at the outset. Figure 5.3 shows that for low energy signals the test interval commences at a time considerably later than that corresponding to -T on the signal envelope. The estimate therefore will contain a number of samples taken after the signal has died out. Noise events occurring later than the signal envelope can compete with the signal and may lead to estimates of appreciably higher echo delay time than warranted by the signal echo delay resolution constant. In spite of this, the estimate will yield only very occasionally to biases in estimation because the probability of a noise-only event exceeding the peak of the correlator output is small for realistic values for the threshold.

Having described the algorithms for estimating the time delay, we now go on to analyze the quality of this estimate. It has been shown in the literature that the maximum likelihood estimate for additive white Gaussian noise is an unbiased estimate [35, 39]. In addition, this estimate is based on a sufficient statistic and hence the Cramer-Rao bound of the variance stated in Equation (2.23) is satisfied with an equality [7]. The estimate is the minimum variance unbiased estimate and we can describe its quality by the variance alone. Alternately, the confidence interval on the estimate is adequate to describe the error in estimation.

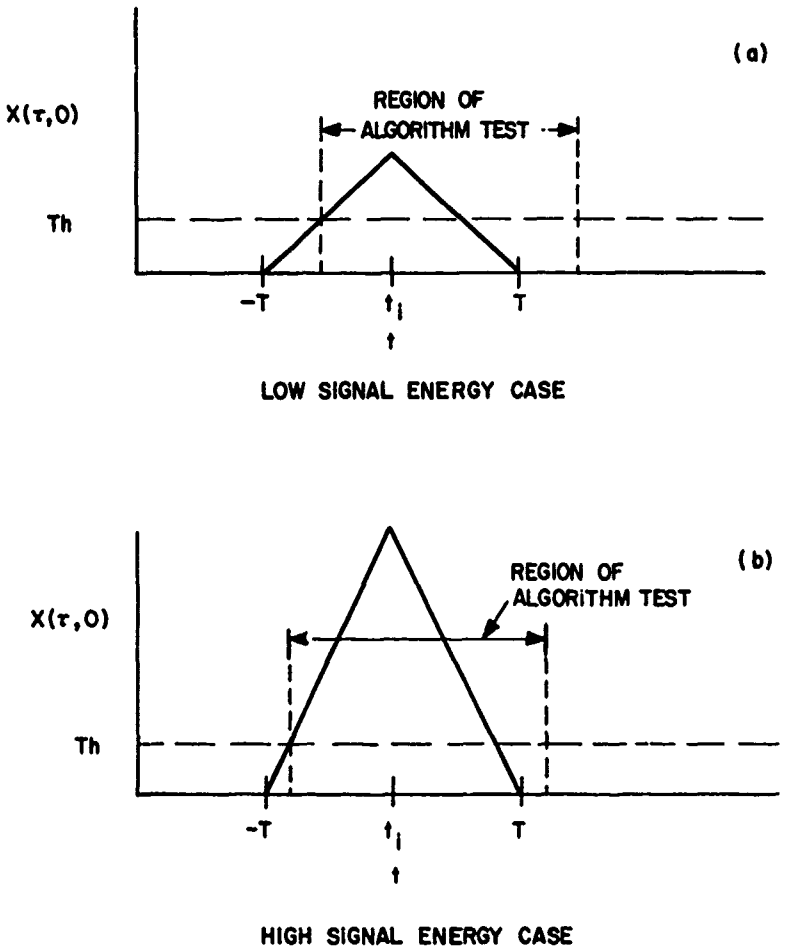

Figure 5.3 Effect of Received Signal Energy on Algorithm Bias

Consider the matched response of a correlator to a monochrome carrier band pulse as developed in Section 4.2. From Equation (4.5), we get

$$|\chi(\tau,0)| = 1 - \frac{|\tau|}{T}$$

for a monochrome pulse with rectangular envelope. However in the presence of noise, the envelope output will be

$$\epsilon(t) = \sqrt{[1 - \frac{|\tau|}{T} + n_c(t)]^2 + n_s^2(t)} \ , \tag{5.1}$$

where n_c and n_s are the quadrature noise components. In the case where

$$[1 - \frac{|\tau|}{T}] >> (n_c(t) \text{ and } n_s(t)) \ , \tag{5.2}$$

$$\epsilon(t) \cong [1 - \frac{|\tau|}{T}] + n_c(t) \quad \text{for almost all } t \text{ [21].}$$

This situation corr ·ponds to those values of

$$X(\tau,0) > \eta,$$

where the threshold η has been chosen so as to give a very low probability of noise only events. The noise on the output of the envelope detector is approximately additive when only samples which exceed the threshold are considered.

The probability that any sample taken at τ_i will exceed the correlator output at $\tau = 0$ due to the noise is then,

$$P\,[X(\tau_i,0) > X(0,0)] =$$

$$P\,\{[X(\tau_i,0) - X(0,0)] > 0\} = P(W > 0)\ , \tag{5.3}$$

where $W = X(\tau_i,0) - X(0,0)$.

The probability densities corresponding to $X(\tau_i,0)$ and $X(0,0)$ have equal variance but different mean values.

Define $\mu_o = E[X(0,0)]$, the mean value of $X(0,0)$, and $\mu_i = E[X(\tau_i,0)]$. The noise events corresponding to these two samples are independent hence the mean values and variances add [16].

The variance of the random variable W will then be $2\sigma^2$ and the mean value will become:

$$\mu_i - \mu_o = \mu_o\,(1 - \frac{|\tau|}{T}) - \mu_o = -\frac{\mu_o|\tau|}{T}\ . \tag{5.4}$$

Since all noise samples are assumed to be independent, the probability of any sample in an interval $\{\tau, -\tau_L < \tau < \tau_L\}$ exceeding that at $\tau = 0$ is given in terms of normal statistics. Here, τ_L is the value of τ defining a confidence interval on $\hat{\tau}$. The parameter $\hat{\tau}$ is the estimate of time delay.

Woodward derives the variance of the estimate of time delay assuming a large signal-to-noise ratio [39]. This result is shown in Equation (5.5). Due to the assumptions, this equation can only be expected to be valid asymptotically as the signal-to-noise ratio become large.

From Woodward, the variance of the estimate of time delay is

$$\sigma_{\hat{\tau}}^2 = \frac{1}{R\beta^2}, \tag{5.5}$$

where R is the signal-to-noise ratio, $2E/N_o$ and $\beta = 2\pi/T$.

Therefore, the variance of the estimate is

$$\sigma_{\hat{\tau}}^2 = \frac{N_o \; T^2}{2E \cdot 4\pi^2}$$

and

$$\sigma_{\hat{\tau}}^2 = \frac{T}{2\pi\sqrt{\frac{2E}{N_o}}} \; . \tag{5.6}$$

The confidence interval on this estimate can be defined and is

$$P(-Z\,\sigma_{\hat{\tau}} < \tau < Z\sigma_{\hat{\tau}}) = P(\tau < Z\sigma_{\hat{\tau}}) - P(\tau < -Z\sigma_{\hat{\tau}}), \tag{5.7}$$

due to the normality of the distribution. Here Z is a real constant.

For the 90 per cent confidence interval, this result is equivalent to

$$P(|\tau| < Z\sigma_{\hat{\tau}}) = 0.95 \tag{5.8}$$

which gives

$$Z = 1.645, |\tau| \leq \frac{0.524\ T}{\sqrt{2E/N_o}}$$

from tables [16].

The behavior of this confidence interval as a function of signal-to-noise ratio R is graphed in Figure 5.4 (Curve b). In order to assess the actual behavior of this estimate at low signal-to-noise ratios the simulation system described in Chapter VI was used to obtain an experimental measure of the confidence interval.

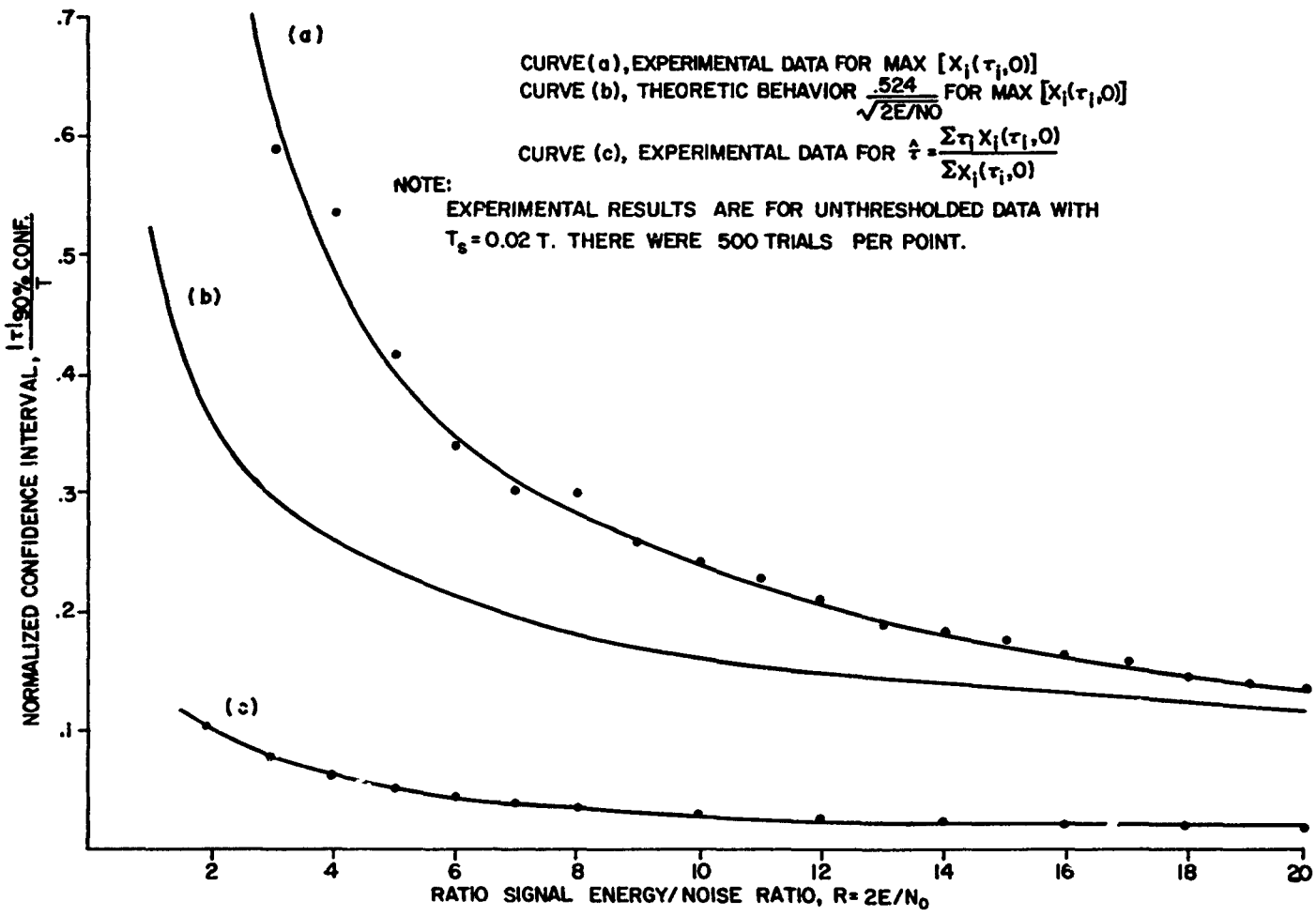

Figure 5.4 Confidence Interval for Estimation Algorithms

These results are also plotted in Figure 5.4 (Curve a.), and it is seen that, in the large signal case, the experimental results do, in fact, converge to the theoretical function. In obtaining these results a sampling interval Ts much smaller than the pulse length was used. Other results which show the effect of sampling time interval and threshold are presented in Chapter VI.

Thus far the estimation algorithm considered has been the one resulting from minimization of the likelihood function as shown in the work leading to Equation (2.21). This result was for a general known signal in additive white Gaussian noise but did not make use of the signals treated herein explicitly. Hence, some other estimation algorithms were considered. It was anticipated that the power of the computer could be used to advantage to improve the accuracy of the estimate for the small class of signals studied. Algorithms which do in fact provide better accuracy in a mean square error sense have been identified. These algorithms lead to a biased estimate of the time delay but it will be shown that the bias is small for realistic signal-to-noise ratios.

Instead of finding the peak value of the correlator it is possible to use the power of the computer to perform more complex estimates. As an example of such an algorithm, consider the estimate

$$\hat{\tau} = \frac{\sum_{i=1}^{m} \tau_i X(\tau_i, 0)}{\sum_{i=1}^{m} X(\tau_i, 0)} , \tag{5.9}$$

where m is the number of time samples in the 2T time interval. It is apparent that such an estimate is less prone to errors caused by isolated noise events.

The variance of this estimate is

$$\mathrm{Var}(\hat{\tau}) = \mathrm{Var}\left\{\frac{\sum_i \tau_i \; X(\tau_i,0)}{\sum_i X(\tau_i,0)}\right\} = \mathrm{Var}\left\{\frac{W}{V}\right\}, \tag{5.10}$$

where W and V are defined as the numerator and denominator terms respectively.

When the τ_i's are chosen so that the time samples are independent in terms of the noise, Equation (5.10) becomes

$$\mathrm{Var}\ (\hat{\tau}) = \mathrm{Var}\left\{\frac{W}{V}\right\}, \text{ W, V both normal.}$$

The variance for the quotient of two random variables is detailed in Appendix C. It is shown there that this estimate has a mean value

$$\mu_{W/V} = \frac{\mu_W}{\mu_V} + \frac{\sigma_V \mu_W}{\mu_V}\left(\frac{\sigma_V}{\mu_V} - \frac{\rho\sigma_W}{\mu_W}\right), \tag{5.11}$$

where ρ is the correlation coefficient of y,x.

In the limit where the second term on the right is very small, the estimate

$$\mu_{W/V} \cong \hat{\tau}\,\frac{\sum_i X(\tau_i,0)}{\sum_i X(\tau_i,0)} = \hat{\tau}.$$

Otherwise, this estimate is a biased one. The experimentally measured confidence interval of this estimate as a function of signal energy is shown in Figure 5.4 (Curve c). This estimate has a smaller confidence interval than the estimate on the basis of peak correlator output. Since the maximum likelihood estimator is optimized on the basis of maximum a posteriori probability, the above finding appears contradictory.

In fact, the estimate based on the peak correlator is the minimum variance unbiased estimate. The variance of a biased estimate cannot be shown to be limited by the Cramer-Rao bound of the variance [35]. The biased estimates studied in this thesis are applicable to only a limited class of signals, and, therefore, lack the generality inherent in the maximum likelihood procedure.

Another estimation algorithm suggested by the work of Hudson consists of fitting a pair of regression lines to the data points [17]. The method is outlined in Appendix C along with a method for finding the confidence interval for the ordinate of intersection for two regression lines. The complex nature of this algorithm seems to preclude its use in a real time system as is dealt with in this thesis. Also, since the confidence interval given by the method of Equation (5.9) is quite small, the gain to be realized by going to greater complexity is questionable.

Other estimation schemes can be conceived but will not be treated here. One method which warrants brief consideration, however, is a scheme which notes the first and last threshold exceeding events

in a fixed time interval and halves this interval to obtain an estimate of echo delay time. The sensitivity of this procedure to noise is very high since the data which is most noise-like is used to generate the estimate.

5.4 Simultaneous Estimation of Frequency and Echo Delay

It has been shown how a computer algorithm may be used to estimate signal parameters when echoes are distinct in time. Such echoes must be spaced at intervals of at least 2T seconds where T is the transmitted pulse length. In many application areas, this time separation cannot be assumed. For a time limited signal, overlap of returns in time implies interaction in the frequency domain. Only in the M-ary digital communication case where the signals are selected to be orthogonal can this frequency interaction be ignored.

Two echo signals which overlap in time will also interact in frequency. In general, two distinct situations can be identified, one will be dealt with in this thesis. When the echoes differ sufficiently in frequency due to differences in target velocity, the interaction between these signals will be small. In keeping with the literature, echo signals differing by at least $2\Delta v$, where Δv is the velocity resolution constant,

$$\Delta v = \frac{c}{2f_o T_e}$$

will be considered as essentially unchanged in the character of the matched response exceeding the threshold η [3]. Figure 5.5 shows the uncertainty surface for two monochromatic r-f pulses of duration T which are clearly distinguishable.

A convenient way to represent the uncertainty surface for multiple returns is by a section parallel to the τ,ν plane such that

$$|Y(\tau,\nu)| = 0.5 \tag{5.12}$$

The planar section for this case represented by Equation (5.12)is shown in Figure 5.6 in heavy shading. The remaining parts of the respective response function is shown in light shading. The frequencies f_1 and f_2 in Figure 5.6 are the matched frequencies for the two responses.

The effect of noise is to deform the uncertainty surface and therefore to distort the area representing.

$$X(\tau,\nu) = |Y(\tau,\nu) + n(0,\sigma_N^2)| = 0.5 \tag{5.13}$$

where the effect of the noise n is no longer negligible. In addition, the prior uncertainty of receiver signal energy for the two echoes requires a threshold η which does not satisfy the requirement of Equation (5.13) for at least one of the echo signals.

In studying Figure 5.6, the similarity to the previous estimation of returns clearly separated in time as outlined in Algorithm 5.2 is apparent. Each echo is characterized by a peak response on the matched correlator at a τ_i such that all related response is distributed within

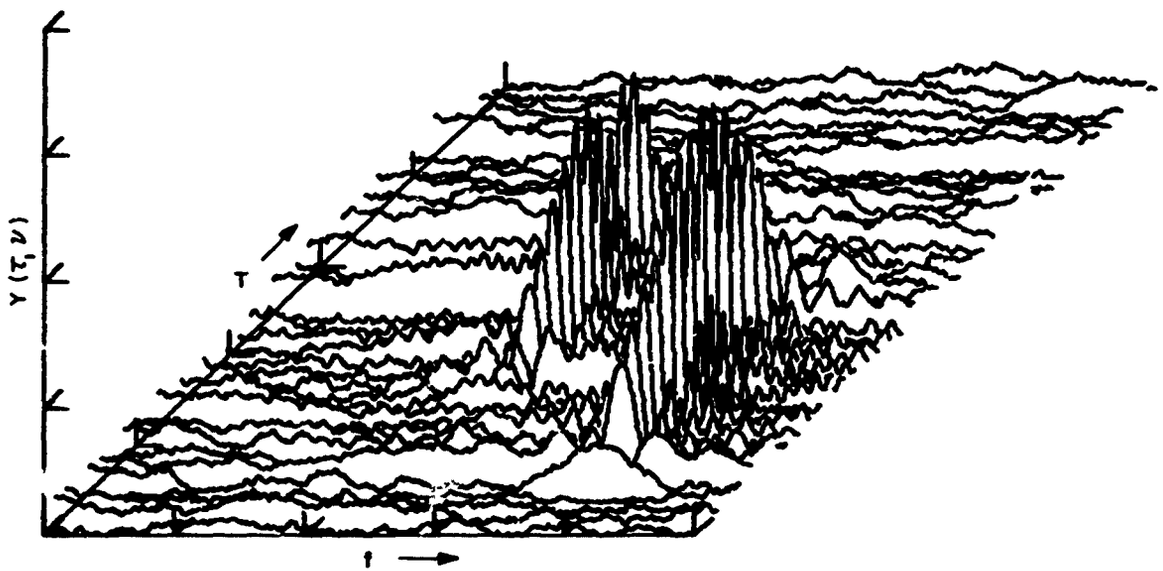

Figure 5.5 ML Detector Response for Two Monochrome Pulses, Large S/N Case

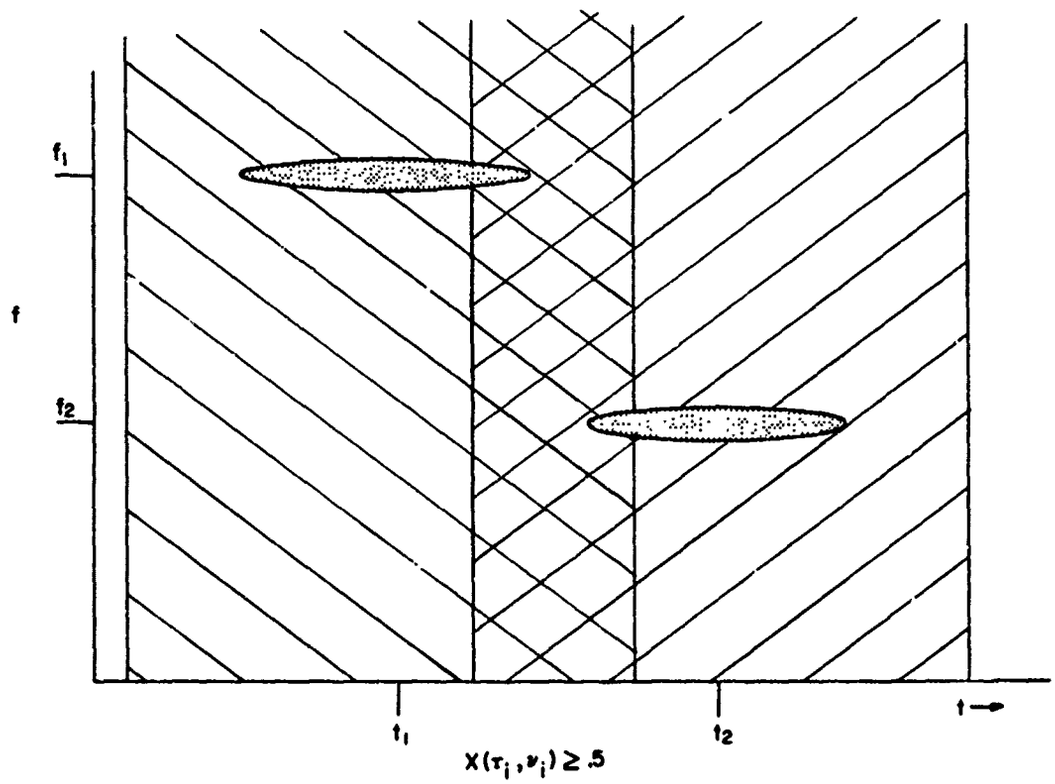

Figure 5.6 Overlapping Monochrome Responses

$$\tau_i - T < t < \tau_i + T .$$

For the monochrome pulse for which each matched response is along a fixed frequency, a method of extending Algorithm 5.2 appears straightforward. If the total frequency range were to be divided into regions 1/T cycles wide, each of these could be treated separately with only minor revision of the algorithm. The special case of a response falling astride this arbitrary division must then be treated by properly grouping data during subsequent processing. If this is the method of attack, it should be noted that samples should be taken at frequency intervals less than 1/T cycles. This precaution insures that a peak response occurring at a doppler dependent frequency not corresponding to the sample frequency will be detected. For example, if

$$f_r = 1/2\ T,$$

where f_r is the frequency at which the sample is taken, then

$$Y(0,\ f_r) = \frac{\sin\ (\pi/2)}{\pi/2} = 0.63.$$

Hence, the sample corresponds to a signal input of 63 per cent of the actual received signal, or the effective signal-to-noise ratio is reduced with associated increased uncertainty in the estimate. The spacing of the frequency shifted reference signals is often dictated by limits imposed by complexity, but a reference spacing which insures that the response is

$$Y\ (0,f_r) \geqq Y\ (0,0) - 0.12$$

requires frequency shifted references spaced 1/2T.

The algorithm needed to accomplish the parameter estimation for overlapping returns in this way is presented in Appendix D (Algorithm D.1). It can be seen that this algorithm does not properly treat signals such as a linear chirp signal for which the response does not occur primarily along a constant frequency. An algorithm which is applicable to such signals as well as the monochrome case is a more general one and can be expected to yield readily to changes in signal characteristics.

The nature of the response of a correlation receiver to overlapping chirp signals is shown in Figure 5.7. The corresponding samples in the frequency/time domain are shown in Figure 5.8.

Referring to Figure 5.7, it can be seen that samples corresponding to two echo signals can be seen to form clearly distinguishable clusters. The first event encountered is associated with an echo delay time t_1 and doppler dependent frequency f_1. All other samples associated with this target lie along a line in the frequency/time plane, the equation of which is dependent on the signal characteristics. The expected spread of the sample points about this line in frequency can be derived directly from the equation of the signal uncertainty function. It was previously shown that, for a large class of linear frequency modulated signals,

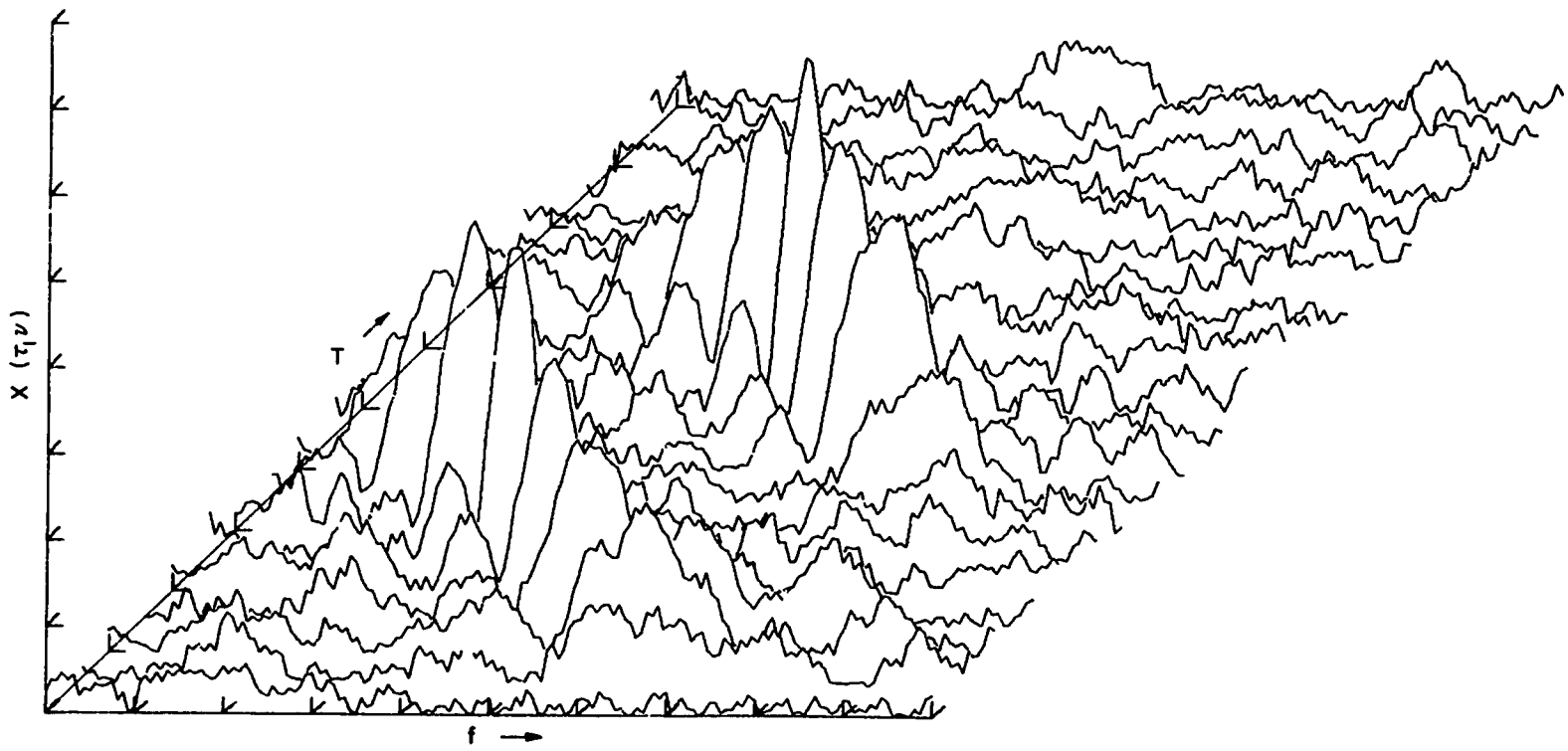

Figure 5.7 Response of a Correlation Receiver to Overlapping Chirp Signals

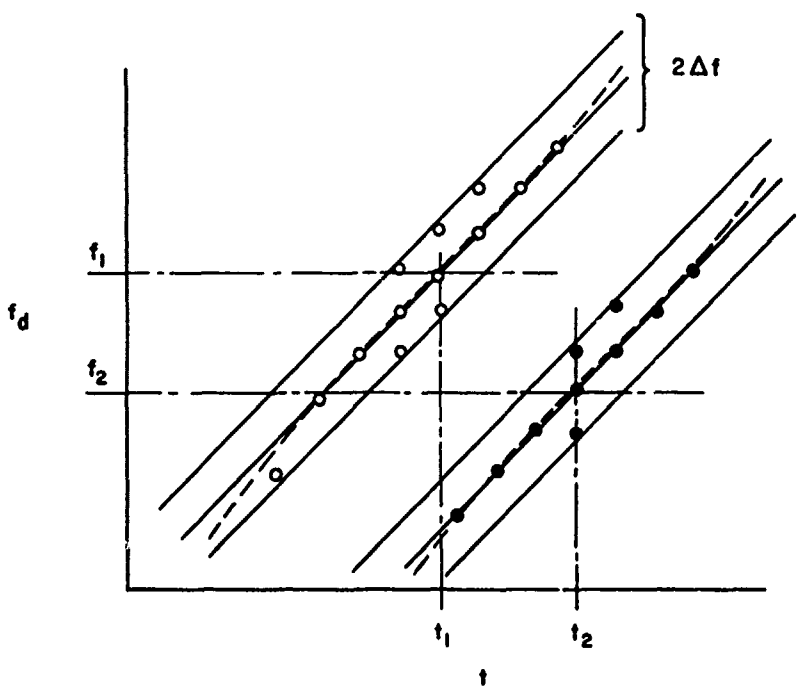

Figure 5.8 Overlapping Echoes for F-M Signal

the effective width in frequency at constant τ, is 1/T, where T is the pulse duration. Also, the trace of the main lobe of the response has constant slope in the time-frequency plane, for values of time delay near the median value. These results suggest a method for treating the general chirp signal case. Given any sample $X(t_i, f_j)$ at t_i, the corresponding sample at t_{i+1} is

$$X(t_{i+1}, f_j + \frac{\Delta f}{\Delta t} + \varepsilon) .$$

The quantity $\Delta f/\Delta t$ is the incremental change in frequency with time which is a function of the signal characteristics. The monochrome signal will have

$$\frac{\Delta f}{\Delta t} = 0.$$

The uncertainty ε is introduced by the fact that neither the sample at t_i nor that t_{i+1} are in synchronism with the signal. If the sample at t_i lies on the ridgeline of the uncertainty surface and near its peak value, then ε is on the order of

$$\varepsilon \cong \pm \frac{1}{2T}$$

in frequency.

In processing the correlator samples, the first sample to exceed the threshold will be most effected by noise. In addition, the non-linear behavior of the FM ridgeline response will cause samples far removed from the peak to exhibit a frequency bias.

Consider the probability density of sample values in the frequency ordinate, this density function will have its peak value approximately on a straight line in the frequency/time domain as delay time increases from the peak of the response. For large values of time delay, however, the density function will be shifted and the maximum probability will no longer coincide with the straight line which defines the ridgeline response near $X(0,\nu)$. The probability distribution

$$F(\nu - \nu_j) = \sum_{i=-\infty}^{(\nu-\nu_j)} f(X_i)$$

where ν_j is the straight line extrapolation of frequency of the ridgeline response near $X(0,\nu)$, is shown in Figure 5.9. Distributions for various signal-to-noise ratio cases are shown. In referring to this figure it can be seen that large signal-to-noise ratios, for which the first sample to exceed the threshold is far removed from the peak of the response, lead to significant biases in initial frequency. Since the first sample of any echo response is used to define the line about which clustering of samples is anticipated, errors introduced by the ridgeline non-linearity must be accounted for by increasing the clustering aperature ε. In practice, a value for ε, such that $\varepsilon = 1/T$, will insure that samples are properly grouped in most cases.

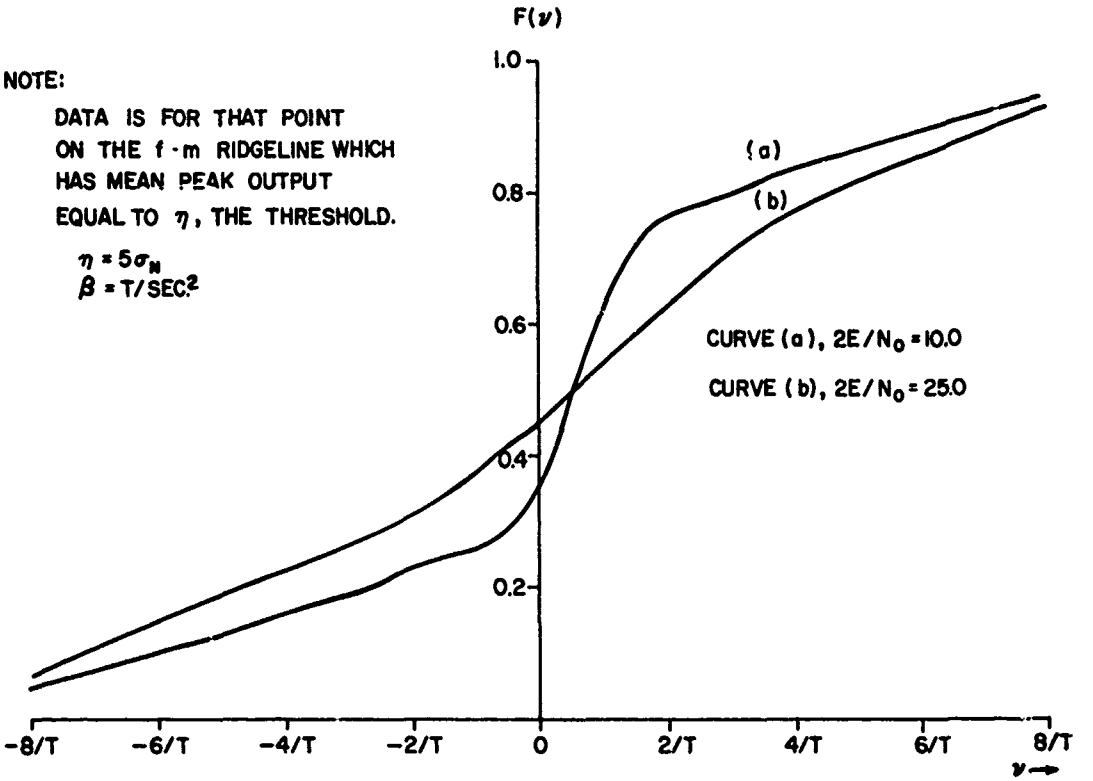

Figure 5.9 Distribution of First Sample Deviation for Linear F-M Signals

The general algorithm then is easily derived and is:

> From all samples lying in the vicinity of a straight line in the frequency/time plane in an interval of time 2T and within $\pm$ 1/T cycles of the frequency ordinate, select the one with maximum amplitude. Report the corresponding values of t_i and f_j as the echo delay time and velocity dependent frequency, respectively.

The functioning of such an algorithm is shown as a general flow diagram in Figure 5.10. The algorithm is detailed in Appendix D (Algorithm D.2). The following observations follow directly from an examination of this diagram.

a. All points associated with a single uncertainty surface are sorted from the total number of samples in a time interval 2T and processed to yield an estimate. Although samples can be processed as they arrive, only samples lying along a line in the time/frequency domain can be used fruitfully in arriving at an estimate. For this reason, the frame length F is

$$F \cong W/\Delta f \ .$$

b. Samples corresponding to other echo returns occurring in the 2T interval must be passed over on the basis of some type of test. The samples therefore must be treated a number of times leading to a cycle repeat count

$$C \cong K/T\Delta f \ ,$$

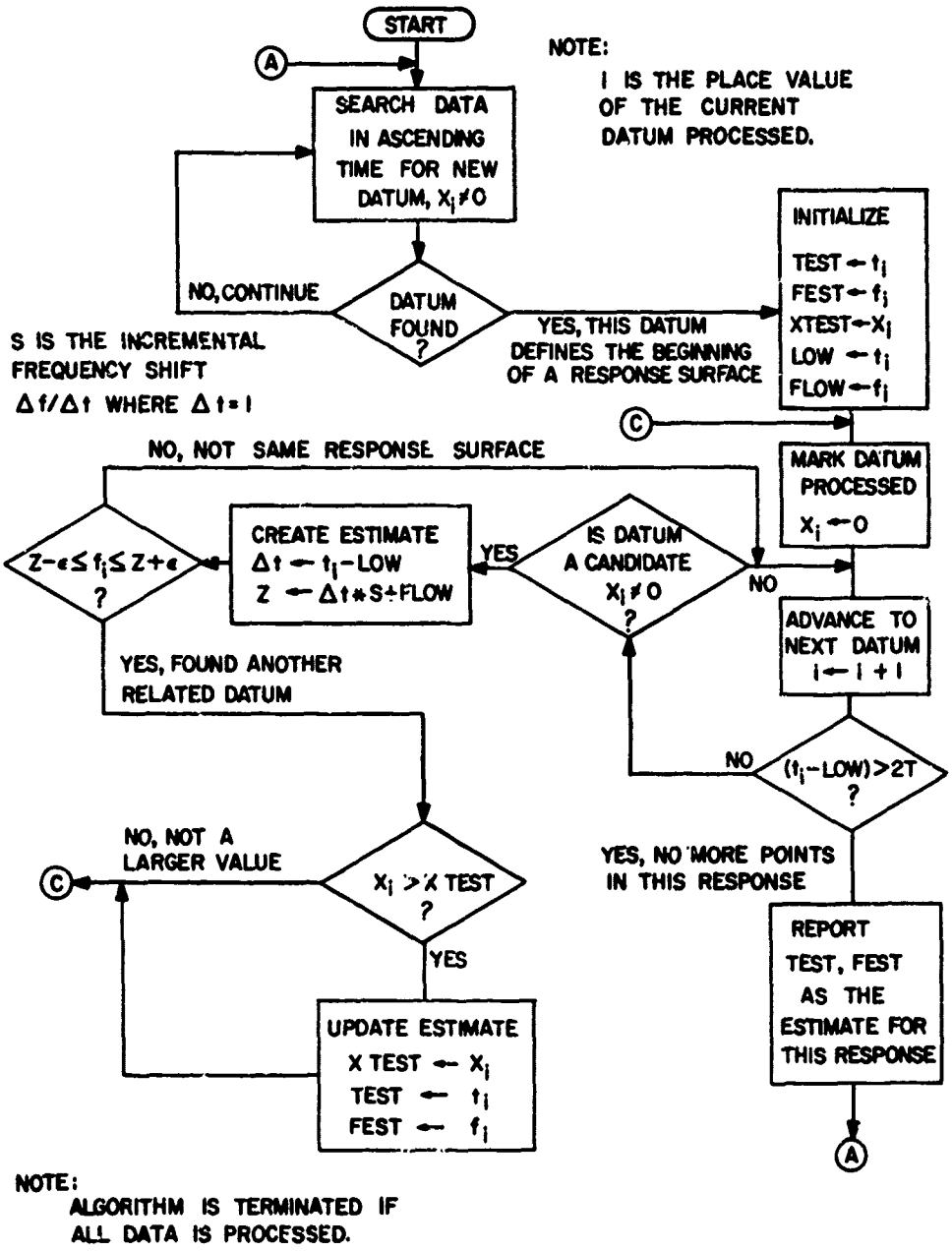

Figure 5.10 General Algorithm for Signals With Linear Ridgeline Response

where K is the mean number of echoes overlapping in a 2T time interval. When Δf is 1/2T as previously described.

$$C \cong 2K \ .$$

c. Samples which have been found to belong to the set of samples defining a specific echo must be somehow marked as being of no further interest. Such marking can be done in a number of ways without requiring additional data storage. In the algorithm shown, this is accomplished by setting the corresponding value of $X(t_i, f_j)$ equal to zero, a unique value for this datum never occurring otherwise.

The significance of the cycle repeat count and frame length will be related to a specific example in Chapter VI. It can be seen that an algorithm which must repeatedly treat the same datum requires more time than one for which C = 1, all other factors being equal.

This situation comes about due to the fact that the samples are interspersed in their order.

By a suitable transformation, it is possible to separate the samples as they are received. Referring to Figure 5.11, it is seen that the operation

$$t_i' = t_i - (f_i \phi) \ ,$$

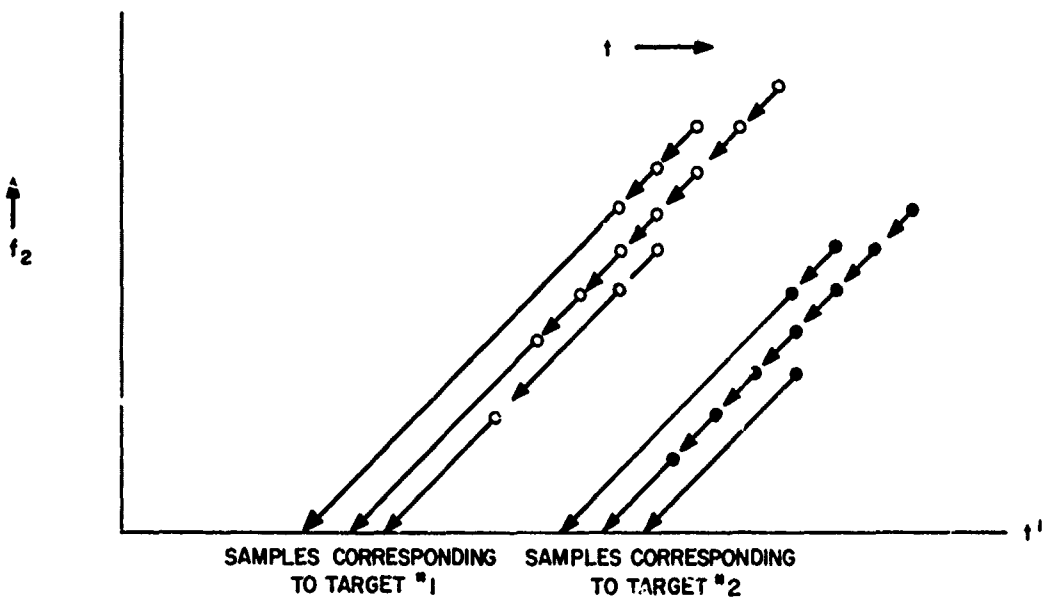

Figure 5.11 Separation of Data Points by Transformation Algorithm

where

$$\phi = \frac{\Delta t}{\Delta f} \quad ,$$

maps all data points belonging to a single echo onto the neighborhood of a point in the one-dimensional space $\{t'\}$ defining the $f = 0$ projection of the echo samples within $\pm$ 1/T cycles of the line defined by the first sample of the signal envelope possibly belong to the same event. The grouping in the space $\{\tau'\}$ must be made over an interval

$$\{t';(t_o' - S/T) \leq t' \leq (t_o' + S/T)\} \ ,$$

where $S = \Delta t/\Delta f = 1/\phi$ and t_o' is the mapping of the first sample from the echo response in question. Note that this algorithm is no longer completely general since for the monochrome signal, $\phi \to \infty$. This is the price which must often be paid in the design of more efficient algorithms. Generality can be retained if this special case is recognized and the projection is then to the $t = 0$ ordinate.

Once this transformation is accomplished, the data points are clearly distinguished as belonging to a specific echo response. The value of t' can then be used to address "bins" which are S/2T in extent. All data points will then be sorted by t' into physically distinct storage cells and tests can be made immediately to see if the current sample exceeds a previous sample with approximately the same t'. Figure 5.12 shows how new samples must be tested against entries in the t' space. A maximum of four tests must be accomplished to test for all points in the vicinity of t'

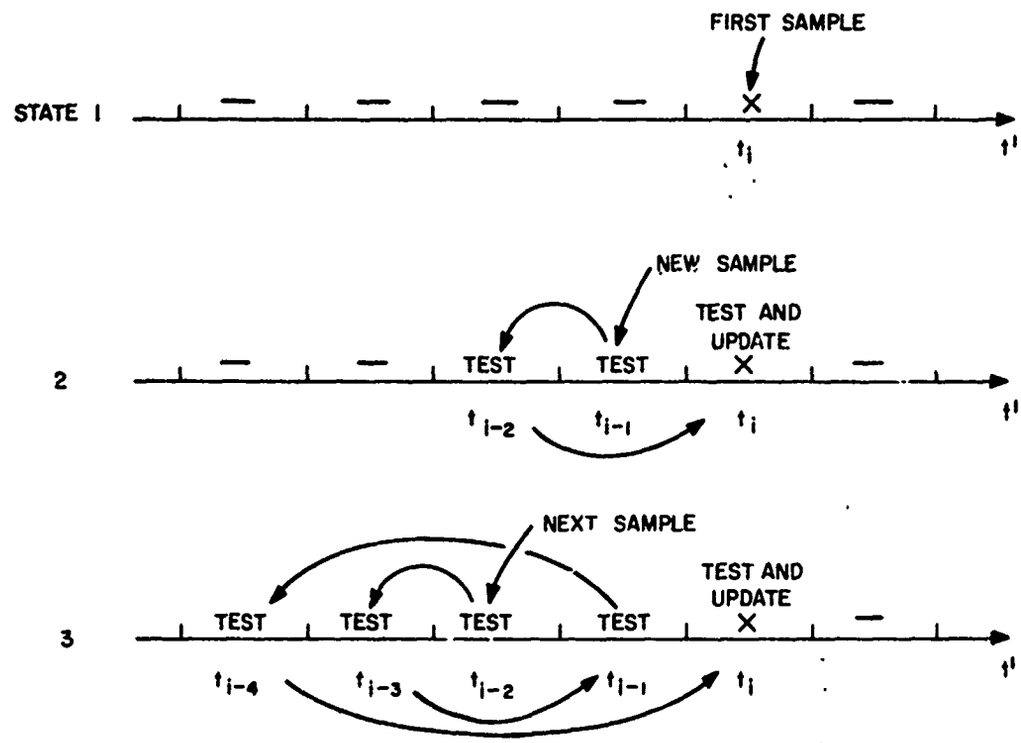

Figure 5.12 Tests of Data Points in the t' Space, Worst Case Example

within a $\pm$ 1/T interval. The average number of tests, as shown in state 2 of Figure 5.12, to find a match will be about two since the data points have maximum probability of occurrence at the center of the response ridgeline.

To reduce the number of storage cells needed in the t' domain, we note that previous entries in this storage which were made at

$$(t_o + 2T) < t_i ,$$

where t_i is the current time sample, can no longer be updated by future samples and can therefore be transferred to the output matrix and the storage space reused. This leads to a folding in the t' domain which is easily accomplished by using modulo arithmetic to generate the address of the target storage cell. Associated with each entry in the t' domain is the value of t_o corresponding to it and these data points are transferred to the output matrix either through tests by new data or at the end of all processing.

This algorithm is detailed in Appendix D (Algorithm D.3). Note that each sample is processed once as available; hence,

$$C = 1, \quad F = 1.$$

However, the processing to be accomplished by the algorithm is rather complex requiring multiplication, modulo arithmetic, and multiple tests of the t' storage elements. For some machines, the additional complexity may not be warranted due to slower execution of the arithmetic functions.

Although the data points can be processed on a one-at-a-time basis, there is, in a typical application, a need for temporary buffering of the input samples as they are received from the digitization process. This precaution insures that, at times when many samples arrive within a short time interval, no data will be lost. The programmed automaton processes data at a fixed upper data rate in a serial fashion and, while it may be able to maintain the required data rate on the average, periods of excessive data transfer from the signal processor can be anticipated.

CHAPTER VI

ILLUSTRATIVE EXAMPLE OF RADAR ESTIMATION

6.1 A Track-While-Scan Radar

In order to relate the previously developed concepts to an actual situation, a ground control radar application will be treated. The choice of system chosen for the model is somewhat arbitrary but conforms generally to the model systems described by Swerling [34]. Table 6.1 gives the pertinent parameters for the system. This a C band radar which continuously scans a 360 degree sector using a linear F-M signal. The beamwidth and scanning rate insure that a target is illuminated with 6 pulses per scan. Tracking of targets is to be accompanied by computer algorithms but, for the initial treatment, no prior knowledge of the target is available. This situation corresponds to the case where the system is just turned on for targets newly arriving in the search area.

The system described should be able to handle a maximum of 1000 aircraft in the total search area. Aircraft are separated by 10 minutes flying distance or in altitude in such a way that up to four aircraft going in different directions can occur in a pulse length, although this is rarely the case. Other systems accomplish aircraft recognition, altitude measurements, and terminal monitoring. Maximum allowed target speeds are Mach 1, or 750 knots.

From Section 4.4, it follows that this system will have a resolution in echo delay of 4 μsec and in target velocity of 75 knots which is adequate to distinguish even low speed aircraft from clutter. Some means must be included for removing the effect of clutter from the maximum likelihood detector since this will lead to unacceptably high false alarm rates at essentially an uninteresting frequency. Such schemes have been reported in the literature and will not be expanded on here [24].

Given the resolution of 4 μsec and 75 knots, it follows that samples will occur at the rate of

$$40/4\mu\text{sec interval} = 10 \text{ MHz rate.}$$

These analog values must be thresholded and A/D converted at a maximum of 10 MHz although the data points surpassing the threshold will arrive in bursts corresponding to target related echoes. This A/D conversion rate is well within current state-of-the-art technological limits and presents no problem. Eight bit quantization at a 10 MHz conversion rate is commercially available.[4]

Eight bits of quantization are deemed adequate for this system. The frequency samples are taken at half the frequency resolution spacing; hence, the maximum error will be 12 per cent. A one bit error of 8 digital states is equivalent to this error. Eight bits

[4]Computer Labs at Greensboro, North Carolina distributes a 10 MHz A/D converter for television digitization of 8 bits - Model HS-810.

Pulse Length	T	= 36 μsec.
Carrier Frequency	f_0	= 5600 MHz
Bandwidth	W	= 250 kHz
F-M Frequency Shift Rate	B	= $1.185 \times 10^{10}/\text{sec}^2$.
Horizontal Beamwidth	b	= 3.6°
Scan Rate	ω	= 10 rpm
Pulse Repetition Rate	f_r	= 100 pps
Target Velocity Maximum	v	= $\pm$ 750 knots

TABLE 6.1 PARAMETERS FOR MODEL RADAR APPLICATION

provide for 255 states or thirty times the nominal number required. This provision is added since the echo energy is unknown at the outset and therefore the peak value of the correlator output will not be known. Automatic gain controls in the analog equipment may be used to compensate for changes in echo level with range but multiple targets at approximately the same range cannot be adequately compensated for. Variations in target strength will cause variations in echo levels aside from purely range determined behavior.

Assuming that the 1000 aircraft are distributed about evenly throughout the search area, there will be 10 aircraft in the beam at once. In the worst case, this will lead to an average of two frequency responses for each of 18 time increments for each aircraft or 360 samples per pulse. There are 100 pulses per second and, therefore, the sample throughput upper limit will be

$$36{,}000 \text{ sample/sec} = 36 \text{ KHz throughput.}$$

In this worst case situation, the time allowed to process each sample is 28 μsec.

Due to the nature of civilian air traffic regulations, the echoes from the various targets will be clearly distinguished in echo time delay and frequency, hence, satisfying the requirements of resolvability previously stated.

6.2 Processing Implications of the Model

In the context of this proposed model of a radar system, it is now possible to analyze the effect of the various measures of algorithm performance.

The cycle repeat count and, to a lesser extent, the frame length are of importance in such a system since very short times are allowed for processing each datum. When the probability of overlapping returns is very small Algorithm D.2 will have

$$C = 2, \qquad F = W/\Delta f.$$

Since there are 40 frequency references, the frame length

$$F = 40, \quad \text{or} \quad T_S = 4\ \mu\text{sec}.$$

The frame length is not an important factor since more than 4 μsec will be needed to process each datum. In this situation where overlapping returns are rare, this algorithm will be faster on most machines than an algorithm involving data transformations since there is less arithmetic computation.

When aircraft are restricted to flight in traffic corridors, the probability of overlapping returns will be higher. The cycle repeat count will then be larger on the average for Algorithm D.2 than for a transformation algorithm. The transformation algorithm (Algorithm D.3) will on many machines, exhibit a higher data throughput rate for this case.

The parameters, accuracy of the estimate, and estimation bias primarily interact with system objectives and cannot be analyzed in the context of the estimation problem alone. One important area where these effects must be considered is in the design of tracking algorithms. So far, in this thesis, we have dealt only with the maximum likelihood estimation in the limit of no a priori knowledge. In tracking a target, however, previous estimates are important.

Recalling the Bayes estimate developed in Chapter I, it is possible to arrive at a solution of the general M-ary communications problem when the a priori density is known. Consider the cost function

$$C(\hat{a},a) = (\hat{a}-a)^2.$$

The Bayes estimate for this problem reduces practically to the estimator shown in Figure 6.1 [35]. The solution is for an additive white noise only but can be extended to the case of "colored" noise by the addition of a whitening filter [21]. The radar system model used here assumes a maximum likelihood estimator for targets for which no prior knowledge exists, but subsequent estimates on the basis of which tracking is performed must make use of the previously estimated velocity and range.

The multiple echoes received from a target on each sweep of the search radar are used to refine the estimate of velocity and range. In addition, the statistical nature of target strength as treated by Swerling requires multiple pulses to maximize the probability of obtaining at least one useful detection per sweep [34]. Target strength fluctuations can be severe.

The possibility of purposeful degrading of performance in such a system will now be treated briefly. The model requires a maximum sample throughput rate of 36 kHz, a large data rate for even high speed computers. It is possible that unusual combinations of high data rate near the maximum range of the system, unusually complex tracking requirements, and other control function requirements will

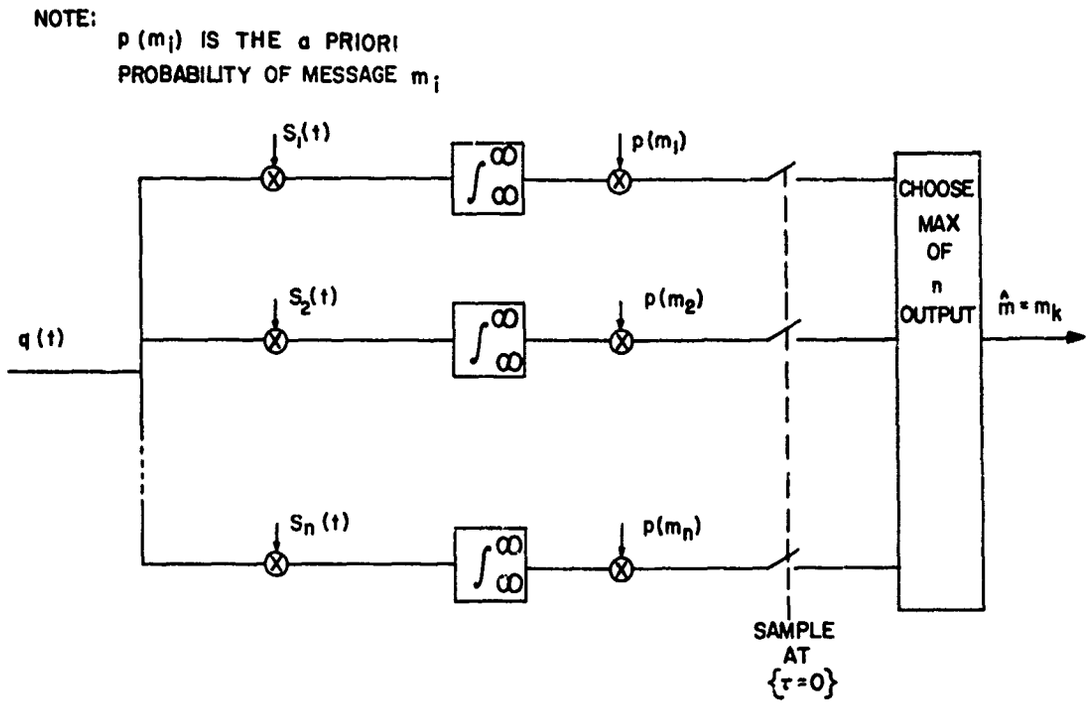

Figure 6.1 Bayes Estimator, M-ary Communications with Known A Priori Density

exceed the processing capability of the computer within the 10 Msec time allowed for each pulse. In this case, instead of causing the system to fail altogether, it is possible to make the decision to not process the data from the next pulse and to finish the pending operations instead. The overall system performance will be degraded but by an anticipated amount. Thus, the logic capability of the computer can be used to advantage in this phase of the system operation.

Another aspect of real systems is demonstrated by the provision for a large range of signal amplitudes to account for differences in target strength and target strength variation due to motion, aspect, and type. In addition to requiring a large number of binary states in the digitization process, the effect of a fixed threshold alluded to previously must be considered. Taking a monochrome pulse as an example,

$$\left| Y(0,\nu) \right| = \left| \frac{\sin \pi \nu T}{\pi \nu} \right| , \tag{6.1}$$

or

$$Y(0,\nu) = F[\psi(t)] ,$$

where $F[\psi(t)]$ is the Fourier transform of the complex time function describing the pulse. Figure 6.2 shows the frequency response to a rectangular envelope of the maximum likelihood receiver for a monochrome pulse. Note that, in addition to the principal peak at $\nu = 0$, there are auxiliary peaks at

$$\pm \frac{3T}{2} , \pm \frac{5T}{2} , \pm \frac{7T}{2} , \ldots .$$

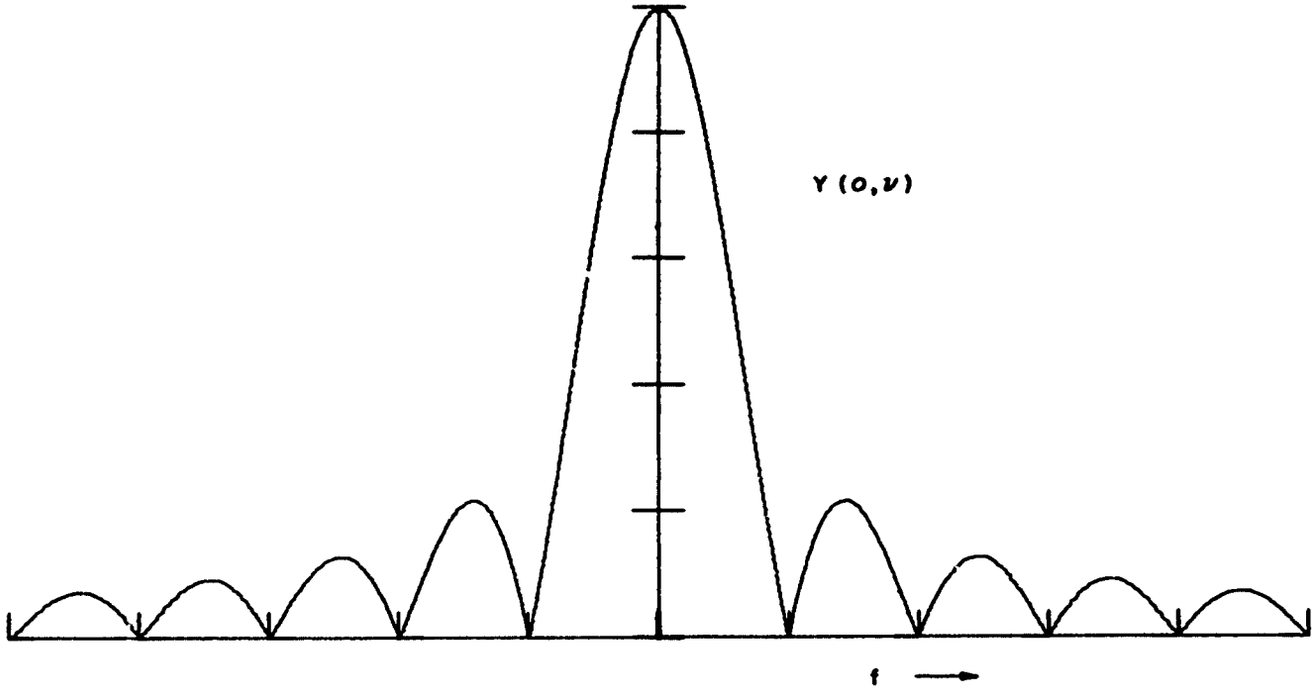

Figure 6.2 Frequency Response of a Maximum Likelihood Receiver to a Monochrome Pulse with Rectangular Envelope

For signals with high energy, these peaks can exceed a fixed threshold and lead to spurious target indications. It is possible to avoid this problem by pulse shaping. For example, the Fourier transform of a Gaussian shaped pulse is also Gaussian, that is, monotonically decreasing from the peak. There are no secondary maxima in this case. The time response on the matched correlator is the autocorrelation function of this pulse envelope and some of the characteristics previously developed for rectangular envelopes must be somewhat revised.

Another method of pulse shaping is one of time weighting of the sample amplitude for the reference signals. One common method is the process of Hamming weighting to reduce the magnitude of secondary peaks in the correlator response. When the transmitted pulse is similarly modulated, a system with bilateral weighting results. Figure 6.3 shows the effect of bilateral Hamming weighting on the magnitude of secondary maxima in a linear FM correlator response.

6.3 A Simulation System

In order to test the functioning of the algorithms described, a general purpose computer was used to generate samples and to perform the algorithm functions. In addition, the computer was used to compile statistical results and to assess the effect of the various sources of error. No attempt was made to simulate the rate at which samples must be processed nor to include the effect of antenna rotation and auxiliary inputs for aircraft height.

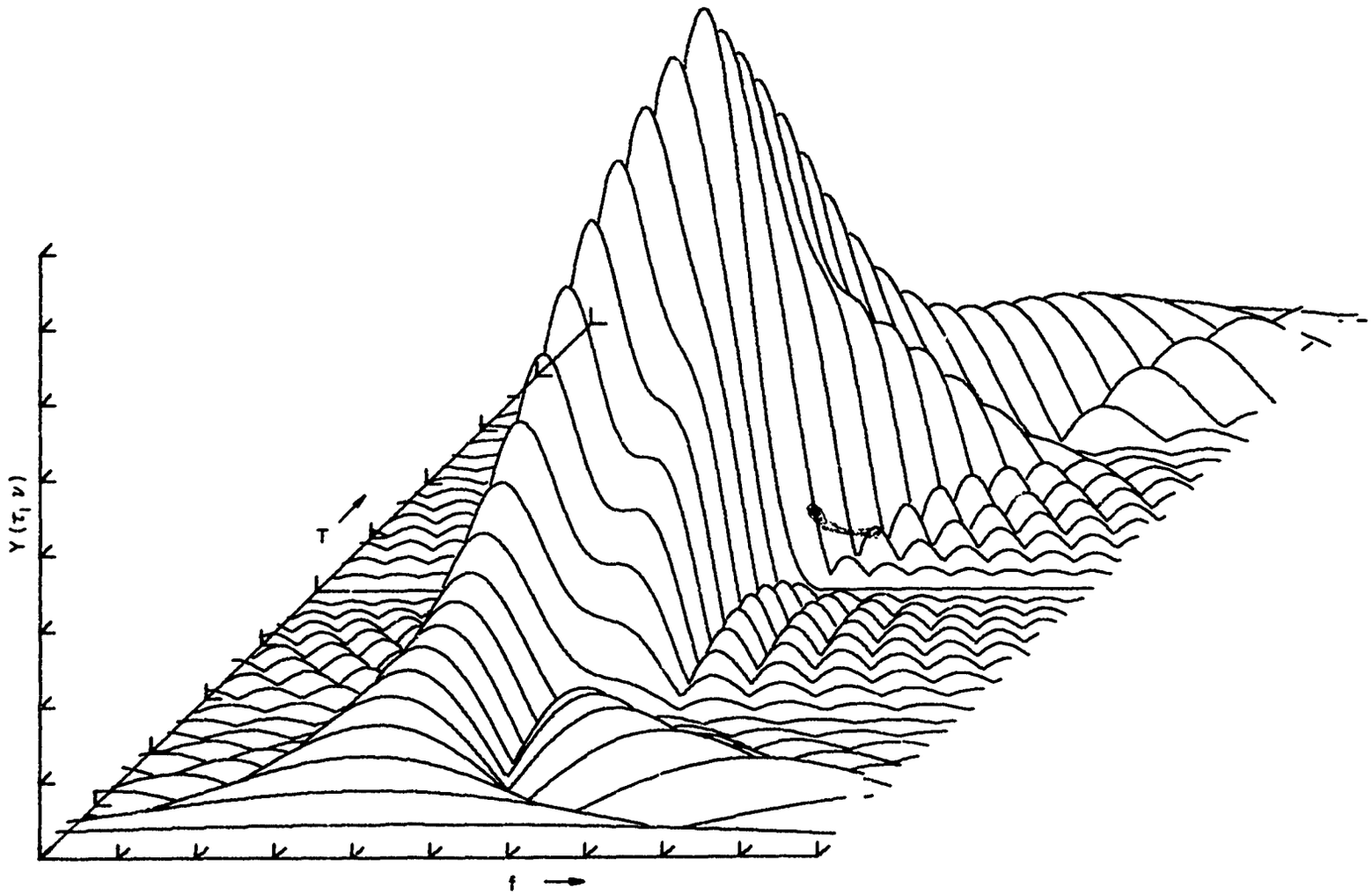

Figure 6.3 The Effect of Bilateral Hamming Weighting on the Secondary Peaks in a Linear F-M Correlator

The simulation was carried out on a Systems Engineering Laboratory Model 840 computer. This is a general purpose computer with approximately 32,000 storage registers, hardware floating point arithmetic unit, and 24 bit word length. Peripheral devices used with the computer were a printer, card reader, and Cal Comp plotter. The plotter was used to generate many of the plots in this thesis.

This machine was programmed in Fortran IV, a higher level language which is well suited to array processing and arithmetic computations. The algorithms described herein were converted to the Fortran language maintaining algorithmic intent since the machine described does not have an Algol processing capability.

Data samples were generated by combining the deterministic value of the uncertainty function with band limited noise. For such a noise, samples separated in time by

$$T_S \geq \frac{1}{2W}$$

are independent. Also, samples in the frequency domain spaced 1/T are independent. A subroutine was used to generate random deviates from a population exhibiting a distribution

$$n(u,\sigma_N^2) \ .$$

Tests of this algorithm show that it exhibits this characteristic to within 1 percent for numbers less than about 4.5 with a somewhat reduced fit at values beyond this limit. The pseodorandom sequence of numbers generated did not repeat in the interval covered by a particular test.

Since frequency samples were taken at intervals of 1/2T, adjacent samples were not independent. Such samples were generated by selecting a random sample with the next sample being selected so as to be correlated with the first. All subsequent samples were chosen with this correlation between neighboring samples. In this way, samples separated by 1/T Hz are independent. The algorithm used to generate these correlated samples is presented in appendix D (Algorithm D.4).

In the various tests of the estimation algorithms all samples were generated at once and stored in a data buffer. Tests included verification of algorithm logical completeness, frame length, and cycle repeat count. The confidence intervals for the various estimation schemes were experimentally obtained using this system.

In experimentally obtaining the confidence interval on the estimate of echo time delay, both the time origin of the sampling schedule and the additive noise were generated using pseudorandom number sequences. The distribution of time origin was selected to be uniformly distributed so that

$$(t_o - T - 1/2\ Ts) \leq t_1 \leq (t_o - T + 1/2\ Ts),$$

where t_o is the true echo time delay, T the pulse length, and Ts the sample interval; t_1 is the first sample generated. The additive noise is an approximation to a Gaussian process with $\mu = 0$, $\sigma^2 = 1.0$.

One topic of investigation using this simulation system was the effect of sampling frequency $f_s = \frac{1}{Ts}$ on the accuracy of the

estimate generated by the algorithms of interest. The results of this investigation for various values of sampling frequency are shown in Figures 6.4 and 6.5. To obtain these curves, 500 trials were made at each data point. The number of occurrences of estimates within a 0.01T interval was recorded. This histogram of occurrences was the input to an algorithm which computes the sample mean, sample variance, and two higher moments of the distribution. The sample standard deviation was then used to define the confidence interval for those trials which could be assumed normally distributed. This is the case for the peak estimate and the estimate based on the quotient when the signal-to-noise ratio is large.

The confidence interval for the quotient algorithm at low signal-to-noise ratios was obtained by printing the histogram and counting the number of cells from the theoretic mean needed to include 30 percent of the occurrences. This interval was found to be very nearly identical to the confidence interval obtained by assuming a normal distribution for the error and using the standard deviation obtained by using the statistical algorithm mentioned above.

Also investigated was the extent of the bias of the quotient algorithm. The results of this study are shown in Figure 6.6. The bias is noticeable only when the sampling frequency f_s is small. Even in this case the actual bias is small in relation to the confidence interval on the estimate. It is unlikely that this bias will ever be of significance in a practical system.

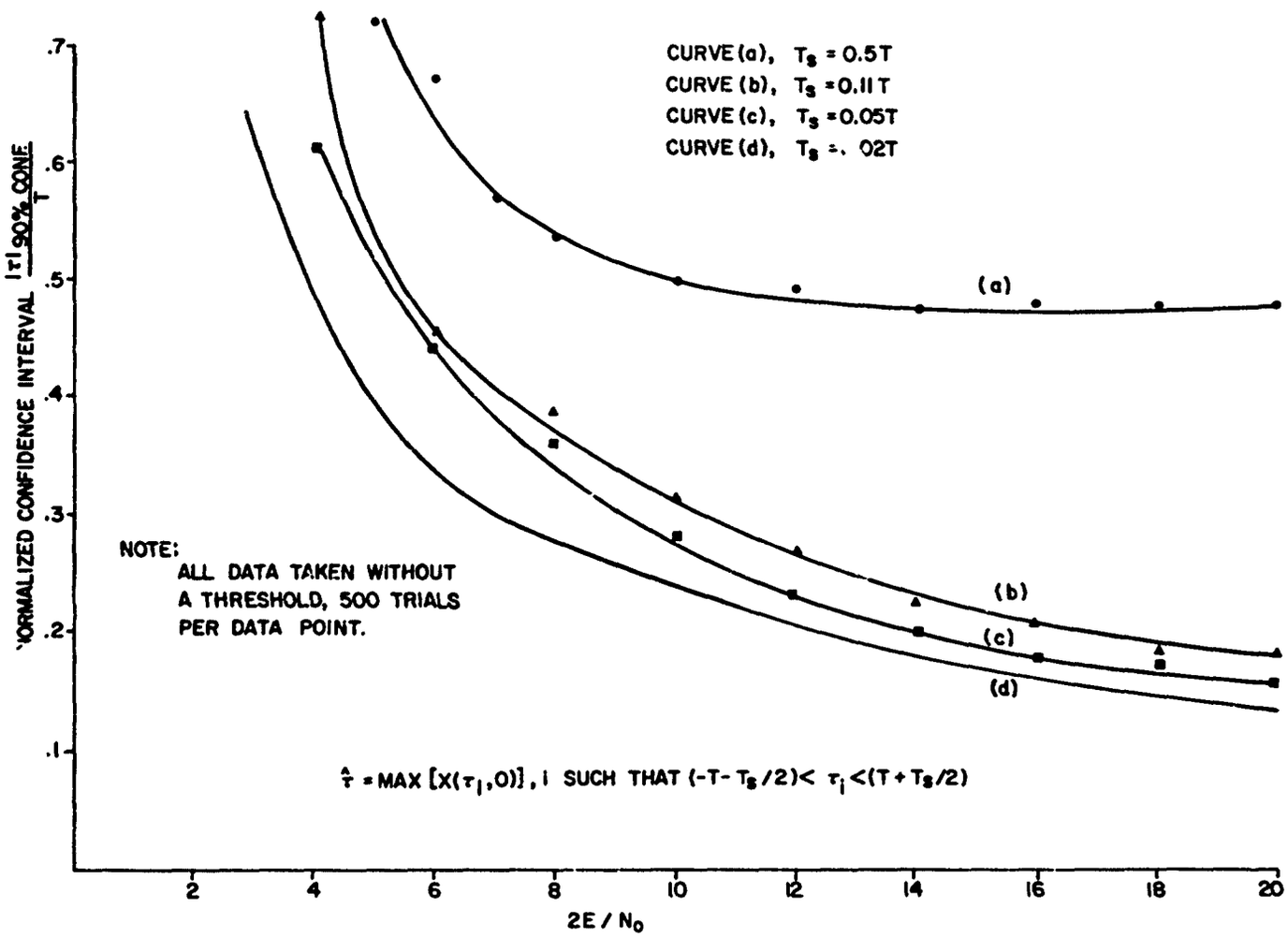

Figure 6.4 Effect of Sampling Rate on Estimate of Time Delay

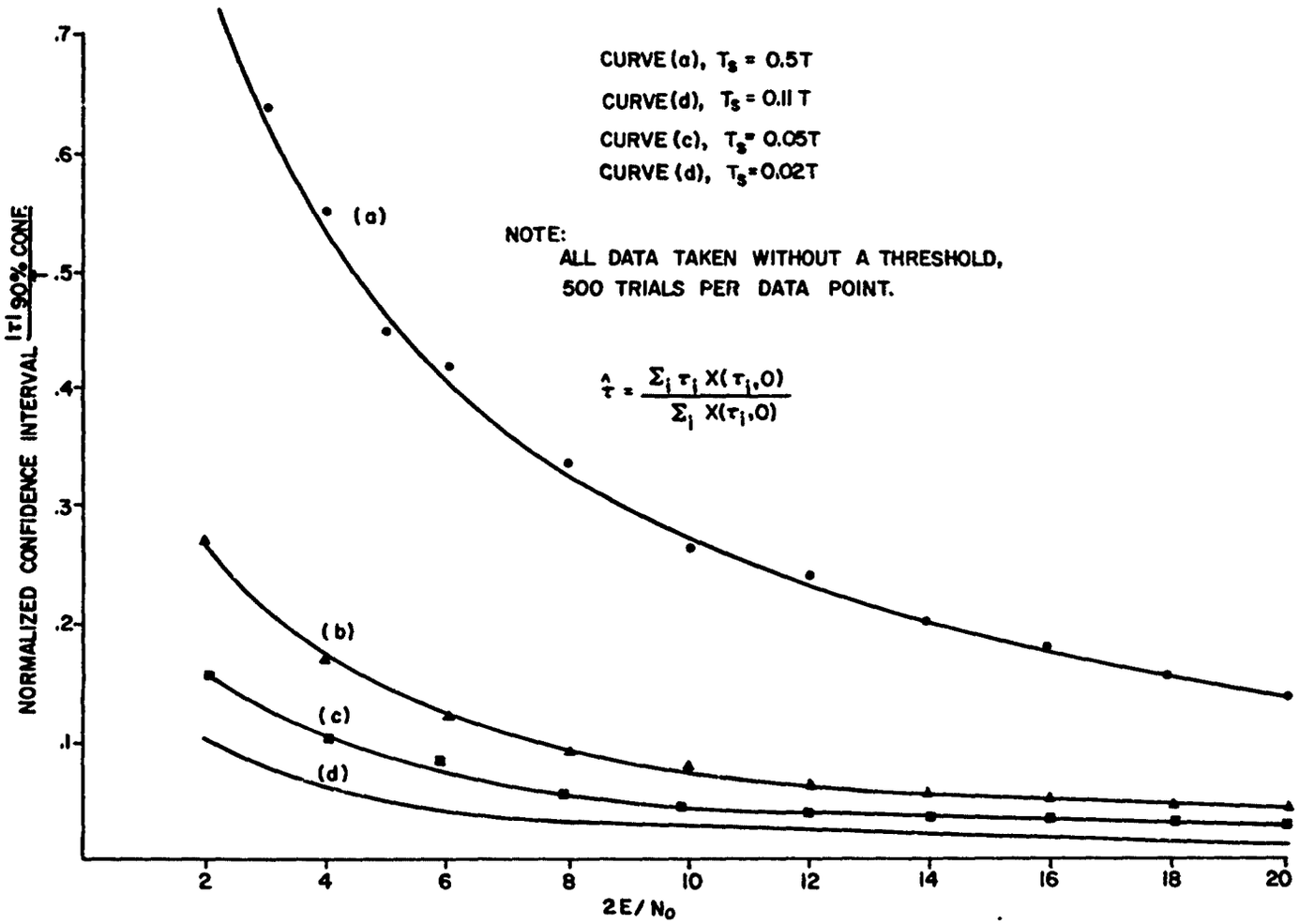

Figure 6.5 Effect of Sampling Rate on Estimate of Time Delay, Quotient Algorithm

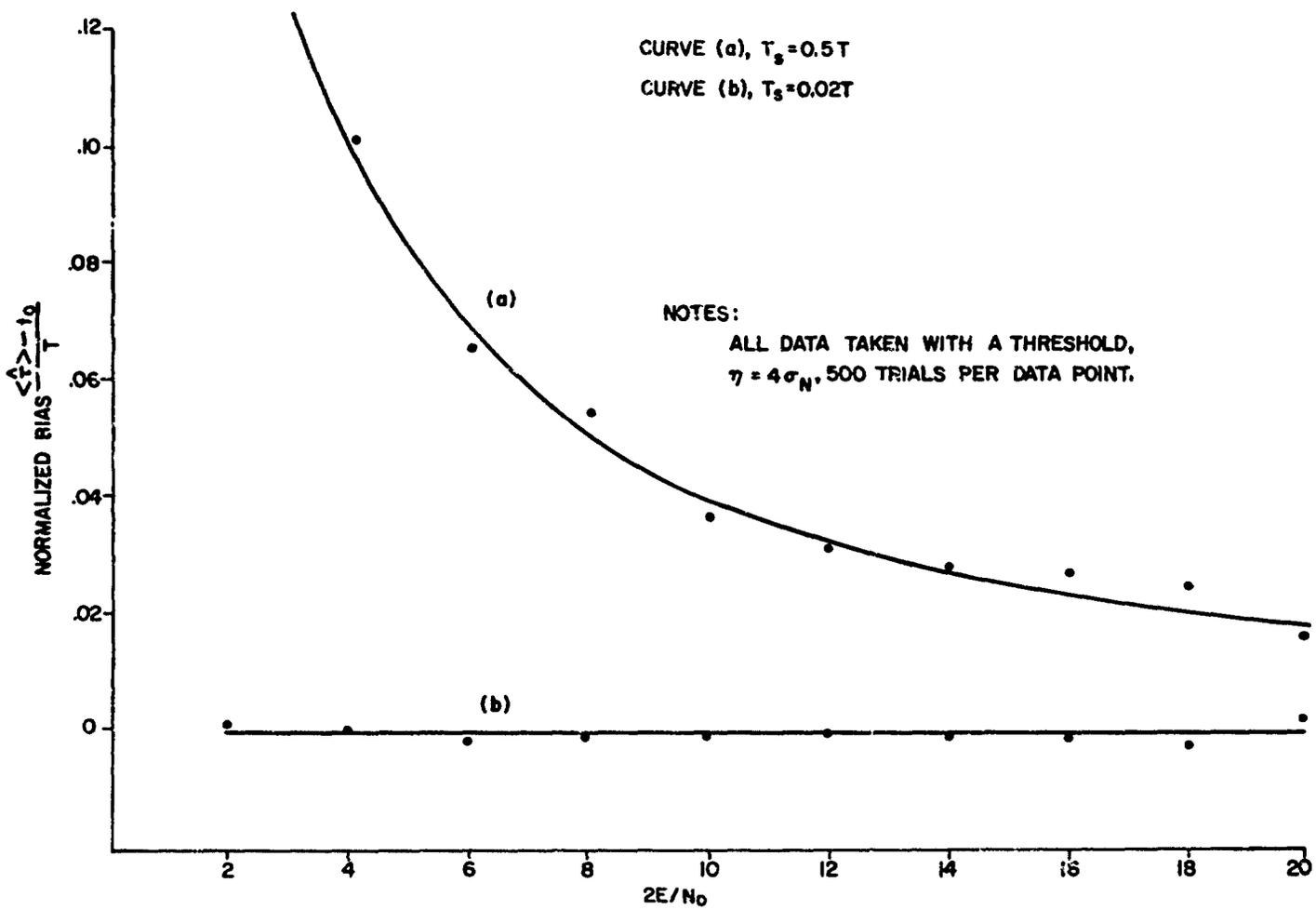

Figure 6.6 Bias of the Quotient Algorithm

The effect of imposing a threshold on the data is shown in Figures 6.7 and 6.8. This threshold is in terms of the correlator output variance and assumes that this noise effect is additive and Gaussian. Hence, a threshold of $\eta = 4$ corresponds to a voltage threshold equivalent to the system mean voltage output

$$\langle x(0,0) \rangle = \frac{2E}{N_o} = 4.$$

Although all of these experimental results were for a monochrome pulse with autocorrelation function

$$|Y(t,0)| = \left(1 - \frac{|\tau|}{T}\right) \frac{2E}{N_o} ,$$

they are applicable as well to the ridgeline response of the linear FM pulse. In this case, however, the confidence interval is in terms of the ridgeline instead of simply the pulse length. For this reason the confidence interval must be scaled by the slope of this ridgeline in the frequency/time domain and the result is:

$$|\tau,\nu|_{\substack{FM \\ 90\% \text{ conf}}} \cong |\tau|_{\substack{\text{monochrome} \\ 90\%}} \times S,$$

where S is $\Delta f/\Delta t$ for the ridgeline response. The equivalence is only approximate because the FM ridgeline response does not define a straight line in the frequency/time domain and it deviates somewhat from the linear decrease from the peak characteristic of the monochrome, rectangular pulse.

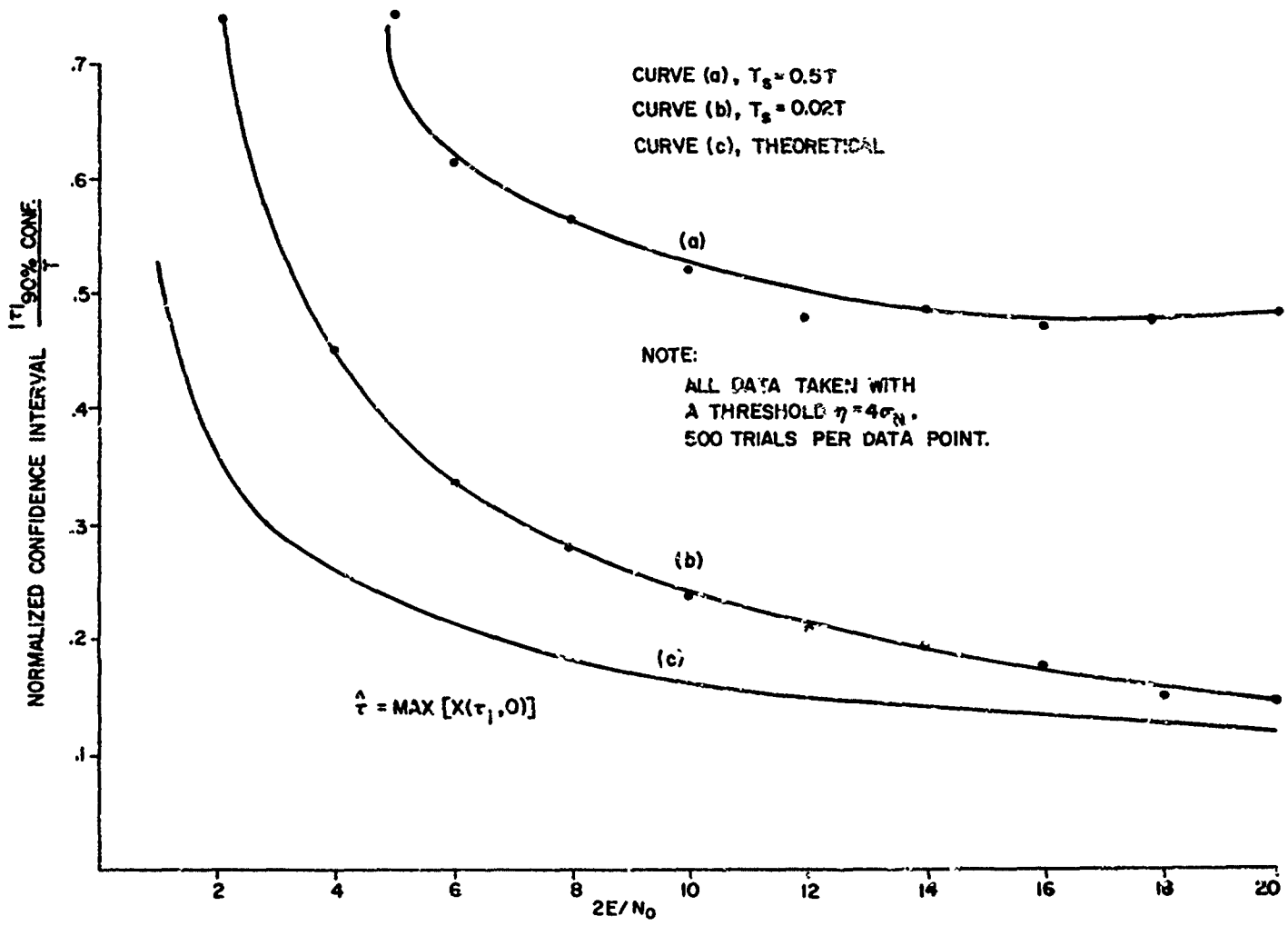

Figure 6.7 Effect of a Threshold on Confidence Interval

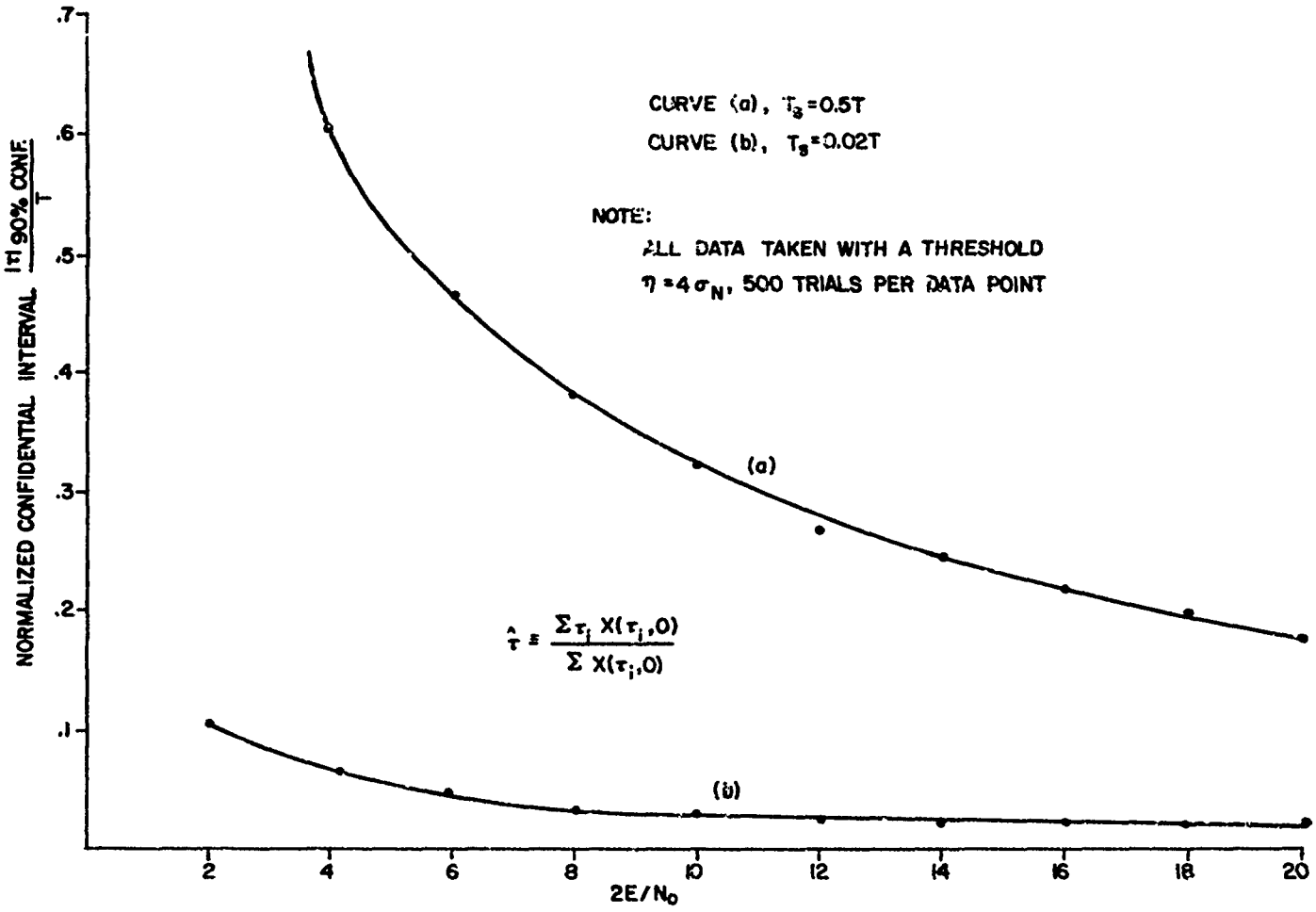

Figure 6.8 Effect of Threshold on Confidence Interval, Quotient Algorithm

The simulation system demonstrated the feasibility of performing parameter estimation using algorithms described in this thesis. In addition, the sensitivity of various algorithms to sampling rate and signal-to-noise ratio was derived experimentally. Some of the results obtained are useful in the design of actual systems since they allow prediction of the estimator performance. For example, by referring to Figure 6.4 and Figure 6.5 it can be seen that for low sampling rates, the proper choice of processing algorithm is as significant a factor as exact sampling rate. For an initial sampling rate such that Ts = 0.5T, replacing the peak estimate by the quotient algorithm is about as effective in reducing the estimation error as is increasing the sampling rate by a factor of ten while retaining the peak estimate. The relative merit of these alternatives is a function of the system design and the decision cannot be made until the respective costs are known. The results presented provide the basis for system tradeoff studies and system performance prediction.

CHAPTER VII

SUMMARY AND CONCLUSIONS

7.1 Statement of the Problem

The general topic discussed in this thesis is the use of algorithms for parameter estimation in a digital signal processor. The work evolved from the current trend toward sampled, digitized data systems, a trend supported by new developments in small digital logic units and the widespread use of programmed automata for system control. Such an algorithmic approach to the estimation problem follows naturally when principal components of the overall system are digital.

7.2 Approach

The approach chosen was to analyze the nature of the estimation problem and then to relate the results of this general analysis to the algorithm functions to be performed. The characteristics of the maximum likelihood estimator were treated and some specific algorithms presented to show how the logic tests can be performed in a computer.

In order to limit the scope of the work, the specific cases treated were the monochrome and linear FM carrier band pulse radar signals. For these signals, the problem of estimating target velocity dependent frequency and echo delay time were chosen as parameters to be estimated. Algorithms to accomplish the estimation

were developed and analyzed on the basis of some measures described in terms of a specific model.

A model of a civil ground control radar was used to assess the effect of performance measures for the more general algorithms.

7.3 Conclusions

It was concluded that digit schemes and the associated algorithms are applicable to a general class of parameter estimation problems. The multi-parameter estimation problem was treated for simple signals and performance measures found. The difficult estimation problem of overlapping FM returns was reduced to a simple problem in pattern recognition on a computer.

The high data rates associated with a multi-target radar case were shown to be within reasonable processing capabilities in a sequential algorithm and a means for selective degradation of the system performance was identified.

In noting the general nature of the algorithms proposed, it can be anticipated that a class of such algorithms will be applicable to a wide variety of parameter estimation problems.

7.4 Suggestions for Further Work

This thesis concentrated on establishing the form which parameter estimation algorithms may take. The types of signals treated were simple ones for which a considerable body of data has been developed. The algorithms are extendable, however, to more complex signals and it is for these that the arithmetic capability of the computer may be best suited.

Some possible applications of such schemes are in situations in which the signal is very noise-like and may, in fact, be unknown until transmitted via an independent data link. Such a situation arises in the use of large seismic arrays used for nuclear test ban monitoring [15].

The treatment in this thesis has avoided the complications resulting from overlapping signals when these are near one another in frequency. This case of interacting signals occurs frequently in communication over a scatter channel, in aircraft tracking when the target cannot be considered a point reflector, and in sonar sounding equipment used for sub-bottom profiling. An investigation of how the flexibility of the computer may be used to improve estimation in these cases is warranted.

APPENDIX A

QUANTIZED CORRELATION FUNCTIONS

As an example of a digital correlation system, the quadrature correlation function will be briefly discussed.

The analytical model of a quadrature correlation function is shown in Figure A.1. This correlator makes use of pairs of samples for both the reference signal and the signal to be processed. The quadrature correlation requires pairs of samples $S_i(2mT_S)$ and $\hat{\hat{S}}_i(2mT_S)$ every $2T_S$ seconds. The real values signal s(t) has $\hat{\hat{s}}(t)$ as its Hilbert transform.

For sample correlation the correlation function is

$$\phi_i(MT_S) = \frac{1}{M} \sum_{m=1}^{M/2} [S_i(2mT_S)g(2mT_S) + \hat{\hat{S}}_i(2mT_S)\hat{g}(2mT_S)] , \qquad (A.1)$$

where T_S is the sampling period and M the number of samples at this sampling rate which define the signal duration. The sampling period T_S is that required by sampling theory to adequately describe a band limited signal.

Similarly,

$$\hat{\hat{\phi}}_i(MT_S) = \frac{1}{M} \sum_{m=i}^{M/2} [S_i(2mT_S)\hat{g}(2mT_S) + \hat{\hat{S}}_i(2mT_S)g(2mT_S)]. \qquad (A.2)$$

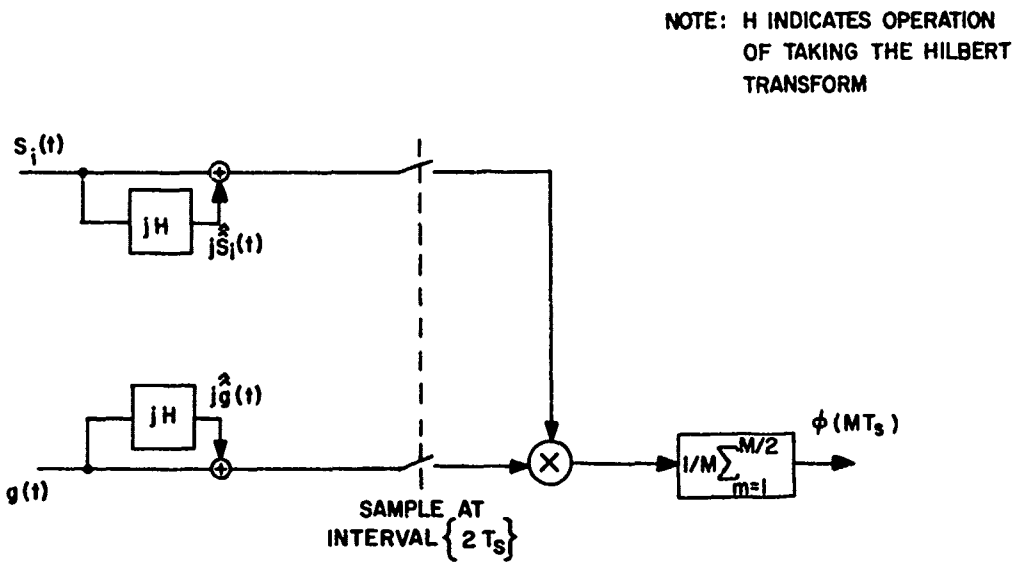

Figure A.1 Analytic Model of a Quadrature Correlator

The envelope output from such a correlator is then

$$\epsilon_i(MT_S) = \sqrt{\phi_1^{\,2}\ (MT_S) + \hat{\phi}_i^{\,2}\ (MT_S)}$$

In referring to Equation (A.1) and comparing this with the analog correlation function,

$$\phi(\tau) = \int_{-T}^{T} q(t)\ S_i(t-\tau)\ dt,$$

it can be seen that the sampled correlation function replaces an integral by a summation. The summation can be accomplished digitally by the use of shift registers, binary multi-stage address, and a digital multiplier unit.

Ackerman has shown that the correlation accuracy, in the limit of many digital state representation approaches that of the analog correlator when the sampling rate [1]

$$f_s = \frac{1}{T_S} = \frac{W}{2}\ .$$

Figure A.2 shows the sampled correlator output variance as a function of sampling rate. It can be seen from this presentation that the errors incurred in digital correlators is due to the digitization error discussed in Chapter V. This error can be made sufficiently small so that the effect of noise received with the signal will be the controlling factor.

Instead of generating the reference signal $s_i(t)$ and then its samples, the samples themselves can be stored in digital form. In referring to Figure A.1, it can be seen that these two techniques are

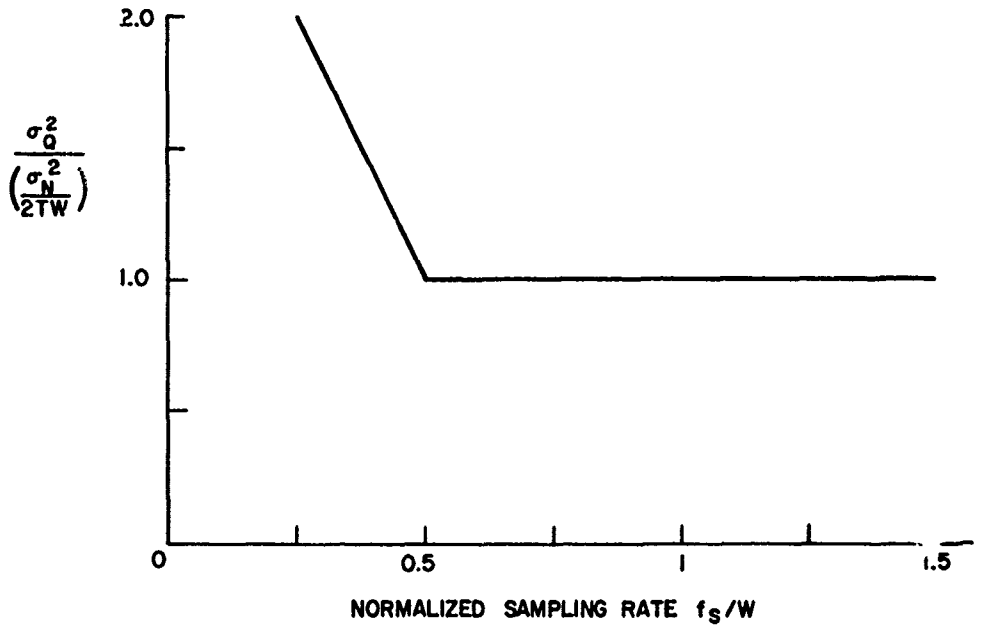

Figure A.2 Quadrature Correlation Function Variance as a Function of Sampling Rate

equivalent. Once the samples have been determined, they need only be recalled from a memory unit in the proper sequence.

APPENDIX B

NON-LINEARITY IN THE LINEAR FM RIDGELINE RESPONSE

The uncertainty function for the linear FM pulse with rectangular envelope is

$$|Y(\tau,\nu)| = \left(1-\frac{|\tau|}{T}\right)\left|\frac{\sin[(B\tau-\pi\nu)(1-\frac{|\tau|}{T})T]}{B\tau-\pi\nu}\right|. \tag{B.1}$$

If we limit our discussion to positive values of τ and make the substitution

$$\beta = [(B\tau-\pi\nu)(1-\frac{\tau}{T})T],$$

Equation (B.1) becomes

$$|Y(\tau,\nu)| = (1-\frac{\tau}{T})\left|\frac{\sin(\beta)}{B\tau\ \pi\nu}\right|. \tag{B.2}$$

To find the equation of the ridgeline, we take the derivative with respect to ν and equate this to zero. It is obvious that removing the absolute value signs does not affect the location of the zeros in the first derivative. Hence,

$$\frac{d}{d\nu}[Y(\tau,\nu)] = (1-\frac{\tau}{T})\frac{d}{d\nu}\ \frac{\sin(\beta)}{B\tau-\pi\nu}\ , \tag{B.3}$$

which is of the form $\frac{d}{d\nu}[\frac{u}{v}]$.

Equation (B.3) yields:

$$\frac{d}{d\nu}\,[Y(\tau,\nu)] = (1-\frac{\tau}{T})\,\frac{(B\tau-\pi\nu)\cos(\beta)(\pi\tau-\pi T)-\sin(\beta)(-\pi)}{(B\tau-\pi\nu)^2}$$

$$= (1-\frac{\tau}{T})\,\frac{\pi[(B\tau-\pi\nu)\cos(\beta)(\tau-T)+\sin(\beta)]}{(B\tau-\pi\nu)^2} \qquad \text{(B.4)}$$

Equating this result to zero and clearing terms, the result is given by:

$$\frac{(B\tau-\pi\nu)\cos(\beta)(\tau-T)+\sin(\beta)}{(B\tau-\pi\nu)^2} = 0$$

or

$$= \frac{1}{(B\tau-\pi\nu)^2}\quad\{\tan[(B\tau-\pi\nu)(1-\frac{\tau}{T})\,T] - (B\tau-\pi\nu)(1-\frac{\tau}{T})T\,\}\,.$$

(B.5)

One condition under which the tangent is equal to its argument is when the argument is zero. Hence,

$$(B\tau-\pi\nu)(1-\frac{\tau}{T})\,T = 0\,,$$

which is, however, not a valid root.

In order to investigate other roots of Equation (B.5), a peak finding algorithm was employed to trace the character of the principal response ridgeline. The general behavior of this response is graphed

in Figure B.1. It can be seen from this figure that the ridgeline is essentially linear in the vicinity of the peak. The equation of the near peak response is

$$\nu = \frac{B\tau}{\pi} \quad .$$

The deviation becomes pronounced for large values of the parameter τ .

Substituting the value of the ridgeline function in Equation (B.1) yields the value of the peak output with delay time. This behavior deviates from the purely linear decrease observed in the monochrome case. Figure B.2 is a graph of this response characteristic.

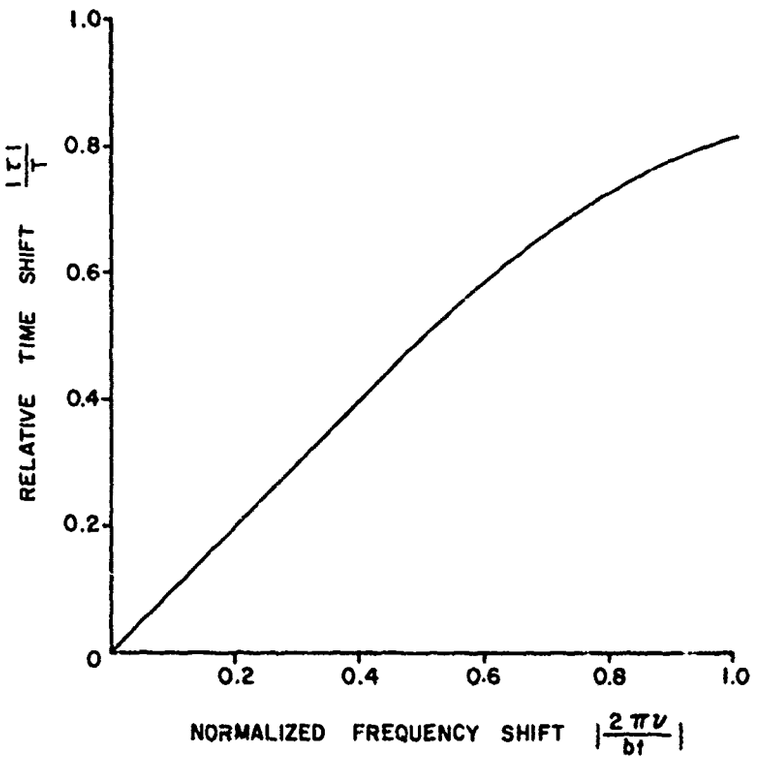

Figure B.1 Slope of Ridgeline Response with Delay Time

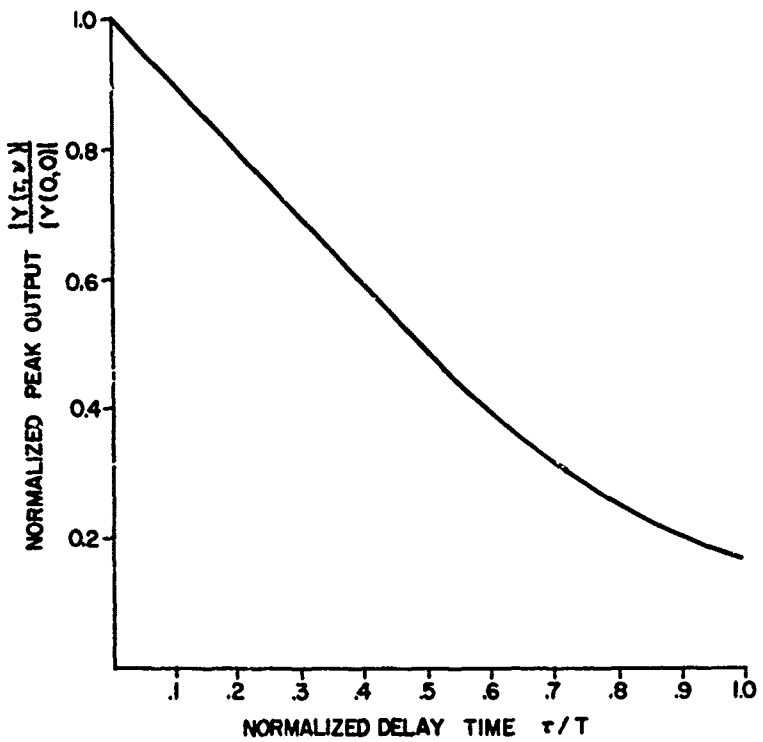

Figure B.2 Behavior of Correlator Peak Output with Delay Time

APPENDIX C

MISCELLANEOUS MATHEMATICS

C.1 Quotient of Random Variables

Consider the case

$$\hat{\tau} = \frac{\sum_i \tau_i X(\tau_i,0)}{\sum_i X(\tau_i,0)} \quad , \tag{C.1}$$

where

$$X(\tau_i,0) = Y(\tau_i,0) + N_i \ .$$

$Y(\tau_i,0)$ is purely deterministic and N_i is $n(0,\sigma_N^2)$.

Then,

$$\mathrm{Var}(\hat{\tau}) = \mathrm{Var}\left\{\frac{\sum_i \tau_i(Y(\tau_i,0) + N_i)}{\sum_i (Y(\tau_i,0) + N_i)}\right\} . \tag{C.2}$$

When the sample spacing is such that all samples N_i are independent, then Var $(\hat{\tau})$ takes the form

$$\sigma_{\hat{\tau}} = \sigma_{w/v} = [\mathrm{Var}\ (w/v)]^{1/2}, \quad w,v \text{ both normal.}$$

By inspection, for an autocorrelation function of the form

$\frac{2E}{N_o}(1-\frac{|\tau|}{T})$,

$$\mu_w = \hat{\tau}\left(\frac{8E}{N_o} - 4\eta\right), \quad \mu_v = \frac{8E}{N_o} - 4\eta,$$

where η is the threshold applied to $X(\tau_i,0)$. The normalization term $2E/N_o$ is the value of $Y(0,0)$.

Also,

$$\sigma_w^{\ 2} = n\sigma_N^{\ 2} \sum_i \tau_i^{\ 2} \ , \ \sigma_v^{\ 2} = n\sigma_N^{\ 2}$$

Then, from Haugen [14],

$$\sigma_{w/v} \cong \frac{\mu_w}{\mu_v}\left[\frac{\sigma_w^{\ 2}}{\mu_w^{\ 2}} + \frac{\sigma_v^{\ 2}}{\mu_v^{\ 2}} - 2\rho \ \frac{\sigma_w\sigma_v}{\mu_w\mu_v}\right]^{1/2} , \tag{C.3}$$

or, more exactly,

$$\sigma_{w/v} = \frac{\mu_w}{\mu_v}\left[\frac{\sigma_v^{\ 2}}{\mu_v^{\ 2}} - 2\rho \ \frac{\sigma_w\sigma_v}{\mu_w\mu_v} + \frac{\sigma_w^{\ 2}}{\mu_w^{\ 2}}\right.$$

$$\left. + 8\,\frac{\sigma_v^{\ 4}}{\mu_v^{\ 4}} - 16\rho \ \frac{\sigma_w^{\ 3}\sigma_v}{\mu_w^{\ 3}\sigma_v} + 3\frac{\sigma_w^{\ 2}\sigma_v^{\ 2}}{\mu_w^{\ 2}\mu_v^{\ 2}} + \cdots\cdot\right]^{1/2} . \tag{C.4}$$

Also,

$$\mu_{w/v} = \frac{\mu_w}{\mu_v}\left[1 + \frac{\sigma_v}{\mu_v}\ \frac{\sigma_v}{\mu_v} - \rho \ \frac{\sigma_w}{\mu_v} \quad 1 + \frac{\sigma_v^{\ 2}}{\mu_v^{\ 2}} + \ldots\right] .$$

If second and higher powers in the last term are ignored,

$$\mu_{w/v} = \frac{\mu_w}{\mu_v} + \frac{\sigma_v\mu_w}{\mu_v}\left(\frac{\sigma_v}{\mu_v} - \frac{\rho\sigma_w}{\mu_w}\right) . \tag{C.5}$$

The random variable $Z = W/V$ will be approximately normal in the case where the coefficients of variation σ_{w/μ_v} and σ_{v/μ_v} both are less than about 10 percent.

In Equations (C.4) and (C.5), the correlation coefficient

$$\rho = \rho_{wv} = \frac{\text{Cov. } (w,v)}{\sigma_w \sigma_v} = \frac{E[(w-\mu_w)(v-\mu_v)]}{\sigma_w \sigma_v} . \tag{C.6}$$

Then,

$$E[(w-\mu_w)(v-\mu_v)] = E\left[\sum_i \tau_i v_i \sum_k v_k\right]$$

$$= E\left[\sum_i \tau_i v_i^2 + \sum_i \sum_k \tau_i v_i v_k\right] , \tag{C.7}$$

where k is a dummy index of summation used to distinguish between the numerator and denominator terms.

The term involving the double sum becomes

$$E \sum_{i \neq} \sum_k \tau_i v_i v_k = \sum_{i \neq} \sum_k \tau_i E(v_i v_k)$$

but the samples are chosen to be independent; hence,

$$\tau_i E(v_i v_k) = \tau_i E(v_i) E(v_k) = 0 .$$

The covariance is given by:

$$E\left(\sum_i \tau_i Y_i^2\right) = \sum_i \tau_i \sigma_N^2 . \tag{C.8}$$

Therefore,

$$\rho_{wv} = \frac{\sum_i \tau_i \sigma_N^2}{\left(\sum_i \tau_i \sigma_N^2\right)^{1/2} \left(\sum_i \sigma_N^2\right)^{1/2}}$$

$$= \frac{\sum_i \tau_i}{\left(\sum_i \tau_i^2\right)^{1/2} \sqrt{n^2}} = \frac{1}{\sqrt{n^2}} , \qquad (C.9)$$

where n is the number of terms summed.

This result insures that when a large number of samples are taken, the numerator and denominator are essentially uncorrelated and the result from Equation (C.5) becomes

$$w/v = \frac{\mu_w}{\mu_v} + \frac{\sigma_v 2 \mu_w}{\mu_v 2}$$

$$= \frac{\mu_w}{\mu_v} + \varepsilon , \qquad (C.10)$$

where ε is a measure of the bias of the estimate. When ε is very small in relation to μ_w/μ_v, the estimate can be considered essentially unbiased.

Writing this term as

$$\varepsilon = \frac{\sigma_v^2}{\mu_v^2} \mu_w ,$$

it is seen that the situation where the coefficient of variation σ_v/μ_v is small, the estimate is unbiased.

For the case of large n and small coefficient of variation,

$$Z = \frac{w}{v} \text{ is distributed as } n\left(\frac{\mu_w}{\mu_v}, \sigma_{w/v}^{\ 2}\right),$$

where

$$\sigma_{w/v}^{\ 2} = \frac{1}{\mu_v}\left(\frac{\mu_w^{\ 2}\sigma_v^{\ 2} + \mu_v^{\ 2}\sigma_w^{\ 2}}{\mu_v^{\ 2} + \sigma_v^{\ 2}}\right)$$

This results in the following:

$$\mu_{w/v} = \frac{\mu_w}{\mu_v} = \hat{\tau} \quad \text{for } \sigma_v/\mu_v < 0.1$$

or $\frac{2E}{N_o} - \eta > 5.$

When the threshold η is set so that $\eta = 4\sigma_N^{\ 2}$, then $2E/N_o$ must be greater than 9.

C.2 Estimation by Intersecting Linear Regression

Consider the totality of sample points corresponding to a single unique event at the correlator output; by knowing the noise free response of the system, it is possible to perform a least squares fit on the data applying either linear or polynomial regression analysis. For the signals treated, this functional form consists of two linear segments. By fitting these two segments using linear regression, the abscissa of their join point will constitute the estimate sought in an estimation algorithm. Hudson develops the method of minimizing the total mean square error between

two regression curve segments and the data points [17]. Since it is not known at the outset which points are to be considered when performing the two regressions, a method must be developed for optimizing the process of fitting the regression lines to the data.

Kastenbaum reports the confidence interval on the abscissa of the join point for two linear regressions [18]. This result is

$$X^2[(b_1-b_2)^2-t^2S^2_{(b_1,b_2)}]-2X[(a_2-a_1)(b_1-b_2)-t^2S_{(a_2,a_1)(b_1,b_2)}]$$

$$+ [(a_2-a_1)^2-t^2S^2_{(a_2,a_1)}] , \qquad (C.11)$$

where the linear regressions $Y_1 = a_1+b_1x$ and $Y_2 = a_2+b_2x$ intersect at X. In Equation (C.11), $S_{(a_2,a_1)}$, $S_{(b_1,b_2)}$ ... are the sample standard deviations of samples grouped to select a_1, a_2, b_1, b_2. The parameter t is the appropriate level of the student distribution for $n_1 + n_2 - 4$ degrees of freedom, where n_1 and n_2 are the number of samples used to generate the two regressions.

By assuming that, on the average, the regression lines will have equal and opposite slope and X is x = 0, Equation (C.11) becomes, after replacing the sample variance with the underlying variance,

$$X^2[2b^2-t^2\sigma_N{}^2]-2X[-t^2\sigma_N] + [-t^2\sigma_N{}^2] = 0.$$

Then, replacing b by $2E/TN_o$ get,

$$X^2 \left[\frac{8E^2}{T^2N_o{}^2} -t^2\sigma_N{}^2\right] +X[2t^2\sigma_N]-[t^2\sigma_N{}^2] = 0.$$

APPENDIX D

MISCELLANEOUS ALGORITHMS

D.1 Algorithm For Estimation, Simple Monochrome Case

```
procedure D.1 (x,t,f,m,tout,fout,xout,n,T,Ts)
integer m,n; integer array x,t,f,tout,fout,xout; value n,T,Ts;
real T,Ts; comment: D.1 selects the largest value of samples within
a 2T interval with time spacing Ts and outputs the parameters of
correlation value, time delay, and frequency as xout, tout, fout.
This process is repeated for all samples.  The frequency domain is
divided into regions 1/T cycles wide.  It is assumed that references
are spaced 1/2 T.  A maximum of n estimates can be output.  The
parameter q below is the number of 1/T frequency increments in the
total range of permitted frequency shifts.
begin
      integer array Testimate [1:q], Festimate [1:q], xtestvalue [1:q],
      low [1:q]; integer k,i,j;
      k:=0;
      for i:=1 step 1 until q do xtestvalue [i]:=low[i]:=0;
      for j:=1 step 1 until m do
          begin
          j:=f[i]/2; if low [j]=0 then
              begin low [j]:=t [i], xtestvalue [j]:= x[i];
              Testimate [j]:= t[i]; Festimate [j]:= t[i] end
```

```
            else if (t[i]-low[j]) > 2T/Ts then SSetE(tout,fout,xout,low,
                Testimate, Festimate, xtestvalue,k,j)
            else if x[i] > xtestvalue [j] then
                begin xtestvalue [j]:=x[i]; Testimate [j]:=t[i];
                Festimate [j]:=f[i] end
            end:
        for i:=1 step 1 until q do
        if low [i]≠0 then SSetE(tout,fout,xout,low,Testimate,Festimate,
            xtestvalue, k,n,i)
end D.1
procedure SSetE(t,f,x,l,T,F,X,k,n,i)integer array t,f,x,l,F,T,X;
integer k,n,i;
comment: This procedure transfers the contents of a temporary
working array to an output array with tests for output array overflow.
begin k:= k+1; if k > n then OVERFLOW else
        begin t[k]:=T[i]; f[k]:=F[i]; x[k]:=X[i];
        l[i]:=0 end
end SSetE
```

D.2 Algorithm For Treating the Linear FM Case, Direct Method.

```
procedure D.2(x,t,f,m,tout,xout,n,T,Ts,S,Eps)
integer m,n; integer array x,t,f,tout,fout,xout; value n,T,Ts,
S,Eps; real T,Ts,Eps;
comment: D.2 searches in the time/frequency domain for samples which
lie within ±Eps of a line defined by the first new sample and the
incremental frequency shift S. Data points once processed have their
value of x(i) set to zero. A total of n estimates can be output.
```

```
begin
integer Testimate,Festimate,xtestvalue,low,i,j,k; real z, Delt; k:=0;
for i:=1 step 1 until m do
A: if x[i] ≠ 0 then
      begin low:=t [i]; j:= [i];
B: Testimate:=t[i]; Festimate:=f[i]; xtestvalue:=x[i];
C: x[i]:=0;
      for j:= j+1 while ((t[i]-low) < 2*T/Ts) ∧ j ≤ m do
          if x[j]≠0 then begin Delt:=t[j]-low; x:= Delt* S;
          if(f[j] ≥ Z-Eps) ∧ (f[j] ≤ Z+Eps) then
              begin if x[j] > xtestvalue then go to B: go to C
              end
          end
      k:=k+1; SSetE(tout,fout,xout,low,Testimate,Festimate,xtestvalue,
          k,n,1)
end of loop A;
end D.2
```

D.3 Algorithm For Treating the Linear Case, Transformation Method.

```
procedure D.3 (x,t,f,m,tout,xout,fout,n,T,Ts,S,Eps)
integer m,n; integer array x,t,f,tout,fout,xout; value n,Eps,
T,Ts,S; real T,Ts,Eps,S;
```

comment: D.3 projects samples in the time/frequency domain onto a linear space by performing the transformation

$$t_i' = t_i - f_i\ (1/S).$$

Tests are made in the t' space and estimates are output whenever a new datum test is made or at the end of all processing. The parameter

q below is the number of intermediate storage units needed to span a 2T time interval.

```
begin
integer q,i,j,k,kk; integer array Tprmx [1:q], Tprmt[1:q],
Tprmf [1:q]; Tprml [1:q]; kk:=0;
for i:=1 step 1 until q do Tprml [i]:=0;
for i:=1 step 1 until m do
        begin
        j:= (t[i]-f[i]/S)/Ts;
        for k:= j,j-1,j+1,j-2,j+2 do
            begin k:= MOD (k,q);
            if Tprml [k] =0 then go to A else
            if (x[i]-Tprmx [k]) ≤ 2*T/Ts then
                begin Tprmx [k]: = x[i]; Tprmt [k]: = t[i];
                Tprmf [k]: = f[i]
                end;
            go to B
            end;
        SSet E(tout,fout,xout,Tprml,Tprmt,Tprmf,Tprmx,kk,n,k)
A:      end
        k: = MOD(j,q); Tprml[k]: = Tprmt[k]: = t[i]; Tprmf[k]:= f[i];
        Tprmx [k]: = x[i]
for i:= 1 step 1 until q do
if Tprml [i] = 0 then
SSetE(tout,fout,xout,Tprml,Tprmt,Tprmf,Tprmx,kk,n,k)
end D.3
```

D.4 Algorithm for Generating Correlated Gaussian Pseudorandom Numbers

```
procedure BVnorm(mu1,mu2,var1,var2,rho12,old,new)
real mu1,mu2,var1,var2,rho12,old,new, value mu1,mu2,var1,var2,rho12;
comment: BVnorm generates a random variable with mean mu2 and
variance var2 which is correlated with a previous sample, old.  The
correlation between samples is rho12.  The parameters mu1 and var1
are the mean and variance from the distribution which lead to the
first sample and are used to scale the input value so that it can
be treated as belonging to a normal distribution with mean 0 and
variance 1.
begin
real temp,x; temp:= (old-mu1)/SQRT(var1); GAUSS(1,0,0);
comment: The routines SQRT and GAUSS are assumed to be standard
library functions the first of which returns a value equal to the
positive square root of the argument and the second is a routine
which sets the parameter x equal to a sample from a distribution
which is normal and has mean zero and variance one;
new:=rho12*temp+SQRT(1-rho12**2); new:=(new*SQRT(var2))+mu2
end BVnorm
```

APPENDIX E

ALGOL 60 LANGUAGE REFERENCE

The algorithm language (ALGOL 60) is the product of an international conference which included the United States. The language has been adopted widely for the purpose of disseminating algorithm intent in publications. It has not found wide acceptance in the United States as a programming language but is used in the literature.

The language exists in three kinds of representations: reference, hardware, and publication. The reference language is in terms of a rigidly and comprehensive syntax which must be adhered to in the hardware or publication implementations. For reasons of variations in card codes, preferred type fonts, and national differences in use, the language provides for variations in representation within the reference language syntax.

Table E.1 provides a compilation of symbols provided by the reference language and as implemented herein for logical consistency and in keeping with available typographic symbols.

The language consists of named or unnamed procedures within which variables are declared, processes are defined, and various repetitive operations and tests are accomplished. All variables must be declared and these may be subscripted. For example, the declaration

<u>real</u> <u>array</u> a[1:3, -6:100, 0:2]

declares the variable a as a triple subscripted floating point array where the bounds on the subscripts are shown. Note that negative or zero subscript values are allowed.

Arithmetic operations and relational tests make no distinction between floating point or integer variables. Integer variables are used primarily to represent quantities which can only take on distinct values, but there is little restriction to use.

The language contains a number of standard operations, some of which are tabulated in Table E.2 along with the logical functioning of these. Operators, declarations, and some other predefined symbols are distinguished by underlining or, where possible, bold face type. Variables may have similar character representation but are presented without underlining or in italics.

Interested readers are referred to Reference 26 for a complete description of the language.

TABLE E.1 SUMMARY OF ALGOL 60 SYMBOLOGY

+	, plus or addition	/	, division
-	, minus or subtraction	**	, exponentiation
*	, multiplication		

RELATIONAL OPERATORS

<	, less than	≥	, greater than or equal to
≤	, less than or equal to	>	, greater than
=	, equal to	≠	, not equal to

LOGICAL OPERATORS

¬	, not	⊃	, implies
∧	, and	≡	, equivalent
∨	, or		

OTHER SYMBOLS

:=	, replacement	<u>begin</u>...<u>end</u>	, statement bracket
()	, arithmetic parentheses	<u>TRUE</u>	, logical value $a \vee \overline{a}$
[]	, subscript bracket	<u>FALSE</u>	, logical value $a \wedge \overline{a}$

TABLE E.2 ALGOL 60 EXPRESSIONS

DECLARATIONS

<u>procedure</u>; <u>integer</u>; <u>real</u>; <u>boolean</u>; <u>integer array</u>; <u>real array</u>; <u>value</u>

COMPOUND STATEMENT

<u>begin</u> ⟨statement⟩ ; ⟨statement⟩ ; ⟨statement⟩ ; <u>end</u>

A compound statement may be used wherever a statement can occur.

TRANSFER OF CONTROL TYPE STATEMENTS

<u>go to</u> ⟨label⟩ ; ⟨statement⟩ ; ⟨label⟩ : ⟨statement⟩

<u>if</u> ⟨logical expression⟩ <u>then</u> ⟨statement⟩ ; ⟨statement⟩

TRUE

FALSE

LOOP STATEMENTS

<u>for</u> ⟨variable⟩ := ⟨for list⟩ <u>step</u> ⟨variable⟩ <u>until</u> ⟨variable⟩
<u>do</u> ⟨statement⟩

-or-

<u>for</u> ⟨variable⟩ := ⟨for list⟩ <u>while</u> ⟨logical expression⟩
<u>do</u> ⟨statement⟩

-for example-

<u>for</u> q:=1 <u>step</u> 5 <u>until</u> 25 <u>do</u> a[q] := b[q]

This example starts with q equal to 1 and steps in units of 5 until the value 25 is exceeded.

BIBLIOGRAPHY

1. Ackerman, C. L., "Effects of Nonuniform Sampling and Limiting on Correlation Function," Ph.D. Dissertation, The Pennsylvania State University, University Park, Pennsylvania 1969.

2. Balakrishnan, A. V., "Computing Algorithms for Detection Problems," Proc. of the Symposium on Comp. Proc. in Comm., April 1969, pp. 603-615.

3. Berkowitz, R. S., editor. Modern Radar Analysis, Evaluation and System Design. New York: John Wiley and Sons, 1965.

4. Beutler, F. J., "Sampling Theorems and Bases in a Hilbert Space," Info. and Control, Vol. 4, 1961, pp. 97-117.

5. Capon, J., "Applications of Detection and Estimation Theory to Large Array Seismology," Proc. IEEE, Vol. 58, No. 5, May 1970, pp. 760-770.

6. Cooley, J. W. and Tukey, J. W., "An Algorithm for the Machine Calculation of Complex Fourier Series," Math. of Computation, Vol. 19, April 1965, pp. 297-301.

7. Cramer, H., Mathematic Methods of Statistics. Princeton: Princeton University Press, 1946.

8. Davenport, W. B. and Root, W. L., An Introduction to the Theory of Random Signals and Noise. New York: McGraw-Hill, 1958.

9. Espensen, L. L , "Evaluation of Track-While-Scan Computer Logics," in Radar Techniques for Detection Tracking and Navigation, ed. W. T. Blackband. New York: Gordon and Breach, 1966.

10. Gold, B. and Rader, C. M., Digital Processing of Signals. New York: McGraw-Hill, 1969.

11. Gushkov, V. M., Introduction to Cybernetics, Trans. ed. G. M. Krang. New York: Academic Press, 1966.

12. Holmos, P. R., Measure Theory. New York: D. Van Nostrand, 1950.

13. Harman, W. W., Principles of the Statistical Theory of Communication. New York: McGraw-Hill, 1963.

14. Haugen, E., Probabilistic Approaches to Design. New York: John Wiley and Sons, Inc., 1968.

15. Helstrom, C. W., Statistical Theory of Signal Detection, London: Pergamon Press, 1968.

16. Hogg, R. V. and Craig, A. T., Introduction to Mathematical Statistics. Toronto: McMillan, 1970.

17. Hudson, D. J., "Fitting Segmented Curves Whose Join Points Have to be Estimated," JASA, Vol. 61, No. 316, December 1966, pp. 1097-1129.

18. Kastenbaum, M., "A Confidence Interval on the Abscissa of the Point of Intersection of Two Fitted Linear Regressions," Biometrics, Vol. 15, 1959, pp. 323-324.

19. Klauder, J. R., "The Design of Radar Signals Having Both High Range Resolution and High Velocity Resolution," Bell System Tech. J., Vol. 39, July 1960, pp. 809-820.

20. Kolmogorov, A. N., "On the Shannon Theory of Information Transmission in the Case of Continuous Signals," IRE Trans. on Info. Theory, Vol. 2, December 1956, pp. 102-108.

21. Lathi, B. P., An Introduction to Random Signals and Communication Theory, Scranton, Pennsylvania: International Textbook Co., 1968.

22. Lee, Y. W., Statistical Theory of Communication. New York: John Wiley and Sons, Inc., 1960.

23. Lerner, R. M., "Design of Signals," MIT Lincoln Laboratory Group Report No. 36-42, February 1960.

24. Mathison, R. P., "Tracking Techniques for Interplanetary Spacecraft," JPL Tech. Report No. 32-284, 1962.

25. Morgera, S. D. and LeBlanc, L. R., "Digital Data Techniques Applied to Real-Time Sonar Data," Proc. Symposium on Computer Processing in Communications, April 1969, pp. 825-845.

26. Naur, P. Editor, "Report on the Algorithmic Language Algol 60," ACM Comm., Vol. 3, No. 5, May 1960, pp. 299-314.

27. Panter, P. F. and Dite, W., "Quantization Distortion in Pulse Code Modulation With Nonuniform Spacing of Levels," Proc. IRE, Vol. 39, January 1951.

28. Papoulis, A., Probability, Random Variables, and Stochastic Processes. New York: McGraw-Hill, 1965.

29. Pickholtz, R. L., "A Recursive Approach to Signal Detection," IEEE Transactions on Information Theory, Vol. 14, No. 3, May 1968.

30. Reboul, L., "Methodes Statistiques En Radiodetection," in Radar Techniques for Detection Tracking and Navigation, ed. W. T. Blackband. New York: Gordon and Breach, 1966.

31. Schlachta, K. V., "Digitalization of Radar Signals and Their Evaluation by a Computer for Automatic Tracking of Targets," Radar Techniques for Detection Tracking and Navigation, ed. W. T. Blackband. New York: Gordon and Breach, 1966.

32. Shannon, C. E., and Weaver, W., The Mathematical Theory of Communication. Urbana, Ill.: U. of Illinois Press, 1949.

33. Sherman, S., "Non-Mean-Square Error Criteria," IRE. Trans. on Information Theory, Vol. 4, No. 3, 1958, pp. 125-126.

34. Swerling, P., "Maximum Angular Accuracy of a Pulsed Search Radar," Proc. IRE, Vol. 44, September 1965, pp. 1146-1155.

35. VanTrees, H. L., Detection, Estimation and Modulation Theory, Pt. I. New York: John Wiley and Sons, 1968.

36. Viterbi, A. J., Principles of Coherent Communication. New York: McGraw-Hill, 1966.

37. Waxman, M. J., "Pattern Recognition Techniques in Detection System Design," Proc. Symp. on Computer Processing in Communications, April 1969.

38. Widrow, B., "Statistical Analysis of Amplitude Quantized Sampled-Data Systems," Trans. AIEE Application and Industry, No. 52, January 1961, pp. 555.

39. Woodward, P. M., Probability and Information Theory with Application to Radar. London: Pergamon Press, 1953.

40. Woodward, P. M. and Davies, I. L., "Information Theory and Inverse Probability in Telecommunication," Proc. IEE, Vol. 99, Pt. III, 1952, p. 37.

41. Young, A. P., "Radar Data-Handling and Display Systems for Use With Pulse Radars," in Radar Techniques for Detection Tracking and Navigation, ed. W. T. Blackband. New York: Gordon and Breach, 1966.

42. Young, G. O., "Array Processing for Target Detection in a Nonuniform Clutter Background," Proc. Symp. on Computer Processing in Communications, April 1969, pp. 727-743.